

GEOMAGNETIC INDUCTION AND THE ELECTRICAL CONDUCTIVITY
OF THE EARTH'S MANTLE

by

DONALD H. ECKHARDT

B.S., Massachusetts Institute of Technology
(1955)

SUBMITTED IN PARTIAL FULFILLMENT
OF THE REQUIREMENTS FOR THE
DEGREE OF DOCTOR OF
PHILOSOPHY

at the

MASSACHUSETTS INSTITUTE OF
TECHNOLOGY
June, 1961

Signature of Author
Department of Geology and Geophysics, May 12, 1961

Certified by
Thesis Supervisor

Accepted by
Chairman, Departmental Committee on Graduate Students

MASSACHUSETTS INSTITUTE OF TECHNOLOGY

GRADUATE THESIS SUBJECT HEADINGS

(To be submitted to Department Headquarters with the original copy of the graduate thesis for transmission to the Library)

WITHDRAWN
FROM
MIT LIBRARY

Author Eckhardt Donald Henry
Last First Middle Full names as appearing on Diploma

Co-Author(s) _____
Last First Middle

Thesis Title Geomagnetic Induction and the Electrical Conductivity of the Earth's Mantle

Submitted to the Department of Geology and Geophysics

For the Degree of Ph.D. in Geophysics

Date Degree Expected June 1961

In order to make your thesis more readily accessible to those who may wish to consult it through national indexing services and library catalogs, you are requested to provide below two or more subject headings. These headings should show the place which your work holds in the fine structure of knowledge in your field. Broad headings such as "organic chemistry," "structures," or "statistics" should be avoided in favor of the most specific terms possible.

Examples: *Semiconductors: Optical properties* is to be preferred to *Solid state physics*; *Sodium graphite reactors to Reactors*; *Isotope effects, Chemical to Reaction mechanisms*; *Control systems, Adaptive to Control systems*; *Computer logic or Assembly programming or Numerical methods to Computers*; *Low lying energy levels or High velocity collisions to Nuclear physics*; *Waste disposal, Atomic to Sanitary engineering*; and *Diffusion indexes or Autoregression* are more descriptive than *Economic forecasting*.

Subject Headings Geomagnetism Earth resistivity

Electromagnetic induction in a sphere

Date May 12, 1961

ABSTRACT

Title: Geomagnetic Induction and the Electrical Conductivity of the Earth's Mantle

Author: Donald H. Eckhardt

Submitted to the Department of Geology and Geophysics on May 12, 1961 in partial fulfillment of the requirements for the degree of Doctor of Philosophy at Massachusetts Institute of Technology.

The ratio of the internal to external source terms of the earth's surface potential for certain geomagnetic fluctuations is indicative of the electrical conductivity of the earth's mantle. Such ratios have already been calculated for harmonics of the diurnal magnetic variation and for storm time variations; in this thesis the ratio for the predominant harmonic of the semiannual variation is calculated but the corresponding ratio for the sunspot variation eludes detection.

A nonlinear first order differential equation is derived for any of these ratios as a function of depth and conductivity in a spherically symmetric earth. This equation may be solved numerically to match an observable surface ratio with a conductivity-depth profile, or it may be solved analytically for a few of the infinite number of possible profiles. This approach departs from earlier, and less flexible, methods which are also reviewed in some detail. The new method provides a deeper insight into the problem of induction in a spherically symmetric earth.

The thin irregular shell of conductivity oceans biases the analyzed ratios for the diurnal and storm time variations. A rough quantitative explanation of this inevitable effect affords an appraisal of the actual significance of the biased ratios.

Since the semiannual variation penetrates more deeply into the mantle and because its analysis is not subject to the same uncertainties due to the influence of the oceans as are the higher frequency variations, it proves a valuable indicator of the possible conductivity structure of the earth. The diurnal ratios are consistent with the semiannual ratio only if there is a rapid rise in conductivity from about 0.3 mhos/meter or less at a depth of 500 kilometers to over 25 mhos/meter at a depth of 600 kilometers.

TABLE OF CONTENTS

	Page
Abstract	2
Lists of Tables and Figures	4
Acknowledgments	6
Chapter I - Introduction	
Purpose	7
Historical Review	7
Contribution of this Thesis	9
The Mantle Conductivity - Other Methods	10
Physical Laws of Conductivity	10
Chapter II - Conventions and Nomenclature	
Units	12
The Geomagnetic Elements	13
Representation of Sinusoidal Variations	14
Legendre Function Normalization	15
Subscripts and Superscripts	15
The Radial Distance	16
Chapter III - The Periodic Geomagnetic Variations	
General	17
The Magnetic Potential and its Sources	17
The Quiet Daily Variation, S_q	19
The Storm Time Variation, Dst	21
Long Period Variations	21
Chapter IV - Induction in an Earth of Spherically Symmetric Conductivity	
General	24
The Vector Helmholtz Equation	25
The Model of Lahiri and Price	26
The Poloidal and Toroidal Modes	28
Boundary Conditions	31
The Solution for a Uniformly Conducting Earth	32
The Solution for the Lahiri and Price Model	34
The Thin Conducting Shell	35
The Thin Insulating Shell	38
Solution by Simultaneous First Order Differential Equations	39
A Differential Equation for S_n	42
Interpretation of Equation 4.30	43
Possible Paths of S_m	48
The Straight Line Path	49
Modifications of the Straight Line Path	53

	Page
Chapter V - Induction Effects of the Irregular Oceans	
General	54
The Thin Shell Insulated on Both Sides	54
The Effects of the Oceans	59
Bias	66
Interpretation of Biased S_q Ratios	70
Chapter VI - Analysis of Long Period Data	
Purpose	76
Zonal Harmonic Analysis	76
Order of Harmonic Analyses	78
Frequency Harmonic Analysis	78
Prefiltering	83
Analysis of Semiannual Variation	87
Analysis of Sunspot Cycle	91
Chapter VII - Conductivity Interpretations of the Mantle	
Resolution of Conductivities	94
The Conductivity of the Mantle - Specific Models	94
The Conductivity of the Mantle - Generalizations	98
Chapter VIII - Suggestions for Future Work	
The Sunspot Cycle	100
Other Cycles	100
Survey of Mantle Models	101
Mantle Shielding	101
Complex Ratios in Geophysics	101
Biographical Note	103
Bibliography	104

LIST OF FIGURES AND TABLES

Figures	Page
4.1	39
4.2, 4.3, 4.4	45
4.5, 4.6, 4.7	47
4.8, 4.9	50
5.1, 5.2 a, b	64
5.3 a, b, c	72
5.4 a, b, c	75

Figures	Page
6.1	77
6.2	82
6.3	88
6.4, 6.5	90
7.1, 7.2	95

Tables	Page
4.1	43
5.1, 5.2	71
6.1	93

ACKNOWLEDGMENTS

I am foremost indebted to my thesis supervisor, Prof. T. R. Madden for having originally introduced me to the topic of this thesis and for having served as adviser and guide throughout the investigation. My association with him has been a most agreeable experience.

I am also grateful to Prof. H. Hughes for having revealed to me the broad geophysical significance to the problem. Others at M.I.T. who have given counsel and aid include Prof. T. Cantwell, Mr. J. Galbraith and Mr. B. Nourbehecht.

Geomagnetic data in punched card form were kindly made available by Prof. M. P. Hagen of Emmanuel College and Mr. P. F. Fougere of Air Force Cambridge Research Laboratories.

Support for the preparation of this work came from the National Science Foundation's Grant NSF-G6602. Machine computations were performed at the M.I.T. Computation Center on the IBM 709. The Standard Oil Company of California awarded me a most welcome fellowship in my terminal year of graduate study.

Miss N. Lawrence typed the manuscript and Mr. N. Hayes performed the drafting. Their assistance during the deadline rush is gratefully acknowledged.

CHAPTER I

INTRODUCTION

Purpose

Among the temporal variations of the magnetic field of the earth, there are several detectable periodic variations whose primary sources are outside of the earth. Secondary source fields induced within the earth can be discriminated from the external source fields, and a comparison of their magnitudes enable us to make estimations of the electrical conductivity of the earth and its variation with depth. This thesis is concerned with reviewing and extending the pertinent theory, discussing its previous application to the diurnal geomagnetic variation, analyzing the semiannual and eleven year variations and applying the theory for the semiannual period.

We are concerned with only one of several different methods for estimating the conductivity of the earth. By the nature of the sources and the relative sizes and conductivities of the crust, mantle and core of the earth, this method is particularly sensitive to the mantle conductivity and it is relatively insensitive to the conductivities of the crust and core.

Historical Review

All previous applications of the process of magnetic induction on a world-wide basis to infer the conductivity of the earth's interior have considered only the diurnal variation of the geomagnetic field and the storm time magnetic transient whose principal composite periods are only a few days.

Chapman and Whitehead (1923) first treated the problem by considering a central "core" (not the core which is now universally accepted in geophysics), surrounded by an insulating shell and capped by a thin conducting shell. In this three layer model the "core" represents, more or less, what is now known as the core and most of the mantle taken together; the insulating shell corresponds to the crust and some of the upper mantle; and the thin conducting shell is an attempt to account for the relatively highly conducting oceans. In matching this model with observed diurnal magnetic variation data, Chapman and Whitehead had three degrees of freedom at their disposal: the thickness of the equivalent oceans, the depth to the "core" and the conductivity of the "core". They found that the equivalent oceans would have to be rather shallow (the total volume being no more than one fifth of the volume of the true oceans) and that the "core" was at a depth of 200-500 kilometers with a conductivity of the order of 0.1 mhos/meter.

Chapman and Price (1930) used the "core" model of Chapman and Whitehead for observed aperiodic storm time magnetic variation data. They calculated "core" conductivities a little higher than those from the diurnal variations. The "core" depth wasn't changed much and the equivalent oceans were still quite shallow.

Lahiri and Price (1939) extended the theory for a "core" whose conductivity varies as some power of the distance from the center of the earth, and they considered both diurnal and storm time variations. Their model required that the earth's conductivity increase very rapidly at a depth of about 700 kilometers. Again the equivalent oceans were very shallow.

All of the above analysts used the data of Chapman (1919). Rikitake (1950) reviewed their work and used the more recent diurnal variation analyses of Benkova (1940), and Hasegawa and Ota (1948). His results were about the same as those of Lahiri and Price. Rikitake also tried to account for the effects of conducting oceans which are not continuous about the earth. Benkova (1957) found similar conductivity structures by applying the theory to new data on storm time variations.

Contributions of this Thesis

The problem of the oceans was never adequately treated, and it is the contention of this thesis that, because of inevitable bias in the data, the problem is insuperable at the frequencies used for any accurate conductivity determinations. The oceans vitiate the data less as the frequencies of the magnetic variations decrease and their effect for the longer period six month and eleven year cycles analyzed in this thesis are negligible. Because of the low signal to noise ratio, the quantitative analysis of these periods is somewhat more complicated than for the diurnal variation. Fortunately, though, the spherical geometry for the long period fields used is very simple; geomagnetic data have been available; and machine computation facilities have been accessible and thoroughly exploited.

The theoretical approach presented by Lahiri and Price adapts itself well to the problem of estimating the mantle conductivity as a function of depth, and much of it is reviewed below. In addition, a new approach to the problem where the conductivity varies with depth is presented. With this method, a better "feel" for the problem is attainable and the solution is more straightforward and flexible insofar as the allowable conductivity structure is concerned. This

new approach is used in the interpretation of the semiannual data.

The Mantle Conductivity - Other Methods

Other methods for estimating the conductivity of the mantle (and core) have most recently been described by Tozer (1959). A few of these which are especially sensitive to the lower mantle conductivity are described here. (For a more complete survey see Tozer or Runcorn, 1956.) Bullard et al (1950) considered the electromagnetic coupling of the core with mantle and the mantle conductivity necessary to account for the observed westward drift of the geomagnetic secular variation. It was calculated that the lower mantle must have a conductivity of at least 10 mhos/meter. Munk and Revelle (1952) were able to explain measured irregularities in the length of the day by a core-mantle electromagnetic coupling if the lower mantle conductivity were of the order of 100 mhos/meter. Runcorn found an upper limit for the conductivity of the lower mantle. By considering the maximum allowable mantle shielding which would allow certain frequently observed and relatively rapid changes in the secular variation field, he found that if the conductivity in the lower two-thirds of the mantle were approximately constant, it could not exceed about 100 mhos/meter. MacDonald (1957) and Yukutake (1959) considered the attenuation in the mantle of a random distribution of secular variation sources at the core boundary. Their lower mantle conductivity estimates range between 45 and 700 mhos/meter.

Physical Laws of Conductivity

Hughes (1953) presented three electrical conduction mechanisms for mantle material: impurity conductivity, electronic conductivity, and ionic conductivity. For the temperatures of the mantle, impurity

conductivity is unimportant, but whether electronic or ionic conductivity dominates at high pressures is a moot point. The conductivities by both of these processes increase with increasing temperature, and at high temperatures the ionic conductivity dominates. There is also a pressure effect which is not well understood, so when both temperatures and pressures are high, as deep in the mantle, the dominant mechanism is uncertain. Hughes (1950) suggests ionic conductivity and Tozer (1959) favors electronic conductivity. It is possible for the conductivity to decrease with depth deep in the mantle if the pressure effects exceed and oppose the temperature effects, but it is generally assumed for the conductivity models in this thesis that the mantle conductivity increases with depth although this assumption need not hold for most of the theoretical development.

Estimates of the conductivity of the upper core have been made by Bullard and Elsasser (1950). Even after possible downward revision suggested by MacDonald and Knopoff (1958) and Tozer, these conductivities are at least of the order of 10^5 mhos/meter. The conductivity below the core boundary is several orders of magnitude greater than it is above the boundary and the core appears as a super-conductor for even the longest period magnetic variation analyzed in this thesis.

CHAPTER II
CONVENTIONS AND NOMENCLATURE

Units

This thesis employs the Giorgi rationalized MKSQ system of units rather than the unnormalized cgs (emu and esu) system which is conventionally used in geomagnetic literature. It is not the purpose of this section to dwell on the advantages of the Giorgi system for they have been adequately demonstrated many times in literature on the subject of units in electromagnetic theory. One very readable account occurs in Sommerfeld's text, "Electrodynamics" (1952).

The nomenclature for the field vectors, \vec{B} , \vec{H} , \vec{E} and \vec{D} is, unfortunately, disparate and often misleading. It is usually safest simply not to give them any names and, except for calling \vec{B} the "magnetic flux density", this is the policy of this thesis.

Sommerfeld shows that \vec{B} and \vec{E} are analogous as "intensity entities" whereas \vec{H} and \vec{D} are analogous as "quantity entities" so, since any field measuring scientific instrument detects "intensity entities", the appropriate vector in which to express the measured magnetic field is \vec{B} . The emu unit for \vec{B} is the gauss; in geomagnetism the gamma (1 gamma = 10^{-5} gauss) is often used in its stead. In the rationalized MKSQ system, the unit of magnetic flux density is the weber per square meter where 1 weber/m² = 10^4 gauss = 10^9 gammas.

The Geomagnetic Elements

The vector \vec{B} may be expressed in terms of its geomagnetic elements. The elements which are the local cartesian components of \vec{B} are known as X, Y and Z. X is defined as positive northward; Y is positive eastward and Z positive downward. If, instead of using geographic north and east, geomagnetic north and east are used in defining the cartesian elements, X and Y are replaced by X' and Y'. The total horizontal component is $H = \sqrt{X^2 + Y^2} = \sqrt{(X')^2 + (Y')^2}$; the total flux density is $F = \sqrt{H^2 + Z^2}$; the declination is $D = \sin^{-1}(Y/H)$; the inclination is $I = \sin^{-1}(Z/F)$.

The geomagnetic elements which are usually tabulated are X, Y and Z or H, D and Z. From the second set we may convert to the first set by using

$$X = H \cos D$$

$$Y = H \sin D$$

For small changes in the elements, we may relate the changes in X and Y with those in H and D by using

$$X + \Delta X = (H + \Delta H) \cos (D + \Delta D) \approx X - Y \Delta D + \cos D \Delta H$$

$$Y + \Delta Y = (H + \Delta H) \sin (D + \Delta D) \approx Y + X \Delta D + \sin D \Delta H$$

$$\Delta X \approx -Y \Delta D + \cos D \Delta H \quad (2.1a)$$

$$\Delta Y \approx X \Delta D + \sin D \Delta H \quad (2.1b)$$

Wherever these elements appear in equations, they are assumed to be complex amplitudes (where $i = \sqrt{-1}$).

Representation of Sinusoidal Variations

In representing a sinusoid in time, t ,

$$u = U_0 \cos \omega (t - t_0)$$

it is often a convenient shorthand to consider the complex function

$$U = U_0 \exp i\omega (t - t_0) = (U_0 e^{-i\omega t_0}) e^{i\omega t}$$

such that

$$u = \text{Re} (U)$$

where Re is the operator which takes the real part of U . $U_0 e^{-i\omega t_0}$ is the complex amplitude of U and $e^{i\omega t}$ is its time variation. Here we wish to extend this shorthand to a product of sinusoids in time, t , and longitude, φ ,

$$u = U_0 \cos \omega (t - t_0) \cos m (\varphi - \varphi_0)$$

for which we now consider the doubly complex function

$$U = U_0 e^{i\omega(t-t_0)} e^{jm(\varphi-\varphi_0)} = (U_0 e^{-i\omega t_0 - jm\varphi_0}) e^{i\omega t} e^{jm\varphi}$$

such that

$$u = \text{Rei} (\text{Rej} (U)) = \text{Rej} (\text{Rei} (U))$$

where Rei is the operator which removes the i -imaginary terms and

Rej is the operator which removes the j -imaginary terms. Thus

$$\text{Rei} (U) = U_0 \cos (t - t_0) \exp jm (\varphi - \varphi_0)$$

$$\text{Rej} (U) = U_0 \exp i\omega (t - t_0) \cos m (\varphi - \varphi_0)$$

$U_0 e^{-i\omega t_0 - jm\varphi_0}$ is the doubly complex amplitude of U ; $e^{i\omega t}$ is its time variation and $e^{jm\varphi}$ is its longitudinal variation. Since i and j are imaginary numbers in their respective domains

$$i^2 = -1$$

$$j^2 = -1$$

although, in general,

$$ij \neq -1$$

It is the convention here that the operator, Re , represents Rei , but never Rej .

Legendre Function Normalization

The associated Legendre functions have the convenient Schmidt normalization (Chapman and Bartels, 1940) which is conventional in geomagnetism. The normalized functions, P_n^m , are defined in terms of the unnormalized functions, $P_{n, m}$, as follows:

$$P_n^m = P_{n, m} \quad m = 0$$

$$P_n^m = 2 \frac{(n - m)}{(n + m)} P_{n, m} \quad m \neq 0$$

Subscript and Superscripts

For scalar quantities which are not components of vectors, the order of a spherical harmonic, n , and of its equatorial sinusoid, m , appear in their usual locations, e. g. $j_n(kr)$, $P_n^m(\cos \vartheta)$. When m is zero, it is omitted. For vectors and vector components, these terms appear as superscripts (when two superscripts are required they are separated by a comma) and components of a vector are identified by subscripts, e. g. \vec{B}^n , $\vec{B}^{n, m}$, $B_\varphi^{n, m}$, Br . Occasional subscripts, such as μ_0 , ω_0 and t_1 have their conventional meanings or are defined where they first appear.

The Radial Distance

To help avoid confusion we define here the many symbols used to denote the distance from the center of the earth, r , to various surfaces.

$r = a$ reference surface for geomagnetic potential.
This is generally the surface of the earth,
 $a = 6370$ kilometers

$r = r_0$ outer surface of conducting mantle $r_0 \leq 6370$ kilometers

$\rho = r/a$ }
 $\eta = r_0/a$ } normalized radial distances

$r = r_s$ radius of superconducting sphere

CHAPTER III
THE PERIODIC GEOMAGNETIC VARIATIONS

General

The changes in the magnetic field of the earth are manifold and complex. They may be considered as the sum of three different kinds of variations: secular, transient and periodic. In this thesis we are mainly concerned with the most easily detectable periodic variations: the diurnal, semiannual and sunspot cycles. The primary sources of these periodic fields are outside the earth and secondary sources are induced within the earth. By comparing these different sources we may make some inferences concerning the conductivity of the earth's mantle. The purpose of this chapter is to describe these variations mathematically and to review the methods for discriminating between internal and external sources.

The Magnetic Potential and its Sources

Let \vec{B} be the periodic magnetic flux density of frequency, $\omega/2\pi$, which is part of the varying magnetic field of the earth, and let it contain time only as the factor $e^{i\omega t}$. For a shell a few kilometers thick, which is bordered on the inside by the earth's surface, we assume that the electrical conductivity, σ , and the current density, \vec{J} , are zero. With $\mu = \mu_0 = \text{constant}$

$$\vec{J} = \nabla \times \vec{H} = 0 = \nabla \times \vec{B}$$

so in this shell \vec{B} is derivable from a potential

$$\vec{B} = -\nabla \Omega$$

In spherical co-ordinates (r , ϑ , φ) the potential takes the form

$$\Omega = \sum_{n=1}^{\infty} \sum_{m=0}^n \Omega_n^m = a \sum_{n=1}^{\infty} \sum_{m=0}^n [\mathcal{E}_n^m \rho^m + \mathcal{L}_n^m \rho^{-m-1}] P_n^m(\cos\vartheta) e^{jm\varphi} e^{i\omega t} \quad (3.1)$$

where $\rho = \frac{r}{a}$ is the normalized distance from the origin and \mathcal{E}_n^m and \mathcal{L}_n^m are doubly complex amplitudes containing the factors $e^{-i\omega t_0}$ and $e^{-jm\varphi_0}$ (see Chapter II). \mathcal{E}_n^m is associated with sources outside the shell, while \mathcal{L}_n^m is associated with sources under the shell, that is, within the earth.

At the earth's surface where $\rho = 1$, the potential is

$$\Omega(a) = a \sum_{n=1}^{\infty} \sum_{m=0}^n \mathcal{B}_n^m Y_n^m e^{i\omega t}$$

where Y_n^m represents $P_n^m e^{jm\varphi}$ and

$$\mathcal{B}_n^m = \mathcal{E}_n^m + \mathcal{L}_n^m = |\mathcal{B}_n^m| e^{-i\omega t_0} e^{-jm\varphi_0}$$

In terms of the X, Y, Z field nomenclature of geomagnetism (see Chapter II)

$$X e^{i\omega t} = -B_{\vartheta}(a) = \frac{\partial \Omega(a)}{a \partial \vartheta} = \sum_{n=1}^{\infty} \sum_{m=0}^n \mathcal{B}_n^m \frac{\partial Y_n^m}{\partial \vartheta} e^{i\omega t} \quad (3.2a)$$

$$Y e^{i\omega t} = -B_{\varphi}(a) = -\frac{1}{a \sin\vartheta} \frac{\partial \Omega(a)}{\partial \varphi} = -\sum_{n=1}^{\infty} \sum_{m=0}^n j^m \mathcal{B}_n^m \frac{Y_n^m}{\sin\vartheta} e^{i\omega t} \quad (3.2b)$$

$$Z e^{i\omega t} = -B_r(a) = \left(\frac{\partial \Omega}{\partial r} \right)_a = \sum_{n=1}^{\infty} \sum_{m=0}^n \mathcal{H}_n^m Y_n^m e^{i\omega t} \quad (3.2c)$$

where

$$\mathcal{H}_n^m = n \mathcal{E}_n^m - (n+1) \mathcal{L}_n^m$$

It is possible to determine \mathcal{E}_n^m and \mathcal{L}_n^m from the measured X, Y and Z periodic field components from observatories distributed around the earth. We may use the horizontal components, X and Y,

to find Ω (a) by numerical line integration. A spherical harmonic analysis of Ω (a) gives \mathcal{B}_m^m while a similar analysis of Z gives \mathcal{H}_m^m . Then the external and internal source terms can be found by

$$(2m + 1) \mathcal{E}_m^m = (m+1) \mathcal{B}_m^m + \mathcal{H}_m^m \quad (3.3a)$$

$$(2m + 1) \mathcal{I}_m^m = m \mathcal{B}_m^m - \mathcal{H}_m^m \quad (3.3b)$$

It is conventional, however, to calculate \mathcal{B}_m^m by analyzing the X or Y field components directly (see Chapman and Bartels, 1940, Chapter 20).

The Quiet Daily Variation, Sq

As may be seen in Vestine et al (1947b) at any geomagnetic latitude the major portion of the quiet daily magnetic variation depends only on local time. Benkova (1940) estimates that, aside from the variation with latitude, about 80 percent of the Sq field is a function only of local time, and most of the harmonic analyses of this field have been made with the assumption that the entire field is so dependent. That part of the field that does not depend on local time may be attributed to the facts that the geomagnetic and geographic axis of the earth do not coincide and that part of the field is caused by currents induced in the irregularly distributed oceans. If we denote local time by γ , we must have

$$\omega_s \gamma = \varphi + \omega_s t$$

$$\frac{2\pi}{\omega_s} = 24 \text{ hours}$$

Rather than having

$$\Omega_m^m(a) = a |\mathcal{B}_m^m| e^{i\omega(t-\tau_0)} e^{jm(\varphi-\varphi_0)} P_m^m$$

we now have

$$\begin{aligned}\Omega_m^m(a) &= a |B_m^m| e^{im\omega_0(\tau - \tau_0)} P_m^m \\ &= a |B_m^m| e^{-im\omega_0\tau_0} e^{im(\omega_0 t + \varphi)} P_m^m \\ &= a B_m^m e^{im(\omega_0 t + \varphi)} P_m^m\end{aligned}$$

This is a more restricted form for Ω_m^m which is imposed by assuming that Ω_m^m is only a function of latitude and local time. It is sufficient only to consider the complex potential associated with the cosine term

$$a B_m^m e^{im\omega_0 t} \cos m\gamma P_m^m$$

Corresponding to this for the vertical field is

$$Z_m^m e^{im\omega_0 t} \cos m\gamma P_m^m$$

At about the time of the equinox, the Sq field harmonics are odd about the equator, primarily of the form, $P_{m+1}^m e^{jm\gamma}$, and harmonics greater than the fourth order are relatively small and unimportant. Analyses of this field have been made by Chapman (1919), Benkova (1940), and Hasegawa and Ota (1941). Their derived complex ratios

$$S_2 = \mathcal{L}_2^1 / \mathcal{E}_2^1 \quad S_3 = \mathcal{L}_3^2 / \mathcal{E}_3^2$$

$$S_4 = \mathcal{L}_4^3 / \mathcal{E}_4^3 \quad \text{are plotted in Figures 5.3a-c}$$

in Chapter V.

The Storm Time Variation, Dst

Since the transient storm time variation, Dst, is symmetric about the earth's geomagnetic axis, and since its geomagnetic north component, X^1 , is symmetric about the geomagnetic equator, the field can be derived from a potential containing only odd zonal harmonics. The field may be considered as composed of two parts. The main part consists only of a few low order harmonics and it is present at all latitudes; another part is very intense and is present only in polar regions where the geomagnetic latitude exceeds 60° (about 13 percent of the earth's area). Using the average characteristics of the Dst field from 40 magnetic storms at geomagnetic north latitude 22° , 40° , and 53° , Chapman and Price (1930) determined \mathcal{L}_m and \mathcal{H}_m for a main field which was assumed to contain only the first, third and fifth order zonal harmonics. They found that the first harmonic coefficients, \mathcal{L}_1 and \mathcal{H}_1 , are, by far, the largest and that the higher harmonics are relatively unimportant.

Long Period Variations

The frequency and intensity of magnetic storms change cyclically with time. There are several detectable cycles which are related, in various ways, to the change in seasons or the sun and its activity. There is, for instance, a 27 day cycle which corresponds to the mean period of rotation of the sun, and there is a yearly cycle which McNish (1959) attributes to an atmospheric dynamo effect. Of greater amplitudes are the cycles with which we shall be concerned in this thesis: a semiannual cycle and an eleven year cycle. The semiannual cycle has most recently been studied by McNish who concluded that peak amplitudes of magnetic activity

indices occur at the equinoxes. The eleven year cycle is known as the sunspot cycle for there is a well-known correlation between magnetic storms and sunspots and both magnetic disturbance indices and sunspot numbers move in phase in an eleven year cycle.

The magnetic storms which are most frequent and intense during the peaks of the semiannual and sunspot cycles combine to give two long period cycles of magnetic flux density variations. Except for scaling, therefore, the harmonics of the potentials of these periodic fields are the same as for the transient field, and the world-wide part can be adequately analyzed in terms only of the first zonal harmonic.

The semiannual cycle in the geomagnetic north component, X^t , is revealed by Vestine et al (1947b) in a graphical presentation of monthly mean departures from yearly means of the X^t , Y^t , Z^t geomagnetic elements. As would be expected for a potential zonal about the geomagnetic axis, the geomagnetic east component, Y^t , shows no periodicity; but the vertical component, Z , is unfortunately so weak that it also shows no periodicity. For the zonal potential the total horizontal component, H , varies the same as the X^t component. Cynk (1941) examined the latitude distribution for H of the daily mean disturbance, Dm , which is calculated from internationally disturbed day means minus internationally quiet day means. He compared this component at geomagnetic north latitudes 22° , 40° and 53° with the mean H component taken from the same Dst field analysis used by Chapman and Price, and he found that the Dm and Dst horizontal components are proportional. In an earlier paper, Cynk (1939) showed that the H component of Dm which is symmetric about the equator has a conspicuous semiannual cycle.

The sunspot cycle is shown graphically by Vestine in a presentation of the yearly means of the geomagnetic elements over three cycles. The geomagnetic north component, X^1 , has a detectable eleven year periodicity and its latitude distribution agrees reasonably well with the X^1 latitude distribution for the daily means of disturbance, Dm . Similar to the semiannual cycle, the Y^1 and Z^1 variations show no periodicity.

Since the semiannual and sunspot cycle potentials can be adequately represented in the nonpolar latitudes with only the first zonal harmonic, only \mathcal{S}_1 and \mathcal{H}_1 need be calculated and the spherical harmonic analysis is simplified. \mathcal{S}_1 is determined from the X^1 variations, but before \mathcal{H}_1 can be calculated for either cycle, the vertical variations must be detectable by a frequency harmonic analysis. However, for either cycle, even if the variations in $Z e^{i\omega t}$ remain below the detection threshold, if we can estimate the threshold level, we can set some limit to \mathcal{S}_1 , \mathcal{E}_1 , and $\mathcal{S}_1/\mathcal{E}_1$. In Chapter VII, new frequency harmonic analyses of the geomagnetic elements are presented for the semiannual and sunspot cycles. The vertical variation is only detected for the semiannual period only.

CHAPTER IV
INDUCTION IN AN EARTH OF SPHERICALLY SYMMETRIC
CONDUCTIVITY

General

The purpose of this chapter is to derive some relations between observable geomagnetic quantities and the radial conductivity structure of a spherical earth. At any depth the conductivity, σ , is assumed to be constant. For the diurnal variations in the earth's magnetic field this assumption loses its validity near the surface where the conductive oceans are inhomogeneously distributed. The problem of allowing for the oceans is treated separately in Chapter V.

The first part of this chapter is a review of the usual method of matching the boundary conditions for Laplace's equation outside the earth with those of the Helmholtz equation inside the earth. With this treatment the complex ratio

$$S_m = \frac{J_m^m}{E_m^m}$$

is related to the solution of a second order differential equation for which the radial distance, r , is the independent variable (see Equation 4.6). The second part of the chapter presents a new approach to the problem in which S_m is considered as a function of r and is shown to satisfy a nonlinear first order differential equation with r as the independent variable (see Equation 4.30). The behavior of this interesting equation is treated in detail for it affords a good understanding of the relationship between r , σ and S_m for any spherically symmetric earth model.

The behavior of the induction coefficient S_m is studied in detail for a constant conductivity earth model. The results are presented in Chapter V.

The Vector Helmholtz Equation

Let the field vectors \vec{E} , \vec{B} , \vec{H} and \vec{J} , contain the time as the factor $e^{i\omega t}$ (rather than the conventional $e^{-i\omega t}$). Using Maxwell's equations, neglecting the displacement current, we find

$$\begin{aligned}\nabla \times \vec{E} &= -i\omega \vec{B} = -i\omega\mu \vec{H} \\ \nabla \times \nabla \times \vec{E} &= -i\omega\mu \nabla \times \vec{H} = -i\omega\mu \vec{J} = -i\omega\mu\sigma \vec{E} = k^2 \vec{E}\end{aligned}\quad (4.1)$$

where $k^2 = k^2(r) = -i\omega\mu\sigma(r)$. Consider \vec{E} as the sum of an irrotational field, \vec{E}_{irr} , and a solenoidal field, \vec{E}_{sol} . Applying (4.1) to \vec{E}_{irr}

$$\nabla \times \nabla \times \vec{E}_{irr} = 0 = k^2 \vec{E}_{irr}$$

If $k^2 \neq 0$, $\vec{E}_{irr} = 0$ and $\vec{E} = \vec{E}_{sol}$. Thus $\nabla \cdot \vec{E} = 0$, and we have the vector Helmholtz equation

$$\nabla \nabla \cdot \vec{E} - \nabla \times \nabla \times \vec{E} + k^2 \vec{E} = \nabla^2 \vec{E} + k^2 \vec{E} = 0 \quad (4.2)$$

where ∇^2 is the vector Laplacian operator. Returning to Maxwell's equations

$$\begin{aligned}\frac{1}{\mu} \nabla \times \vec{B} &= \nabla \times \vec{H} = \vec{J} \\ \frac{1}{\mu} \nabla \times \nabla \times \vec{B} &= \nabla \times \vec{J} = \nabla \times (\sigma \vec{E}) = \nabla \sigma \times \vec{E} + \sigma \nabla \times \vec{E} \\ \nabla \times \nabla \times \vec{B} &= \mu \nabla \sigma \times \vec{E} - i\omega\mu\sigma \vec{B} \\ \nabla \times \nabla \times \vec{B} &= -\frac{\nabla k^2}{i\omega} \times \vec{E} + k^2 \vec{B}\end{aligned}\quad (4.3)$$

In spherical co-ordinates (r, θ, φ) , if ψ is a scalar which satisfies the scalar Helmholtz equation

$$\nabla^2 \psi + k^2 \psi = 0 \quad (4.4)$$

then three mutually orthogonal solutions to (4.2) may be derived from ψ (see Stratton (1941), Section 7.11) as

$$\vec{E} = \vec{L} = \nabla \psi \quad (4.5a)$$

$$\vec{E} = \vec{M} = \nabla \times \vec{r} \psi \quad (4.5b)$$

$$\vec{E} = \vec{N} = (1/k) \nabla \times \vec{M} \quad (4.5c)$$

By separation of variables, the solution for ψ is found to be

$$\psi = \sum_{m=1}^{\infty} \psi_m = \sum_{m=1}^{\infty} R_m V_m = \sum_{m=1}^{\infty} R_m \sum_{m=0}^m a_m^m P_m^m(\cos \theta) e^{jm\varphi} e^{i\omega t}$$

where R_m is the solution to the differential equation

$$r^2 \frac{d^2 R_m}{dr^2} + 2r \frac{dR_m}{dr} + [k^2 r^2 - m(m+1)] R_m = 0 \quad (4.6)$$

The Model of Lahiri and Price

The case where k^2 is allowed to vary with depth in the form

$$k^2(r) = k_0^2 \rho^{-\alpha} \quad \rho < 1$$

$$= 0 \quad \rho \geq 1$$

where

$$\rho = r/r_0$$

$$r_0 \leq a = \text{earth's radius}$$

was first investigated by Lahiri and Price (1939). Substituting for r and k^2 , (4.6) becomes

$$\rho^2 \frac{d^2 R_m}{d\rho^2} + 2\rho \frac{dR_m}{d\rho} + [k_0^2 r_0^2 \rho^{2-\alpha} - m(m+1)] R_m = 0 \quad (4.7)$$

For a uniformly conducting sphere, $\alpha = 0$ and the two independent solutions to (4.5) are the spherical Bessel functions $j_m(kr)$ and $n_m(kr)$. In order to have the solution remain finite at $r = 0$, only the $j_m(kr)$ solution is used and we have

$$R_m = j_m(kr), \quad \alpha = 0$$

For the special case, $\alpha = 2$, the two independent solutions to (4.7) are $\rho^{-\frac{1}{2} + \sqrt{(m+\frac{1}{2})^2 - k_0^2 r_0^2}}$ and $\rho^{-\frac{1}{2} - \sqrt{(m+\frac{1}{2})^2 - k_0^2 r_0^2}}$. Again, in order to have the solution remain finite at the origin, only the first form is chosen and

$$R_m = \rho^{-\frac{1}{2} + \sqrt{(m+\frac{1}{2})^2 - k_0^2 r_0^2}}, \quad \alpha = 2$$

For the case $\alpha \neq 2$, the two independent solutions to (4.7) may be chosen as $\rho^{-\frac{1}{2}} I_p(\eta)$ and $\rho^{-\frac{1}{2}} K_p(\eta)$ where $I_p(\eta)$ and $K_p(\eta)$ are, respectively, the modified Bessel function of the first and second kind, and

$$\eta = -\frac{2ik_0 r_0}{2-\alpha} \rho^{\frac{2-\alpha}{2}} = \beta_0 \rho^{\frac{2-\alpha}{2}}$$

$$p = \frac{2m+1}{2-\alpha}$$

(See for instance, Hildebrand, 1948, pp. 166-67.)

As $\eta \rightarrow 0$

$$I_p(\eta) \rightarrow \frac{1}{\Gamma(p+1)} \left(\frac{\eta}{2}\right)^p$$

$$K_p(\eta) \rightarrow \frac{1}{2} \Gamma(p) \left(\frac{\eta}{2}\right)^{-p}$$

so since $\eta = \beta_0 \rho^{(2-\alpha)/2}$, in order that the solution remain finite

as $\rho \rightarrow 0$, R_m takes the following forms

$$R_m = (-1)^p \rho^{-\frac{t}{2}} I_p(z) = \rho^{-\frac{t}{2}} I_p(-z) = \rho^{-\frac{t}{2}} I_\nu(z) \quad \alpha < 2$$

$$R_m = \rho^{-\frac{t}{2}} K_p(z) = \rho^{-\frac{t}{2}} K_{-p}(z) = \rho^{-\frac{t}{2}} K_\nu(z) \quad \alpha > 2$$

where

$$z = \frac{2ik_0 r_0}{|2-\alpha|} \rho^{\frac{2-\alpha}{2}} = z_0 \rho^{\frac{2-\alpha}{2}}$$

$$\nu = \frac{2m+1}{|2-\alpha|}$$

The Poloidal and Toroidal Modes

For the problem at hand, only the solenoidal solutions for \vec{E} (4.5b, c) are applicable. Corresponding to $\psi_m = R_m V_m$, let us consider the two cases $\vec{E}^m = \vec{M}^m$ and $\vec{E}^m = \vec{N}^m$

where

$$\vec{M}^m = \nabla \times \vec{r} \psi_m$$

$$\vec{N}^m = \frac{1}{k} \nabla \times \vec{M}^m$$

Their components are

$$M_r^m = 0 \quad M_\theta^m = \frac{1}{\sin\theta} \frac{\partial \psi_m}{\partial \varphi} \quad M_\varphi^m = -\frac{\partial \psi_m}{\partial \theta}$$

$$N_r^m = \frac{n(n+1)}{kr} \psi_m \quad N_\theta^m = \frac{1}{kr} \frac{\partial^2 (r\psi_m)}{\partial r \partial \theta} \quad N_\varphi^m = \frac{1}{kr \sin\theta} \frac{\partial^2 (r\psi_m)}{\partial r \partial \varphi}$$

Just above the boundary $r=r_0$, the conductivity is zero and there can be no radial component of current. Just below the boundary, where the conductivity is not zero, there still can be no radial current so

$$J_r^m(r_0) = \sigma E_r^m(r_0) = E_r^m(r_0) = 0 \quad (4.8)$$

Since the \vec{M}^m form of the solution has no radial component, it may be identified with \vec{E}^m , and boundary condition (4.8) is satisfied.

Let us take

$$\vec{E}^m = -i\omega \vec{M}^m \quad (4.9a)$$

Then, since $\nabla \times \vec{E}^m = -i\omega \vec{B}^m$

$$\vec{B}^m = \nabla \times \vec{M}^m = k \vec{N}^m \quad (4.9b)$$

The magnetic field for this form of solution is said to be in the poloidal mode.

We may verify, now, that $\vec{B}^m = k \vec{N}^m$ satisfies (4.3). Using (4.5c) and (4.9a, b)

$$\vec{B}^m = k \vec{N}^m = \nabla \times \vec{M}^m$$

$$\nabla \times \vec{B}^m = \nabla \times \nabla \times \vec{M}^m = k^2 \vec{M}^m$$

$$\nabla \times \nabla \times \vec{B}^m = \nabla k^2 \times \vec{M}^m + k^2 \nabla \times \vec{M}^m$$

$$\nabla \times \nabla \times \vec{B}^m = -\frac{\nabla k^2}{i\omega} \times \vec{E}^m + k^2 \vec{B}^m$$

If we make an attempt to match \vec{E}^m with \vec{N}^m in the form, say,

$$\vec{E}^m = k \vec{N}^m$$

then boundary condition (4.8) can only be met if

$$E_r^m(r_0) = \frac{m(m+1)}{r_0} \psi_m(k_0 r_0) = 0$$

$$\psi_m(k_0 r_0) = R_m(k_0 r_0) = 0$$

Therefore

$$\nabla \times \vec{E}^m = \nabla \times (k \vec{N}^m) = \nabla \times \nabla \times \vec{M}^m = k^2 \vec{M}^m$$

$$i\omega \vec{B}^m = -k^2 \vec{M}^m$$

$$i\omega B_r^m(r_0) = 0$$

$$i\omega B_\theta^m(r_0) = -k^2 R_m(k_0 r_0) \frac{\partial V_m}{\sin^2 \theta \partial \varphi} = 0$$

$$i\omega B_\varphi^m(r_0) = k^2 R_m(k_0 r_0) \frac{\partial V_m}{\partial \theta} = 0$$

The magnetic field for this form of solution is said to be in the toroidal mode. At the boundary $r = r_0$, \vec{B}^m vanishes in all components so the magnetic lines of flux are completely enclosed inside the conducting earth and they have no effect at the surface. The toroidal mode cannot be induced by external source fields so, in the absence of internal sources, it corresponds to a decaying field. For example, for a uniformly conducting sphere in the toroidal mode

$$R_m(k_0 r_0) = j_m(k_0 r_0) = 0$$

The real roots to $j_m(k_0 r_0) = 0$ correspond to imaginary frequencies or, physically, to exponentially decaying fields. For any reasonable uniform earth model, the relaxation time, σ / ϵ , is considerably less than one second. Even when σ is not uniform, we have shown above that $\nabla \cdot \vec{E} = 0$ and thus there is no charge density. For any radial conductivity distribution for which $\frac{d\sigma}{dr} \neq 0$ and for which the charge density and its time derivative are everywhere zero

$$\nabla \cdot \vec{J}^m = \vec{E}^m \cdot \nabla \sigma + \sigma \nabla \cdot \vec{E}^m = \vec{E}^m \cdot \nabla \sigma = 0$$

Consequently

$$\vec{E}^m \cdot \vec{r} = 0$$

and \vec{E}^m must have no radial component; that is, the solution must be in the poloidal mode. From here on we shall consider only the poloidal mode.

Boundary Conditions

At the boundary, $r = r_0$, on the conducting side, the poloidal components of $\vec{B}^{m,m}$ are

$$B_r^{m,m}(r_0) = \frac{n(m+1)}{r_0} R_n(k, r_0) a_n^m Y_n^m e^{i\omega t} \quad (4.10a)$$

$$B_\theta^{m,m}(r_0) = \frac{1}{r_0} \left[\frac{d(rR_n)}{dr} \right]_{k, r_0} a_n^m \frac{\partial Y_n^m}{\partial \theta} e^{i\omega t} \quad (4.10b)$$

$$B_\phi^{m,m}(r_0) = \frac{1}{r_0} \left[\frac{d(rR_n)}{dr} \right]_{k, r_0} a_n^m j^m \frac{Y_n^m}{\sin \theta} e^{i\omega t} \quad (4.10c)$$

On the nonconducting side, from (3.2 a, b, c), if $a = r_0$ the components are

$$B_r^{m,m}(r_0) = -\mathcal{A}_n^m Y_n^m e^{i\omega t} \quad (4.11a)$$

$$B_\theta^{m,m}(r_0) = -\mathcal{B}_n^m \frac{\partial Y_n^m}{\partial \theta} e^{i\omega t} \quad (4.11b)$$

$$B_\phi^{m,m}(r_0) = -j^m \mathcal{B}_n^m \frac{Y_n^m}{\sin \theta} e^{i\omega t} \quad (4.11c)$$

The boundary conditions are that $B_r^{m,m}$ is continuous across the boundary and, since $\mu = \text{constant}$, that $B_\theta^{m,m}$ and $B_\phi^{m,m}$ are also continuous. Equating (4.10a, b or c) and (4.11a, b or c)

$$\frac{n(m+1)}{r_0} R_n(k, r_0) a_n^m = -\mathcal{A}_n^m \quad (4.12a)$$

$$\frac{1}{r_0} \left[\frac{d(rR_n)}{dr} \right]_{k, r_0} a_n^m = -\mathcal{B}_n^m \quad (4.12b)$$

Using (3.3a, b) we have

$$\frac{J_n^m}{E_n^m} = \frac{n E_n^m - H_n^m}{(m+1) E_n^m + H_n^m} = \left\{ \frac{n \frac{d(\rho R_n)}{d\rho} - n(m+1) R_n}{(m+1) \frac{d(\rho R_n)}{d\rho} + n R_n} \right\}_{\rho=a}$$

In the above equation, we have assumed that the boundary of the conducting earth, $r = r_0$, is the same as the surface where the magnetic field is observed, $r = a$. If, instead, the field is observed at $a > r_0$, going from r_0 to a , J_n^m decreases by the factor $(a/r_0)^{-m-1}$ and E_n^m increases by the factor $(a/r_0)^m$. The net result is that the observed amplitude ratio at $r = a$ has decreased from the ratio at $r = r_0$ by a factor $(r_0/a)^{2m+1} = g^{2m+1}$. This ratio

$$S_n(a) = \frac{n}{m+1} g^{2m+1} \left\{ \frac{\frac{d(\rho R_n)}{d\rho} - (m+1) R_n}{\frac{d(\rho R_n)}{d\rho} + n R_n} \right\}_{\rho=a} \quad (4.13)$$

depends on n , but not on m . Since it contains no j imaginaries,

J_n^m and E_n^m are in the same angular phase.

The Solution for a Uniformly Conducting Earth

For a uniformly conducting earth

$$\frac{d(\rho R_n)}{d\rho} = R_n + kr R_n' = j_n^m + kr j_n^{m'}$$

where the prime denotes the derivative with respect to the whole argument, kr .

$$S_n(a) = \frac{n}{m+1} g^{2m+1} \left\{ \frac{kr \frac{j_n^{m'}}{j_n^m} - m}{kr \frac{j_n^{m'}}{j_n^m} + (m+1)} \right\}_{r_0}$$

Using the identities

$$j'_m = \frac{1}{2m+1} [m j_{m-1} - (m+1) j_{m+1}]$$

$$j_m = \frac{kr}{2m+1} [j_{m-1} + j_{m+1}]$$

we find that

$$kr \frac{j'_m}{j_m} = \frac{m j_{m-1} - (m+1) j_{m+1}}{j_{m-1} + j_{m+1}}$$

and therefore

$$S_m(a) = -\frac{m}{m+1} g^{2m+1} \frac{j_{m+1}(kr_0)}{j_{m-1}(kr_0)}$$

For a large kr_0

$$S_m(a) \rightarrow -\frac{m}{m+1} g^{2m+1} \frac{\cos(kr_0 - \frac{m+2}{2}\pi)}{\cos(kr_0 - \frac{m}{2}\pi)} = \frac{m}{m+1} g^{2m+1} \quad (4.14)$$

This is the ratio for a superconductor. We may easily verify this independently by noticing that at $g = 1$ on the surface of the superconductor, the radial magnetic field must vanish. Consequently

$$B_r^{nm}(r_0) = 0$$

$$\mathcal{H}_r^m = 0 = m E_m^m - (m+1) \mathcal{J}_m^m$$

$$S_m(r_0) = \frac{m}{m+1}$$

For a small kr_0 , using $j_m(kr_0) \approx (2kr_0)^m \frac{m!}{(2m+1)!}$

$$S_m(a) \rightarrow -g^{2m+1} \frac{2k^2 r_0^2 m}{2m+1} = g^{2m+1} \frac{2im\omega\mu_0 r_0^2}{2m+1}$$

Going from a superconductor to a poor conductor, the absolute value of the ratio decreases and the corresponding phase lead changes from 0 to $\pi/2$.

The Solution for the Lahiri and Price Model

The Lahiri and Price distribution ratio, $S_m(a)$, is derived as follows:

$$Z_p(z) = \begin{cases} I_p(z) & \alpha < 2 \\ K_p(z) & \alpha > 2 \end{cases}$$

$$R_m = \rho^{-\frac{1}{2}} Z_p(z) \quad \rho R_m = \rho^{\frac{1}{2}} Z_p(z)$$

$$\frac{d[\rho R_m]}{d\rho} = \rho^{\frac{1}{2}} Z_p'(z) \frac{dz}{d\rho} - \frac{1}{2} \rho^{-\frac{1}{2}} Z_p(z)$$

$$\frac{dz}{d\rho} = \frac{2-\alpha}{2} z_0 \rho^{-\alpha/2} = \frac{2m+1}{\rho} z_0 \rho^{-\alpha/2}$$

$$\left[\frac{d(\rho R_m)}{d\rho} \right]_{\rho=z_0} = \frac{(2m+1)z_0 Z_p'(z_0)}{2\rho Z_p(z_0)} - \frac{1}{2} = \frac{1}{2} \left[(2m+1) \frac{Z_{p-1}(z_0) + Z_{p+1}(z_0)}{Z_{p-1}(z_0) - Z_{p+1}(z_0)} - 1 \right] = \frac{m Z_{p-1}(z_0) + (m+1) Z_{p+1}(z_0)}{Z_{p-1}(z_0) - Z_{p+1}(z_0)}$$

(See Hildebrand, Chapter 4, Equations 105a - 106b). Finally, substituting the above into (4.13) we find

$$S_m(a) = \frac{m}{m+1} g^{2m+1} \frac{Z_{p+1}(z_0)}{Z_{p-1}(z_0)}$$

For $\alpha < 2$

$$S_m(a) = \frac{m}{m+1} g^{2m+1} \frac{I_{p+1}(z_0)}{I_{p-1}(z_0)} = \frac{m}{m+1} g^{2m+1} \frac{I_{\nu+1}(z_0)}{I_{\nu-1}(z_0)}$$

For $\alpha > 2$

$$S_m(a) = \frac{m}{m+1} g^{2m+1} \frac{K_{p+1}(z_0)}{K_{p-1}(z_0)} = \frac{m}{m+1} g^{2m+1} \frac{K_{-\nu}(z_0)}{K_{-1-\nu}(z_0)} = \frac{m}{m+1} g^{2m+1} \frac{K_{\nu+1}(z_0)}{K_{\nu-1}(z_0)}$$

Of the many special cases one of the most useful occurs when z_0 is small and $\alpha > 2m+3$ and, thus, $\nu < 1$. Then

$$\frac{K_{\nu-1}(z_0)}{K_{\nu+1}(z_0)} = \frac{K_{1-\nu}(z_0)}{K_{1+\nu}(z_0)} \rightarrow \frac{\Gamma(1-\nu)}{\Gamma(1+\nu)} \left(\frac{z_0}{2}\right)^{2\nu} =$$

$$\frac{\Gamma(1-\nu)}{\Gamma(1+\nu)} \left(\frac{r_0}{\alpha-2}\right)^{2\nu} (-k_0^2)^\nu = \frac{\Gamma(1-\nu)}{\Gamma(1+\nu)} \left(\frac{r_0}{\alpha-2}\right)^{2\nu} (i\omega\mu\sigma_0)^\nu$$

and

$$S_m(a) = \frac{m}{m+1} g^{2m+1} \frac{\Gamma(1-\nu)}{\Gamma(1+\nu)} \left[\left(\frac{r_0}{\alpha-2}\right)^2 \omega\mu\sigma_0 \right]^\nu \left[\cos \frac{\nu\pi}{2} + i \sin \frac{\nu\pi}{2} \right]$$

The Thin Conducting Shell

The thin conducting spherical shell of constant conductivity and bounded on both surfaces by insulators was first treated by Chapman and Whitehead (1923) in a manner similar to that given below. Unlike this treatment, however, they made no use of the now well-known properties of the spherical Bessel functions. In Chapter V, an alternative approach to this problem is given.

Let the shell have a thickness δ with its outer surface at $r = a$ and its inner surface at $r = a - \delta$. The conductivity times the thickness, $\sigma\delta$, is taken as some non-zero quantity which remains constant as we make the shell infinitesimally thin while, at the same time, making the conductivity infinitely large. Symbolically,

$$\sigma\delta = \text{constant}$$

$$\sigma \rightarrow \infty$$

$$\delta \rightarrow 0$$

$$\text{Since } k^2 = -i\omega\mu\sigma$$

$$k^2 a\delta = \text{constant}$$

$$ka \rightarrow \infty$$

$$k\delta \rightarrow 0$$

For the n, m harmonic, above the shell we have the potential

$$a \left[\mathcal{E}_n^m \rho^n + \mathcal{L}_n^m \rho^{-n-1} \right] Y_n^m e^{i\omega t}$$

On the underside of the shell, ignoring δ with respect to a , we have the potential

$$a \left[(\mathcal{E}_n^m - \Delta \mathcal{E}_n^m) \rho^n + (\mathcal{L}_n^m - \Delta \mathcal{L}_n^m) \rho^{-n-1} \right] Y_n^m e^{i\omega t}$$

$\Delta \mathcal{E}_n^m, \Delta \mathcal{L}_n^m$ are the unknowns sought.

In the shell the solution is the same as that for the uniformly conducting sphere, but without the condition that the solution remain finite at the origin. The solution, then, is a linear combination of $j_n(kr)$ and $n_n(kr)$ times $Y_n^m e^{i\omega t}$.

Let

$$a_n^m R_n = (C_{n,1}^m j_n(kr) + C_{n,2}^m n_n(kr))$$

With r , replaced by a , the boundary conditions (4.12a, b) become

$$\frac{n(n+1)}{a} \left[C_{n,1}^m j_n(ka) + C_{n,2}^m n_n(ka) \right] = -n \mathcal{E}_n^m + (n+1) \mathcal{L}_n^m \quad (4.15a)$$

$$\frac{1}{a} \left[\frac{d}{dr} (C_{n,1}^m r j_n(kr) + C_{n,2}^m r n_n(kr)) \right]_a = -\mathcal{E}_n^m - \mathcal{L}_n^m \quad (4.15b)$$

For $ka \gg 1$

$$j_n(ka) = \frac{1}{ka} \cos(ka - \frac{n+1}{2}\pi) = n_n'(ka) \quad (4.16a)$$

$$n_n(ka) = \frac{1}{ka} \sin(ka - \frac{n+1}{2}\pi) = -j_n'(ka) \quad (4.16b)$$

$$\left[\frac{d(r j_n(kr))}{dr} \right]_a = j_n(ka) + ka j_n'(ka) = j_n(ka) - ka n_n(ka)$$

$$\left[\frac{d(r n_n(kr))}{dr} \right]_a = n_n(ka) + ka n_n'(ka) = n_n(ka) + ka j_n(ka)$$

and (4.15a, b) become

$$C_{m,1}^m j_m(ka) + C_{m,2}^m n_m(ka) = -a \left(\frac{E_m^m}{m+1} - \frac{L_m^m}{m} \right) \quad (4.17a)$$

$$-C_{m,1}^m n_m(ka) + C_{m,2}^m j_m(ka) = -\frac{1}{k} \left(\frac{m}{m+1} E_m^m + \frac{m+1}{m} L_m^m \right) \quad (4.17b)$$

Making use of the Wronskian

$$j_m^2(ka) + n_m^2(ka) = \frac{1}{(ka)^2} \quad (4.18)$$

we may now solve for $C_{m,1}^m$ and $C_{m,2}^m$.

$$C_{m,1}^m = ka^2 \left[n_m(ka) \left(\frac{m}{m+1} E_m^m + \frac{m+1}{m} L_m^m \right) - ka j_m(ka) \left(\frac{E_m^m}{m+1} - \frac{L_m^m}{m} \right) \right] \quad (4.19a)$$

$$C_{m,2}^m = ka^2 \left[-j_m(ka) \left(\frac{m}{m+1} E_m^m + \frac{m+1}{m} L_m^m \right) - ka n_m(ka) \left(\frac{E_m^m}{m+1} - \frac{L_m^m}{m} \right) \right] \quad (4.19b)$$

Using (4.16a, b) in a first order Taylor series expansion of $j_m(k(a-\delta))$ and $n_m(k(a-\delta))$, we have

$$j_m(k(a-\delta)) \approx j_m(ka) + k\delta n_m(ka) \quad (4.20a)$$

$$n_m(k(a-\delta)) \approx n_m(ka) - k\delta j_m(ka) \quad (4.20b)$$

Corresponding to (4.17a, b), we have the inner boundary conditions which are, to the first order

$$C_{m,1}^m j_m(ka) + C_{m,2}^m n_m(ka) = -a \left(\frac{E_m^m - \Delta E_m^m}{m+1} - \frac{L_m^m - \Delta L_m^m}{m} \right) \quad (4.21a)$$

$$-C_{m,1}^m (n_m(ka) - k\delta j_m(ka)) + C_{m,2}^m (j_m(ka) + k\delta n_m(ka)) = -\frac{1}{k} \left(\frac{m}{m+1} (E_m^m - \Delta E_m^m) + \frac{m+1}{m} (L_m^m - \Delta L_m^m) \right) \quad (4.21b)$$

Subtracting (4.17a) from (4.21a) gives

$$\frac{\Delta E_n^m}{m+1} - \frac{\Delta d_n^m}{n} = 0 \quad (4.22a)$$

which is simply the condition that $B_r^{m,m}$ is continuous across both boundaries. Subtracting (4.17b) from (4.21b) gives

$$\frac{m\Delta E_n^m}{m+1} + \frac{(m+1)\Delta d_n^m}{n} = C_{m,1}^m k^2 \delta j_m(ka) + C_{m,2}^m k^2 \delta n_m(ka) \quad (4.22b)$$

Finally, combining (4.22a, b, 4.19a, b) and (4.18), we find

$$\frac{\Delta E_n^m}{m+1} = \frac{\Delta d_n^m}{n} = -\frac{k^2 a \delta}{2m+1} \left(\frac{E_n^m}{m+1} - \frac{d_n^m}{n} \right) \quad (4.23a)$$

$$m\Delta E_n^m = (m+1)\Delta d_n^m = \frac{i\omega\mu_0 \delta a}{2m+1} (mE_n^m - (m+1)d_n^m) = \frac{i\omega\mu_0 \delta a}{2m+1} H_n^m \quad (4.23b)$$

$$m(m+1)\Delta d_n^m = i\omega\mu_0 \delta a H_n^m = -k^2 a \delta H_n^m \quad (4.23c)$$

The Thin Insulating Shell

Let us suppose that the potential (3.1), is to be developed by analytic continuation about $r = a$, where a is now considered as a variable describing the potential reference level. Accordingly, the terms,

$$a E_n^m \rho^n = E_n^m \frac{r^n}{a^{n-1}}$$

and

$$a d_n^m \rho^{-n-1} = d_n^m \frac{r^{-n-1}}{a^{-n-2}}$$

must vary only with r , where the potential is evaluated, and not with a , which is an arbitrary reference level. Thus

$$\begin{aligned} E_n^m &\propto a^{m-1} \\ \mathcal{L}_n^m &\propto a^{-m-2} \end{aligned}$$

For a small Δa ,

$$\frac{\Delta E_n^m}{E_n^m} = (m-1) \frac{\Delta a}{a} \tag{4.24a}$$

$$\frac{\Delta \mathcal{L}_n^m}{\mathcal{L}_n^m} = -(m+2) \frac{\Delta a}{a} \tag{4.24b}$$

Solution by Simultaneous First Order Differential Equations

Now consider a sequence of alternating thin conducting and insulating spherical shells. We wish to find how E_n^m and \mathcal{L}_n^m , evaluated in the insulators, change with a . It is sufficient to consider the change across one pair of shells as from 1 to 3 in

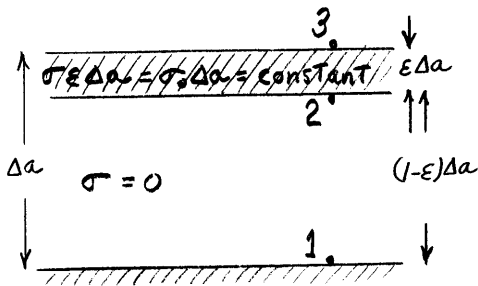


FIGURE 4.1

Figure 4.1. Let $\sigma = \sigma_0/\epsilon$ so that the conductivity times the thickness of the conducting shell

$$\sigma \epsilon \Delta a = \sigma_0 \Delta a$$

is constant. By (4.24 a, b), the change in going from 1 to 2 is

$$\Delta_1 E_n^m = (m-1) \frac{(1-\epsilon)\Delta a}{a} E_n^m$$

$$\Delta_1 \mathcal{L}_n^m = -(m+2) \frac{(1-\epsilon)\Delta a}{a} \mathcal{L}_n^m$$

If $\epsilon \Delta a$ is made small (4.23) may be used in going from 2 to 3, with σd replaced by $\sigma_0 \Delta a$.

$$m \Delta_2 E_n^m = (n+1) \Delta_2 \mathcal{L}_n^m = -\frac{k^2 a \Delta a}{2m+1} [m(E_n^m + \Delta_1 E_n^m) - (n+1)(\mathcal{L}_n^m + \Delta_1 \mathcal{L}_n^m)]$$

Letting $\epsilon \rightarrow 0$

$$\frac{\Delta E_n^m}{\Delta a} = \frac{\Delta_1 E_n^m + \Delta_2 E_n^m}{\Delta a} = \frac{(m-1)}{a} E_n^m - \frac{k^2 a}{n(2n+1)} \left(m(E_n^m + \Delta_1 E_n^m) - (m+1)(L_n^m + \Delta_1 L_n^m) \right)$$

$$\frac{\Delta L_n^m}{\Delta a} = \frac{\Delta_1 L_n^m + \Delta_2 L_n^m}{\Delta a} = -\frac{(m+2)}{a} L_n^m - \frac{k^2 a}{(m+1)(2m+1)} \left(m(E_n^m + \Delta_1 E_n^m) - (m+1)(L_n^m + \Delta_1 L_n^m) \right)$$

Now, letting $\Delta_1 E_n^m, \Delta_2 E_n^m, \Delta_1 L_n^m, \Delta_2 L_n^m \rightarrow 0$ as $\Delta a \rightarrow 0$ replacing a by r , we have

$$\frac{dE_n^m}{dr} = -\frac{k^2 r}{n(2n+1)} \left(mE_n^m - (m+1)L_n^m \right) + \frac{(m-1)E_n^m}{r} \quad (4.25a)$$

$$\frac{dL_n^m}{dr} = -\frac{k^2 r}{(m+1)(2m+1)} \left(mE_n^m - (m+1)L_n^m \right) - \frac{(m+2)L_n^m}{r} \quad (4.25b)$$

It has been shown earlier in this chapter that there are no radial currents so, naturally, the insulating shells can have no effect on these currents. The horizontal currents are also unaffected because the effective horizontal conductivity is unchanged. Therefore (4.25a, b) are a pair of first order differential equations in the external and internal components of the Y_n^m term of an effective potential for conductivity distributions which depend only on r . If we were interested in the flux density vector as a function of depth rather than the nature of the field sources, the following pair of equations, derived from (4.25a, b) using (3.3a, b) would be more direct

$$\frac{dB_n^m}{dr} = -\frac{k^2 r}{n(n+1)} Z_n^m + \frac{Z_n^m - B_n^m}{r} \quad (4.26a)$$

$$\frac{dZ_n^m}{dr} = \frac{n(n+1)B_n^m - 2Z_n^m}{r} \quad (4.26b)$$

It is shown in Chapter V that these equations can be derived directly from Maxwell's equations with the same condition as used above: that there are no radial currents.

It is easy to verify that either pair of first order differential equations (4.25a, b) or (4.26a, b) is equivalent to the second order differential equation (4.6). Since each pair is simply a linear recombination of the other, we shall consider only (4.26a, b). By (4.12a), at any r , $r^2 \mathcal{H}_m^m$ should satisfy the same differential equation in r as R_m . Differentiating (4.26a, b) we have

$$\frac{d}{dr}(r \mathcal{H}_m^m) = r \frac{d \mathcal{H}_m^m}{dr} + \mathcal{H}_m^m = m(m+1) \mathcal{B}_m^m - \mathcal{H}_m^m \quad (4.27)$$

$$\begin{aligned} \frac{d^2}{dr^2}(r \mathcal{H}_m^m) &= m(m+1) \frac{d \mathcal{B}_m^m}{dr} - \frac{d \mathcal{H}_m^m}{dr} = \\ &= -k^2 r \mathcal{H}_m^m + m(m+1) \frac{\mathcal{H}_m^m}{r} - \frac{2m(m+1) \mathcal{B}_m^m}{r} + \frac{2 \mathcal{H}_m^m}{r} \end{aligned} \quad (4.28)$$

We may eliminate \mathcal{B}_m^m between (4.27) and (4.28) by multiplying the former by 2 and the latter by r and summing

$$\begin{aligned} r \frac{d^2}{dr^2}(r \mathcal{H}_m^m) + 2 \frac{d}{dr}(r \mathcal{H}_m^m) &= -k^2 r \mathcal{H}_m^m + m(m+1) \mathcal{H}_m^m \\ r^2 \frac{d^2}{dr^2}(r \mathcal{H}_m^m) + 2r \frac{d}{dr}(r \mathcal{H}_m^m) + [k^2 r^2 - m(m+1)](r \mathcal{H}_m^m) &= 0 \end{aligned}$$

which is the same as (4.6). Thus we have shown that $r \mathcal{H}_m^m$ does satisfy the same differential equation as R_m . It follows that $r^2 \mathcal{H}_m^m$ satisfies the same differential equation as $r R_m$ and $\frac{1}{r} \frac{d}{dr}(r^2 \mathcal{H}_m^m)$ satisfies the same differential equation as $\frac{1}{r} \frac{d}{dr}(r R_m)$. But we have

$$\frac{1}{r} \frac{d}{dr}(r^2 \mathcal{H}_m^m) = 2 \mathcal{H}_m^m + r \frac{d \mathcal{H}_m^m}{dr} = m(m+1) \mathcal{B}_m^m$$

and, therefore, in agreement with (4.12b), B_n^m satisfies the same differential equation as $\frac{1}{r} \frac{d}{dr}(rR_n)$.

For a thin conducting shell, (4.26a, b) become

$$\frac{dB_n^m}{dr} = -\frac{k^2 r}{n(n+1)} H_n^m \quad \frac{dH_n^m}{dr} = 0$$

Therefore

$$\begin{aligned} \frac{d^2 B_n^m}{dr^2} &= -\frac{k^2}{n(n+1)} H_n^m \\ \frac{d^s B_n^m}{dr^s} &= 0 \quad s \geq 3 \end{aligned}$$

By Taylor series expansion

$$B_n^m(r+\delta) = B_n^m(r) - \frac{k^2 r \delta}{n(n+1)} H_n^m(r) \left(1 + \frac{\delta}{r}\right)$$

Since δ/r is small compared with 1

$$\Delta B_n^m = -\frac{k^2 r \delta}{n(n+1)} H_n^m(r) \quad (4.29)$$

is linear in $k^2 \delta$ for a thin conducting shell.

A Differential Equation for S_n

From (4.25a, b) we may derive a first order, but nonlinear, differential equation for the complex ratio $S_n = \frac{L_n^m}{E_n^m}$. Earlier, we derived formulas for $S_n(a)$ for special conductivity distributions where $a \geq r_0$, and r_0 is the outer limit of the conducting earth.

Now, for any r

$$\begin{aligned} \frac{dS_n}{dr} &= \frac{d}{dr} \left(\frac{L_n^m}{E_n^m} \right) = \frac{1}{E_n^m} \left[\frac{dL_n^m}{dr} - \frac{L_n^m}{E_n^m} \frac{dE_n^m}{dr} \right] = \\ \frac{1}{E_n^m} &\left[\frac{-k^2 r}{(n+1)(2n+1)} (nE_n^m - (n+1)L_n^m) - \frac{(n+2)}{r} L_n^m + \frac{k^2 r}{n(2n+1)} \frac{L_n^m}{E_n^m} (nE_n^m - (n+1)L_n^m) - \frac{(n-1)}{r} L_n^m \right] = \\ &\frac{1}{E_n^m} \left[-\frac{k^2 r}{2n+1} \left(\frac{nE_n^m}{n+1} - 2L_n^m + \frac{(n+1)}{n} \left(\frac{L_n^m}{E_n^m} \right)^2 \right) - \frac{(2n+1)}{r} L_n^m \right] \end{aligned}$$

$$\frac{dS_m}{dr} = - \frac{k^2 r (m+1)}{(2m+1)n} \left(S_m - \frac{n}{m+1} \right)^2 - \frac{2m+1}{r} S_m \quad (4.30)$$

For a thin conducting shell $S_m + \Delta S_m$ may be found by using (4.29)

$$\begin{aligned} S_m + \Delta S_m &= \frac{I_m^m + \Delta I_m^m}{E_m^m + \Delta E_m^m} = \frac{E_m^m S_m + \frac{n}{2m+1} \Delta E_m^m}{E_m^m + \frac{m+1}{2m+1} \Delta E_m^m} = \frac{E_m^m S_m - \frac{k^2 r d}{(m+1)(2m+1)} \mathcal{H}_n^m}{E_m^m - \frac{k^2 r d}{n(2m+1)} \mathcal{H}_n^m} = \\ &= \frac{S_m - \frac{k^2 r d}{(m+1)(2m+1)} (n - (m+1) S_m)}{1 - \frac{k^2 r d}{n(2m+1)} (n - (m+1) S_m)} \\ S_m + \Delta S_m &= \left(\frac{n}{m+1} \right) \frac{(2m+1) S_m + k^2 r d \left(S_m - \frac{n}{m+1} \right)}{(2m+1) \frac{n}{m+1} + k^2 r d \left(S_m - \frac{n}{m+1} \right)} \quad (4.31) \end{aligned}$$

Interpretation of Equation 4.30

Except near $S_m = 0$ or $S_m = n/(n+1)$, the relative importance of the two terms on the right hand side of (4.30) is determined by the magnitude of $\left(\frac{kr}{2m+1} \right)^2$. When this is a large number the first term predominates. When r is taken as the radius of the earth, the values of σ necessary in order that $kr = ka = \frac{1}{10}, 100$ are given in Table 4.1 for 24 hour, semiannual and eleven year periods.

Table 4.1 Conductivities in mhos/meter

Period	24 hours	6 months	11 years
For $ka = 100$	0.3	50	1100 - High conductivity
For $ka = \frac{1}{10}$	0.0003	0.05	1.1 - Low conductivity

Let us consider two extreme cases of (4.30). When $\left(\frac{kr}{2m+1}\right)^2$ is large and $\left(S_m - \frac{m}{m+1}\right)$ is not small the equation becomes

$$\frac{dS_m}{dr} = \frac{i\omega\mu\sigma r}{(2m+1)} \frac{(m+1)}{m} \left(S_m - \frac{m}{m+1}\right)^2 \quad (4.32)$$

On the other hand, when $\left(\frac{kr}{2m+1}\right)^2$ is small and S_m is not small, (4.30) becomes

$$\frac{dS_m}{dr} = -\frac{2m+1}{r} S_m \quad (4.33)$$

In (4.32), the term $\frac{\omega\mu\sigma r(m+1)}{(2m+1)m}$ only affects the rate at which S_m travels along any of the characteristic curves which are solutions of

$$\frac{dS_m}{dr} = i \left(S_m - \frac{m}{m+1}\right)^2$$

In Figure 4.2, let S_m be in the direction $\exp i(\pi - \alpha_m)$ from $\frac{m}{m+1}$ and let P be a point on the real axis such that S_m is in the direction $\exp i(\pi - 2\alpha_m)$ from P . The direction from the origin to $\left(S_m - \frac{m}{m+1}\right)$ is $\exp i(\pi - \alpha_m)$; to $\left(S_m - \frac{m}{m+1}\right)^2$ the direction is $\exp 2i(\pi - \alpha_m) = \exp -2i\alpha_m$; and to $\left(S_m - \frac{m}{m+1}\right)^2$ it is $\exp i\left(\frac{\pi}{2} - 2\alpha_m\right)$. Thus $\frac{dS_m}{dr}$ moves in the direction $\exp i\left(\frac{\pi}{2} - 2\alpha_m\right)$ from S_m and is perpendicular to the line $P-S_m$. The characteristic curves are, therefore, circles whose centers are on the real axis and about which S_m travels in a clockwise manner as r increases. When $\alpha_m = \frac{\pi}{2}$, the derivative has no real part so it must be crossing the real axis. This can only happen at $\frac{m}{m+1}$, so all the characteristic circles must pass through this point. However, as $\left(S_m - \frac{m}{m+1}\right) \rightarrow 0$, $\frac{dS_m}{dr} \rightarrow 0$ so S_m can never cross the real axis from the positive imaginary to the negative imaginary side. Figure 4.3 is a plot of the characteristic paths that S_m may take as r increases for this case.

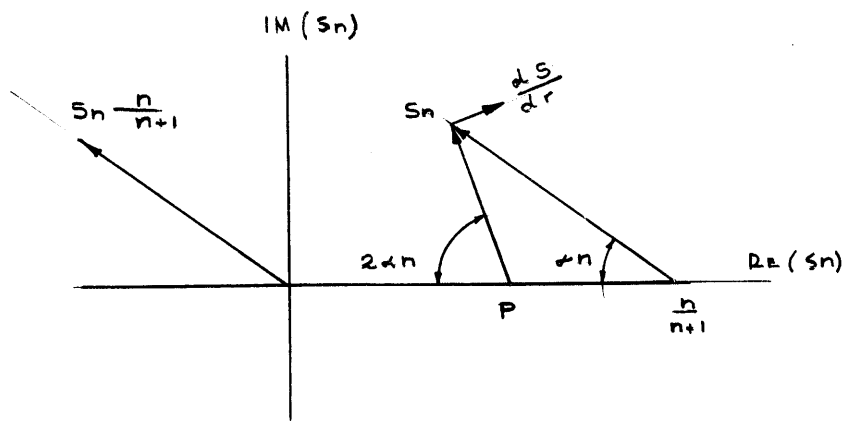


FIGURE 4.2

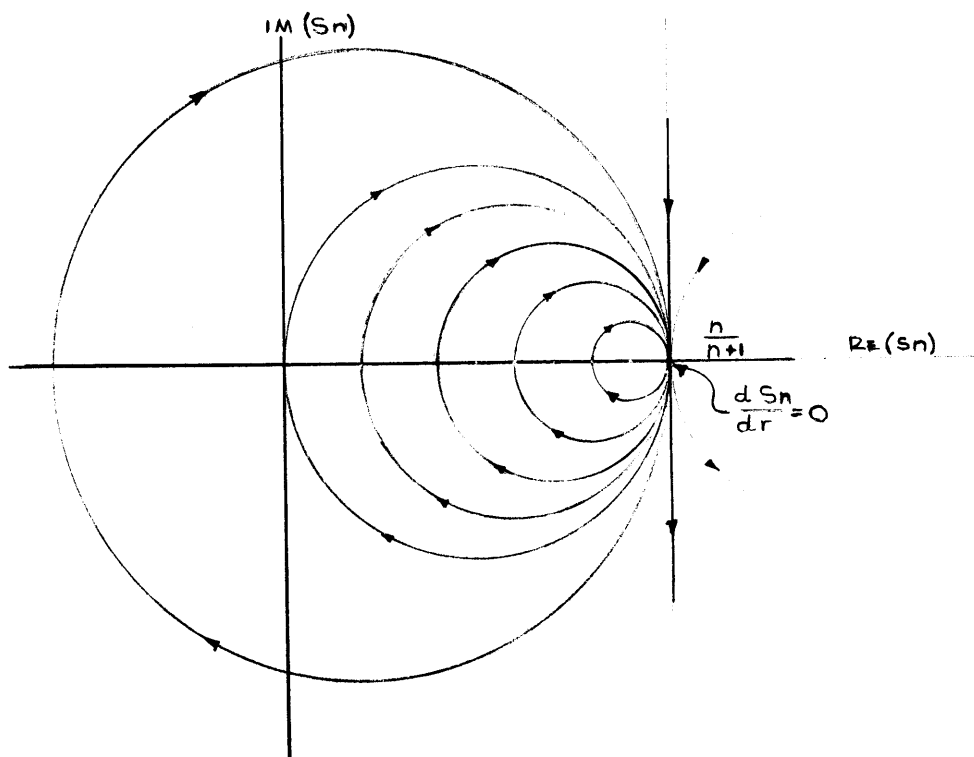


FIGURE 4.3

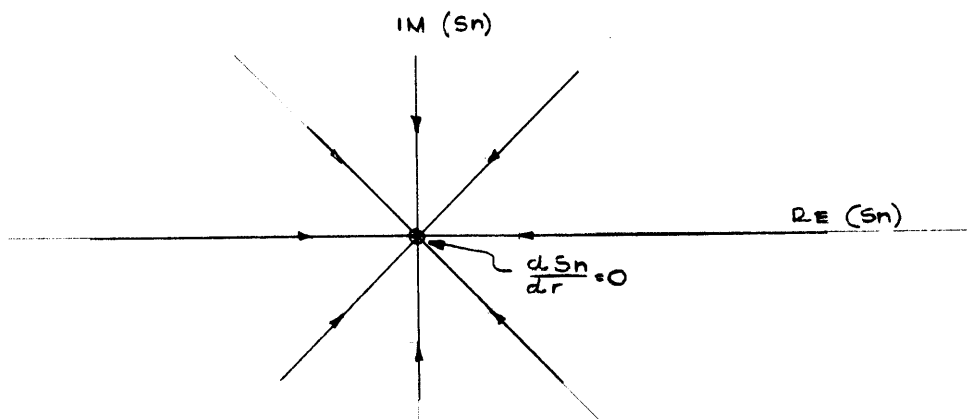


FIGURE 4.4

In (4.33), as r increases, S_n decreases along a straight line toward the origin, and, as $S_n \rightarrow 0$, $\frac{dS_n}{dr} \rightarrow 0$. These characteristic paths are shown in Figure 4.4.

In the general case which is governed by (4.30), $\frac{dS_n}{dr}$ travels in a direction which is a combination of the directions from the two extreme cases.

It has already been shown (see 4.14) that on the surface of a superconducting sphere S_n lies on the real axis and has the value

$$S_m = \frac{m}{m+1}$$

It is obvious that when evaluated on the surface of a uniform insulator S_n has the value

$$S_m = 0$$

Any possible radial conductivity distribution can be synthesized by using a small superconducting or insulating sphere as a nucleus and surrounding the nucleus by concentric shells of arbitrary conductivities. Starting at $S_m = 0$ and $S_m = \frac{m}{m+1}$, and referring to Figures 4.3 and 4.4 it is seen that, whatever the conductivity structure, S_n is restricted to a semicircular region in the first quadrant of the complex plane. This region is depicted in Figure 4.5. Mathematically, the conditions that S_n must satisfy are as follows:

$$2 \left| 2 S_n - \frac{m}{m+1} \right| \leq \frac{m}{m+1} \quad (4.34a)$$

$$\text{Im}(S_n) \geq 0 \quad (4.34b)$$

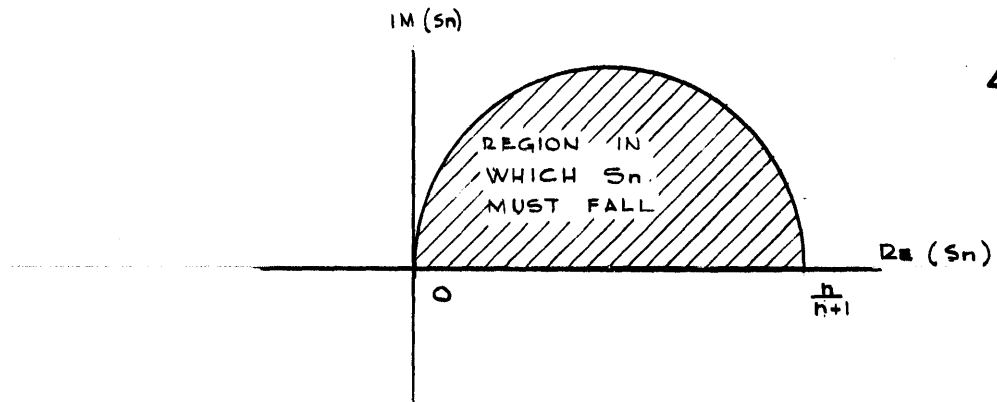


FIGURE 4.5

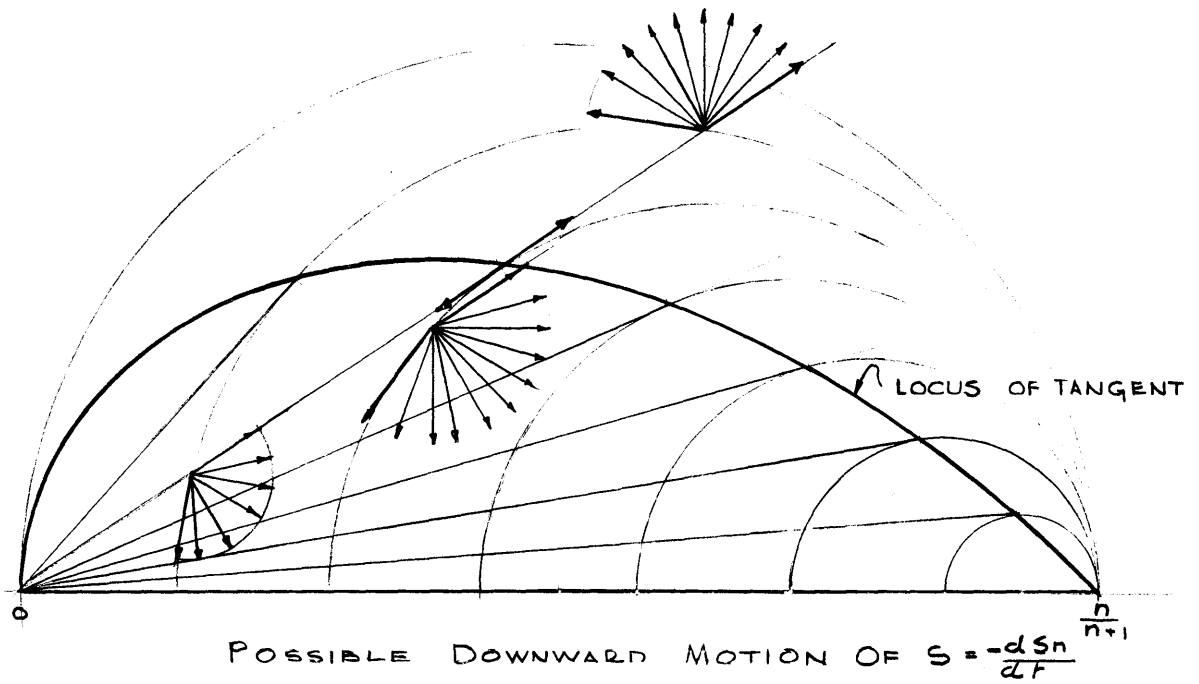
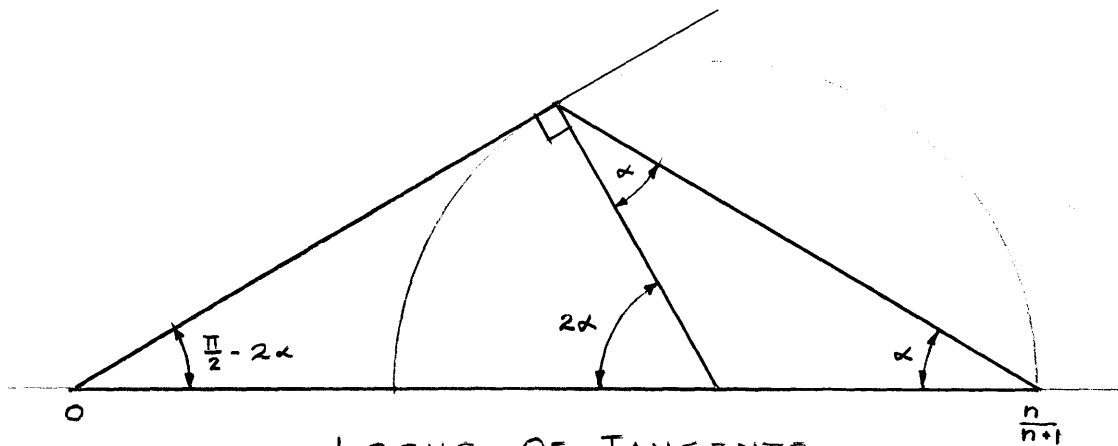


FIGURE 4.6



LOCUS OF TANGENTS

FIGURE 4.7

Since at the nucleus $\text{Im}_j(S_m) = 0$, by (4.30) the j -imaginary part of S_m is always zero. Thus E_m^m and I_m^m must have the same j^m phase.

Equation (4.30) may be solved numerically, working downwards from the surface of the earth where S_m is known. The conductivity as a function of depth may be arbitrarily chosen until S_m leaves the region defined by (4.34). From this point the path that S_m can take is uniquely specified and the corresponding conductivity distribution is also unique (except, of course, superconducting sphere cannot be discriminated from a superconducting shell). If S_m leaves the region across the real axis, the remaining earth consists of a superconducting sphere surrounded by an insulating shell; if it leaves across the semicircular border, the remaining earth consists of an insulating sphere covered by a thin highly conducting shell.

Possible Paths of S_m

Now let us examine the nature of the possible paths that S_m may take going downwards. By varying the conductivity we may alter the relative importance of either term on the right hand side of (4.30) so from any point, S_m may move in any direction which is a linear combination of these two terms. Where these terms move in parallel, that is, where the curves in Figures 4.3 and 4.4 are tangent, except for the sign, there is only one possible direction in which S_m may move. This locus of tangents is plotted in Figure 4.6. It is easily constructed, graphically, for it is the intersection of two straight lines passing through the origin and $\frac{m}{m+1}$.

Their slopes are related as shown in Figure 4.7 which is self-explanatory. As may be seen by examining Figure 4.6, below this curve the angular change of S_m about the origin is clockwise with increasing depth and above the curve this change is counter-clockwise. Anywhere below the locus of tangents it is possible to move directly toward $\frac{m}{m+1}$ and anywhere above it is possible to move directly away from $\frac{m}{m+1}$; it is impossible to move in either of these directions from a point exactly on the curve.

Suppose that $S_m(r)$ is known at $r = r_0$ and we assume that the conductivity increases with depth such that eventually S_m takes on the superconducting ratio

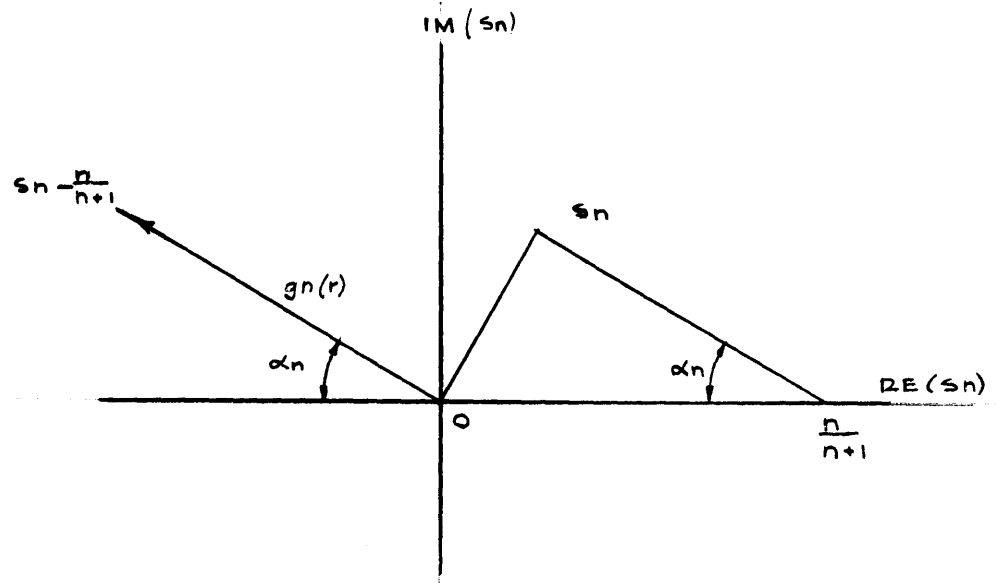
$$S_m = \frac{m}{m+1}$$

There are, of course, an infinite number of possible paths S_m may take as long as it stays inside the borders of the restricting semi-circle. If $S_m(r_0)$ falls below the locus of tangents, one possible path is the straight line between $S_m(r_0)$ and $\frac{m}{m+1}$. Let us examine the conductivity structure for this path.

The Straight Line Path

Let us replace $(S_m - \frac{m}{m+1})$ in (4.30) by $-g_m e^{-i\alpha_m}$ (see Figure 4.8) where $g_m = g_m(r)$ is a real function of r and the angle $\alpha_m = \text{constant}$. We seek the path for which $g_m(r)$ decreases from $g_m(r_0)$ to zero. We now have

$$\frac{d g_m}{d r} e^{-i\alpha_m} = -\frac{i\omega\mu\sigma r}{(2m+1)} \frac{(m+1)}{m} g_m^2 e^{-2i\alpha_m} = \frac{2m+1}{r} \left(g_m e^{-i\alpha_m} - \frac{1}{m+1} \right) \quad (4.35)$$



THE STRAIGHT LINE PATH
FIGURE 4.8

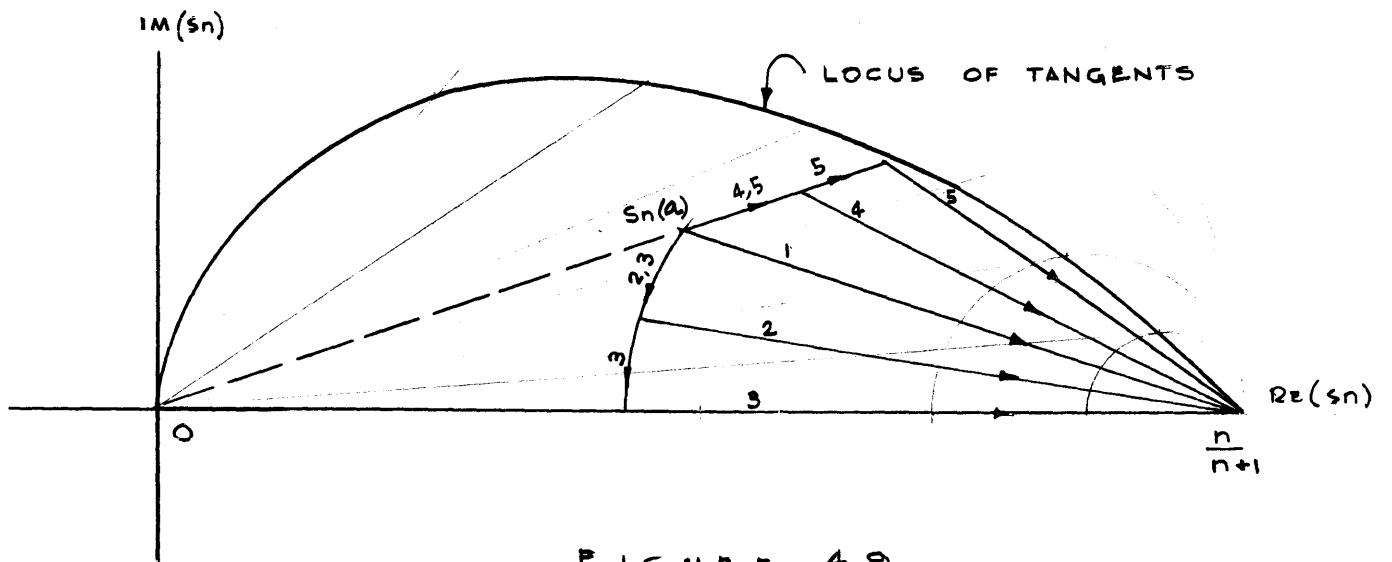


FIGURE 4.9

If we divide (4.35) by $g_m e^{-i\alpha_m}$ we have

$$\frac{dg_m}{dr} = -\frac{i\omega\mu\sigma r}{(2m+1)} \frac{(m+1)}{m} g_m e^{-i\alpha_m} - \frac{2m+1}{r} \left(1 - \frac{m}{m+1} \frac{e^{i\alpha_m}}{g_m}\right)$$

Now $\frac{dg_m}{dr}/g_m$ is real, so the imaginary part of the right hand side must be zero

$$-\frac{\omega\mu\sigma r g_m (m+1)}{(2m+1)m} \cos\alpha_m + \frac{(2m+1)m}{r g_m (m+1)} \sin\alpha_m$$

$$\sigma r^2 g_m^2 = \left[\frac{(2m+1)m}{m+1}\right]^2 \frac{\tan\alpha_m}{\omega\mu} \quad (4.36)$$

This equation tells us that as r and g_m decrease, σ must increase. If

now we take the imaginary part of (4.35) and substitute into it (4.36)

we get

$$-\frac{dg_m}{dr} \sin\alpha_m = -\frac{\omega\mu\sigma r g_m^2 (m+1)}{(2m+1)m} \cos 2\alpha_m + \frac{2m+1}{r} g_m \sin\alpha_m$$

$$\frac{dg_m}{dr} + \frac{2m+1}{r} g_m = \frac{(2m+1)m}{r(m+1)} \frac{\tan\alpha_m \cos 2\alpha_m}{\sin\alpha_m} = \frac{(2m+1)m}{r(m+1)} \frac{\cos 2\alpha_m}{\cos\alpha_m}$$

$$\frac{d}{dr} (r^{2m+1} g_m) = r^{2m} \frac{(2m+1)m}{m+1} \frac{\cos 2\alpha_m}{\cos\alpha_m}$$

$$g_m = \frac{m}{m+1} \frac{\cos 2\alpha_m}{\cos\alpha_m} + \frac{\text{constant}}{r^{2m+1}}$$

The constant is evaluated at $r = r_0$ and the equation becomes

$$\left[g_m(r) - \frac{m}{m+1} \frac{\cos 2\alpha_m}{\cos\alpha_m} \right] = \left(\frac{r_0}{r} \right)^{2m+1} \left[g_m(r_0) - \frac{m}{m+1} \frac{\cos 2\alpha_m}{\cos\alpha_m} \right] \quad (4.37)$$

When $\alpha_m = 0$, $S_m + g_m = \frac{m}{m+1}$ and this equation reduces to the integral of (4.33). At the superconductor, $g_m(r_s) = 0$ and

$$\left(\frac{r_s}{r_0}\right)^{2m+1} = 1 - g_m(r_0) \frac{(m+1) \cos \alpha_m}{m \cos 2\alpha_m} \quad (4.38)$$

Combining (4.36) and (4.37), the conductivity may be calculated as a function of $r > r_s$ where r_s is calculated from (4.38).

If $g_m(r_0)$ were originally chosen so that

$$g_m(r_0) = \frac{m}{m+1} \frac{\cos 2\alpha_m}{\cos \alpha_m} \quad (4.39)$$

then, by (4.37), $g_m(r) = g_m(r_0) = \text{constant}$. Since g_m cannot increase or decrease, S_n can neither move directly toward nor away from $n/(n+1)$ and it must, therefore, fall on the locus of tangents. Equation (4.39) describes the locus of tangents.

If, in (4.36), (4.37) and (4.38), the projection of g_m on the real axis, $g_m \cos \alpha_m$, is replaced by

$$h_m = g_m \cos \alpha_m$$

and we let

$$\delta_m = 2\alpha_m$$

the equations are modified into the following forms:

$$\sigma r^2 h_m^2 = \left[\frac{(2m+1)m}{m+1} \right]^2 \frac{\sin \delta_m}{2\omega\mu} \quad (4.40)$$

$$h_m = \frac{m}{m+1} \cos \delta_m \left[1 - \left(\frac{r_s}{r}\right)^{2m+1} \right] \quad (4.41)$$

$$\left(\frac{r_3}{r_0}\right)^{2m+1} = 1 - \frac{m+1}{m} \frac{h_m(r_0)}{\cos \delta_m} \quad (4.42)$$

Used in the order (4.42), (4.41), and (4.40), these equations are, computationally, slightly more simple for deriving the radial conductivity distribution of the straight line model.

Modifications of the Straight Line Path

In Figure 4.9, the path taken by S_m labelled as Number 1 is the straight line path investigated above. By first assuming that at the surface there is a thin highly conducting shell which modifies S_m according to (4.31) and then using the straight line method, we get alternate paths such as Numbers 2 and 3. Each of these paths corresponds, at one point, to a discontinuous decrease in conductivity with depth. Path 3, for instance, represents a thin highly conducting shell separated from a superconducting sphere by an insulator. On the other hand, before using the straight line method we may assume that the initial outer material has no conductivity; in this case S_m must be modified according to the method described in the paragraph preceding Equation 4.13. Numbers 4 and 5 are two paths corresponding to this assumption. Path 5 makes its abrupt turn just short of the locus of tangents. Here h_m remains relatively constant as r changes until r approaches zero, and, by (4.40), over the bulk of the conducting material for this model, $\sigma \propto r^{-2}$. Like Numbers 2 and 3, Paths 4 and 5 represent models with conductivity discontinuities, but unlike the others, the conductivity never decreases with depth.

CHAPTER V
INDUCTION EFFECTS OF THE IRREGULAR OCEANS

General

Chapter IV was concerned exclusively with a spherical earth whose conductivity is a function only of the distance from the origin. This sort of conductivity was necessary in order to separate the partial differential equation (4.4), and to prevent radial currents. Although there may be good reason to assume that the conductivity of the earth is relatively constant at any depth deep inside the earth, such is not the case near the surface, particularly because of the irregular distribution of the conducting oceans. Since the oceans are comparatively thin and are surrounded above, below and landward by relatively poor conductors, the problem resolves into the case of a thin shell, insulated inside and out, whose conductivity is a function of the colatitude ϑ , and east longitude, φ .

The Thin Shell Insulated on Both Sides

We shall start by writing down, from (3.2 a-c) the vector components of the n, m harmonic of the flux density.

$$B_{\vartheta}^{n, m} = -\mathcal{G}_n^m \frac{\partial Y_n^m}{\partial \vartheta} e^{i\omega t} \quad (5.1a)$$

$$B_{\varphi}^{n, m} = -jm\mathcal{G}_n^m \frac{Y_n^m}{\sin\vartheta} e^{i\omega t} \quad (5.1b)$$

$$B_r^{n, m} = -\mathcal{H}_n^m Y_n^m e^{i\omega t} \quad (5.1c)$$

From these, we derive

$$\frac{\partial B_{\theta}^{m,m}}{\partial r} = -\frac{d\mathcal{L}_m^m}{dr} \frac{\partial Y_m^m}{\partial \theta} e^{i\omega t} \quad (5.2a)$$

$$\frac{\partial B_{\varphi}^{m,m}}{\partial r} = -jm \frac{d\mathcal{L}_m^m}{dr} \frac{Y_m^m}{\sin\theta} e^{i\omega t} \quad (5.2b)$$

$$\frac{\partial B_r^{m,m}}{r\partial\theta} = -\frac{1}{r} \mathcal{H}_m^m \frac{\partial Y_m^m}{\partial\theta} e^{i\omega t} \quad (5.2c)$$

$$\frac{\partial B_r^{m,m}}{r\sin\theta\partial\varphi} = -\frac{jm}{r} \mathcal{H}_m^m \frac{Y_m^m}{\sin\theta} e^{i\omega t} \quad (5.2d)$$

Since $\vec{J} = \nabla \times \vec{H}$

$$\sum_{n=1}^{\infty} \sum_{m=0}^n \mu\sigma(\theta, \varphi) E_{\theta}^{n,m} = \sum_{n=1}^{\infty} \sum_{m=0}^n \text{curl}_{\theta} \vec{B}^{n,m} = \sum_{n=1}^{\infty} \sum_{m=0}^n \left[\frac{1}{r\sin\theta} \frac{\partial B_r^{n,m}}{\partial\varphi} - \frac{\partial B_{\varphi}^{n,m}}{\partial r} - \frac{B_{\varphi}^{n,m}}{r} \right]$$

Substituting from (5.1b), (5.2b,d) we have

$$\sum_{n=1}^{\infty} \sum_{m=0}^n \mu\sigma(\theta, \varphi) E_{\theta}^{n,m} = \sum_{n=1}^{\infty} \sum_{m=0}^n -\frac{jm}{r} \left[-r \frac{d\mathcal{L}_m^m}{dr} - \mathcal{L}_m^m + \mathcal{H}_m^m \right] \frac{Y_m^m}{\sin\theta} e^{i\omega t} \quad (5.3a)$$

Similarly, using (5.1a), (5.2a, c), we have

$$\begin{aligned} \sum_{n=1}^{\infty} \sum_{m=0}^n \mu\sigma(\theta, \varphi) E_{\varphi}^{n,m} &= \sum_{n=1}^{\infty} \sum_{m=0}^n \text{curl}_{\varphi} \vec{B}^{n,m} = \sum_{n=1}^{\infty} \sum_{m=0}^n \left[\frac{\partial B_{\theta}^{n,m}}{\partial r} + \frac{B_{\theta}^{n,m}}{r} - \frac{\partial B_r^{n,m}}{r\partial\theta} \right] = \\ &= \sum_{n=1}^{\infty} \sum_{m=0}^n \frac{1}{r} \left[-r \frac{d\mathcal{L}_m^m}{dr} - \mathcal{L}_m^m + \mathcal{H}_m^m \right] \frac{\partial Y_m^m}{\partial\theta} e^{i\omega t} \end{aligned} \quad (5.3b)$$

Let us, for the nonce, set

$$\left[-r \frac{d\mathcal{L}_m^m}{dr} - \mathcal{L}_m^m + \mathcal{H}_m^m \right] e^{i\omega t} = C_m^m$$

Then (5.3 a, b) can be rewritten as

$$\sum_{n=1}^{\infty} \sum_{m=0}^n \mu\sigma(\theta, \varphi) E_{\theta}^{n,m} = \sum_{n=1}^{\infty} \sum_{m=0}^n -\frac{1}{r\sin\theta} \frac{\partial Y_m^m}{\partial\varphi} C_m^m \quad (5.4a)$$

$$\sum_{n=1}^{\infty} \sum_{m=0}^n \mu\sigma(\theta, \varphi) E_{\varphi}^{n,m} = \sum_{n=1}^{\infty} \sum_{m=0}^n \frac{1}{r} \frac{\partial Y_m^m}{\partial\theta} C_m^m \quad (5.4b)$$

and therefore

$$\sum_{n=1}^{\infty} \sum_{m=0}^n \mu \sigma(\vartheta, \varphi) \operatorname{curl}_r \vec{E}^{n,m} = \sum_{n=1}^{\infty} \sum_{m=0}^n \left[\frac{1}{r^2 \sin^2 \vartheta} \frac{\partial}{\partial \vartheta} \left(\sin^2 \vartheta \frac{\partial Y_n^m}{\partial \vartheta} \right) + \frac{1}{r^2 \sin^2 \vartheta} \frac{\partial^2 Y_n^m}{\partial \varphi^2} \right] C_n^m =$$

$$\sum_{n=1}^{\infty} \sum_{m=0}^n C_n^m \nabla_{\vartheta, \varphi}^2 Y_n^m$$

where $\nabla_{\vartheta, \varphi}^2$ is the operator composed of the ϑ and φ partial derivatives of the Laplacian, ∇^2 , in spherical co-ordinates. Y_n^m is a surface harmonic so $r^m Y_n^m$ is a solid harmonic which is a solution of Laplace's equation,

$$\nabla^2 (r^m Y_n^m) = 0 = r^m \nabla_{\vartheta, \varphi}^2 Y_n^m + Y_n^m \frac{1}{r^2} \frac{d}{dr} (r^2 \frac{dr^m}{dr})$$

Therefore

$$r^2 \nabla_{\vartheta, \varphi}^2 Y_n^m = -m(m+1) Y_n^m$$

$$\sum_{n=1}^{\infty} \sum_{m=0}^n \mu \sigma(\vartheta, \varphi) \operatorname{curl}_r \vec{E}^{n,m} = \sum_{n=1}^{\infty} \sum_{m=0}^n -\frac{m(m+1)}{r^2} C_n^m Y_n^m = \sum_{n=1}^{\infty} \sum_{m=0}^n \frac{m(m+1)}{r} \left[r \frac{dB_n^m}{dr} + B_n^m - \mathcal{L}_n^m \right] Y_n^m e^{i\omega t}$$

$$\text{Since } \nabla \times \vec{E} = -i\omega \vec{B}$$

$$\sum_{n=1}^{\infty} \sum_{m=0}^n \mu \sigma(\vartheta, \varphi) \operatorname{curl}_r \vec{E}^{n,m} = \sum_{n=1}^{\infty} \sum_{m=0}^n -i\omega \mu \sigma(\vartheta, \varphi) B_r^{n,m} = \sum_{n=1}^{\infty} \sum_{m=0}^n i\omega \mu \sigma(\vartheta, \varphi) \mathcal{L}_n^m Y_n^m e^{i\omega t}$$

and, therefore

$$\sum_{n=1}^{\infty} \sum_{m=0}^n \frac{m(m+1)}{r^2} \left[r \frac{dB_n^m}{dr} + B_n^m - \mathcal{L}_n^m \right] Y_n^m = \sum_{n=1}^{\infty} \sum_{m=0}^n i\omega \mu \sigma(\vartheta, \varphi) \mathcal{L}_n^m Y_n^m$$

$$\sum_{n=1}^{\infty} \sum_{m=0}^n m(m+1) \frac{dB_n^m}{dr} Y_n^m = \sum_{n=1}^{\infty} \sum_{m=0}^n \left[-\mathcal{L}^2(\vartheta, \varphi) r \mathcal{L}_n^m + m(m+1) \frac{\mathcal{L}_n^m - B_n^m}{r} \right] Y_n^m \quad (5.5a)$$

If σ (or, equivalently, k^2) is constant with respect to ϑ and φ , respective n , m harmonics can be equated in the above equation making it just a restatement of (4.26a). Since (4.26b) doesn't contain σ , it still holds for the nonuniform shell. This may be shown by independently deriving it as follows

$$H_n^m = m E_n^m \rho^{n-1} - (m+1) d_n^m \rho^{-n-2}$$

$$\frac{dH_n^m}{dr} = \frac{n(n-1)}{r} E_n^m + \frac{(m+1)(m+2)}{r} d_n^m \quad \text{at } \rho=1$$

Therefore

$$\frac{dH_n^m}{dr} = \frac{n(n+1)E_n^m - 2H_n^m}{r}$$

Naturally this equation still holds when it is multiplied by either $m P_n^m$ or $(m+1) P_n^m$ and summed over n and m .

$$\sum_{n=1}^{\infty} \sum_{m=0}^n m \frac{dH_n^m}{dr} Y_n^m = \sum_{n=1}^{\infty} \sum_{m=0}^n m \left[\frac{n(n+1)E_n^m - 2H_n^m}{r} \right] Y_n^m \quad (5.5b)$$

$$\sum_{n=1}^{\infty} \sum_{m=0}^n (m+1) \frac{dH_n^m}{dr} Y_n^m = \sum_{n=1}^{\infty} \sum_{m=0}^n (m+1) \left[\frac{n(n+1)E_n^m - 2H_n^m}{r} \right] Y_n^m \quad (5.5c)$$

Combining (5.5a) with (5.5b) and (5.5a) with (5.5c) we get

$$\sum \sum n(2m+1) \frac{dE_n^m}{dr} Y_n^m = \sum \sum \left[-k^2 r (mE_n^m - (m+1)d_n^m) + \frac{(m-1)n(2m+1)E_n^m}{r} \right] Y_n^m \quad (5.6a)$$

$$\sum \sum (m+1)(2m+1) \frac{dE_n^m}{dr} Y_n^m = \sum \sum \left[-k^2 r (mE_n^m - (m+1)d_n^m) - \frac{(m+1)(m+2)(2m+1)d_n^m}{r} \right] Y_n^m \quad (5.6b)$$

If the conductivity does not vary within the shell (5.6 a, b) reduce to (4.25 a, b). Finally, for the very thin conducting shell for which $k^2 r^2$ is very large the second term inside the brackets on the right hand side of (5.5a) is negligible with respect to the first. Across the shell we have

$$\sum_{m=1}^{\infty} \sum_{m=0}^m n(m+1) \Delta \mathcal{B}_n^m Y_n^m = - \sum_{m=1}^{\infty} \sum_{m=0}^m k^2 r \delta \mathcal{H}_n^m Y_n^m \quad (5.7)$$

and since the radial flux density is continuous across this shell

$$\Delta \mathcal{H}_n^m = 0 = n \Delta \mathcal{E}_n^m - (m+1) \Delta \mathcal{L}_n^m$$

$$\Delta \mathcal{E}_n^m = \frac{(m+1) \Delta \mathcal{B}_n^m}{(2m+1)} \quad (5.8a)$$

$$\Delta \mathcal{L}_n^m = \frac{n \Delta \mathcal{B}_n^m}{(2m+1)} \quad (5.8b)$$

Using (5.8 a, b) in (5.7), we have the analog to the uniform thin shell equation, (4.23).

Because we have allowed the conductivity to vary with θ and φ in the above derivations, it was necessary to consider the conducting shell as thin and insulated on both sides in order to avoid radial currents. If the conductivity $\sigma = \sigma(r)$, these restrictions are unnecessary and we have the same conditions as applied to the unsummed equations in Chapter IV.

The change in the potential function of $\vec{H} = \frac{1}{\mu} \vec{B}$ across the thin shell at r , whose thickness is δ , is its magnetic moment per unit area

$$\frac{1}{\mu} \Delta \Omega = \frac{r}{\mu} \sum_{m=1}^{\infty} \sum_{m=0}^m \Delta \mathcal{B}_n^m Y_n^m e^{i\omega t}$$

The magnetic moment per unit area is the same as the current function, F , from whose surface gradient may be obtained the surface current density vector (Chapman and Bartels, 1940, pp. 630, 1) by

$$\vec{J}\delta = \nabla F \times \frac{\vec{F}}{r}$$

This is easily verified by referring to (5.4 a, b) and writing for C_m^m its approximate value in the conductor,

$$C_m^m \approx -r \frac{\Delta \mathcal{B}_m^m}{\mathcal{J}}$$

giving

$$\sum_{m=1}^{\infty} \sum_{m'=0}^m J_{\vartheta}^{m,m'} \delta = \sum_{m=1}^{\infty} \sum_{m'=0}^m \frac{1}{r \sin \vartheta} \frac{\partial}{\partial \varphi} \left[\frac{r}{\mu} \Delta \mathcal{B}_m^m Y_m^m \right] e^{i\omega t} = \frac{1}{r \sin \vartheta} \frac{\partial}{\partial \varphi} \left(\frac{\Delta \Omega}{\mu} \right)$$

$$\sum \sum J_{\varphi}^{m,m'} \delta = \sum \sum -\frac{\partial}{r \partial \vartheta} \left[\frac{r}{\mu} \Delta \mathcal{B}_m^m Y_m^m \right] e^{i\omega t} = -\frac{1}{r} \frac{\partial}{\partial \vartheta} \left(\frac{\Delta \Omega}{\mu} \right)$$

which are the components of $\nabla F \times \frac{\vec{F}}{r}$ if F is replaced by $(\Delta \Omega / \mu)$.

The Effects of the Oceans

In (5.7) it has been assumed that k^2 varies with ϑ and φ while δ remains constant. Since k^2 and δ appear only together in the term $k^2 \delta$ we may consider k^2 as constant, and δ as variable (or their product as variable). Let

$$\text{Rej}(\mathcal{B}_m^m e^{j m \varphi}) = g_m^m \cos m \varphi \quad \text{Imj}(\mathcal{B}_m^m e^{j m \varphi}) = \delta_m^m \sin m \varphi$$

$$\text{Rej}(\mathcal{H}_m^m e^{j m \varphi}) = h_m^m \cos m \varphi \quad \text{Imj}(\mathcal{H}_m^m e^{j m \varphi}) = \eta_m^m \sin m \varphi$$

Then (5.7) becomes

$$\sum_{m=1}^{\infty} \sum_{m'=0}^m m(m+1) [\Delta g_m^m \cos m \varphi + \Delta \delta_m^m \sin m \varphi] P_m^m = - \sum_{m=1}^{\infty} \sum_{m'=0}^m k^2 a \delta(\vartheta, \varphi) [h_m^m \cos m \varphi + \eta_m^m \sin m \varphi] P_m^m$$

Now let us multiply this equation by $\left\{ \begin{array}{l} \cos r \varphi \\ \sin r \varphi \end{array} \right\} P_s^r(\omega \vartheta)$ and integrate over the surface of the unit sphere.

$$\frac{4\pi S(s+1)}{2s+1} \begin{Bmatrix} \Delta g_s^r \\ \Delta \gamma_s^r \end{Bmatrix} = -k^2 a \sum_{m=1}^{\infty} \sum_{m=0}^m \int_0^{2\pi} \int_0^{\pi} \delta(\vartheta, \varphi) (\lambda_m^m \cos m\varphi + \eta_m^m \sin m\varphi) \begin{Bmatrix} \cos r\varphi \\ \sin r\varphi \end{Bmatrix} P_m^m P_s^r \sin\vartheta d\vartheta d\varphi \quad (5.9)$$

If $\delta(\vartheta, \varphi)$ is expressed as a sum of surface harmonics, the integral in the above equation is over three such harmonics and difficult to evaluate. The average value of δ , δ_0 say, would occur in an integral involving the products of only two surface harmonics which is readily integrated to

$$\frac{4\pi \delta_0}{2s+1} \begin{Bmatrix} h_s^r \\ \gamma_s^r \end{Bmatrix}$$

It would contribute to Δh_n^m the same change as that of a shell of uniform depth, δ_0 . If the oceans were randomly distributed, the expected value of the remaining contributions would be zero.

Rather than expressing $\delta(\vartheta, \varphi)$ as a surface harmonic, let us assume that in the northern and southern hemispheres it is a function only of longitude and, therefore, can be developed into alternate Fourier series expansions.

$$\delta(\varphi) = \delta^N(\varphi) = \delta_0^N + \delta_0^N \sum_{k=1}^{\infty} (a_k^N \cos k\varphi + b_k^N \sin k\varphi) \quad 0 \leq \vartheta \leq \frac{\pi}{2} \quad (5.10a)$$

$$\delta(\varphi) = \delta^S(\varphi) = \delta_0^S + \delta_0^S \sum_{k=1}^{\infty} (a_k^S \cos k\varphi + b_k^S \sin k\varphi) \quad \frac{\pi}{2} < \vartheta \leq \pi \quad (5.10b)$$

For Dst, semiannual and sunspot cycle variations, the field is composed predominantly of odd zonal harmonics. If we wish to examine the effects of an ocean of the above type we may take $r = m = 0$ and write

$$\begin{aligned}
\frac{4\pi s(s+1)}{2s+1} \Delta g_s = & -k^2 a \sum_{m=1}^{\infty} h_m \left[\int_0^{2\pi} \left[\delta_0^N + \delta_0^S \sum_{k=1}^{\infty} (a_k^N \cos ky + b_k^N \sin ky) dy \int_0^{\pi} P_m P_s \sin \vartheta d\vartheta \right. \right. \\
& \left. \left. + \int_0^{2\pi} \left[\delta_0^S + \delta_0^N \sum_{k=1}^{\infty} (a_k^S \cos ky + b_k^S \sin ky) dy \int_0^{\pi} P_m P_s \sin \vartheta d\vartheta \right] \right] = \\
& -2\pi k^2 a \sum_{m=1}^{\infty} h_m \left[\delta_0^N \int_0^{\pi/2} P_m P_s \sin \vartheta d\vartheta + \delta_0^S \int_0^{\pi/2} P_m P_s \sin \vartheta d\vartheta \right] \quad (5.11)
\end{aligned}$$

The zonal harmonics are orthogonal, integrated from 0 to π

$$\int_0^{\pi} P_m P_s \sin \vartheta d\vartheta = \begin{cases} \frac{2}{2s+1} & m=s \\ 0 & m \neq s \end{cases}$$

Since both n and s are odd, $P_n P_s$ is even about the equator, and the orthogonality must hold from 0 to $\frac{\pi}{2}$ and $\frac{\pi}{2}$ to π .

$$\int_0^{\pi/2} P_m P_s \sin \vartheta d\vartheta = \int_{\pi/2}^{\pi} P_m P_s \sin \vartheta d\vartheta = \begin{cases} \frac{1}{2s+1} & m=s \\ 0 & m \neq s \end{cases} \quad m+s = \text{even}$$

Consequently, (5.11) becomes

$$s(s+1) \Delta g_s = -k^2 a \frac{\delta_0^N + \delta_0^S}{2} h_s = -k^2 a \delta h_s$$

where δ_0 is the mean depth of all the oceans. Any oceanic distribution in which the oceans in the northern and southern hemispheres are, separately, functions only of the longitude and whose oceans have a mean depth, δ_0 , modifies odd zonal fields to the same extent as a uniform ocean of depth, δ_0 . The combination of zonal fields and sectoral seas will cause some tesseral harmonic field terms, but these are assumed to be negligible.

Let us now consider the daily Sq variation during equinoctial days. There are no zonal harmonics and aside from its latitude dependence, the variation is a function mainly of local time. Since the frequencies $r\omega_0/2\pi$ and $m\omega_0/2\pi$ must be the same, we must take $r = m \geq 1$, and make use of the orthogonality of the normalized associated Legendre functions

$$\int_0^\pi P_m^r P_s^r \sin^r \vartheta d\vartheta = \begin{cases} \frac{1}{2^{s+1}} & m=s \\ 0 & m \neq s \end{cases} \quad r \geq 1$$

The equinoctial variations are predominantly odd about the equator, so if we only consider the odd harmonics which are of the form P_{m+1}^m , P_{m+3}^m , etc., we must have

$$\int_0^{\pi/2} P_m^r P_s^r \sin^r \vartheta d\vartheta = \int_{\pi/2}^\pi P_m^r P_s^r \sin^r \vartheta d\vartheta = \begin{cases} \frac{2}{2^{s+1}} & m=s \\ 0 & m \neq s \end{cases} \quad \begin{matrix} m+s = \text{even} \\ r \geq 1 \end{matrix}$$

Using (5.10 a, b) in (5.9), we have

$$s(s+1) \begin{Bmatrix} \Delta g_s^r \\ \Delta \chi_s^r \end{Bmatrix} = -k^2 a_0 \left[\frac{1}{\pi} \sum_{k=1}^{\infty} \int_0^{2\pi} (a_k \cos k\varphi + b_k \sin k\varphi) (h_m^m \cos r\varphi + \eta_m^m \sin r\varphi) \begin{Bmatrix} \cos r\varphi \\ \sin r\varphi \end{Bmatrix} d\varphi + \begin{Bmatrix} h_s^r \\ \eta_s^r \end{Bmatrix} \right] \quad (5.12)$$

where $\delta_0 = \frac{1}{2}(\delta_0^N + \delta_0^S)$

$$\delta_0 a_k = \frac{1}{2} (\delta_0^N a_k^N + \delta_0^S a_k^S)$$

$$\delta_0 b_k = \frac{1}{2} (\delta_0^N b_k^N + \delta_0^S b_k^S)$$

The trigonometric integral is of the form

$$\frac{1}{8} \int_0^{2\pi} (e^{jr\varphi} \pm e^{-jr\varphi}) (e^{jkr\varphi} \pm e^{-jkr\varphi}) (e^{jk\varphi} \pm e^{-jk\varphi}) d\varphi \quad \begin{matrix} r \geq 1 \\ k \geq 1 \end{matrix}$$

In order that the integral doesn't vanish over 2π , it is necessary that the product of its terms be

$$\frac{1}{8}(e^{j0} + e^{-j0}) = \frac{1}{4} \cos 0 = \frac{1}{4}$$

This will be so if the product of the three ambiguous signs is positive, and if $2m = k$. Thus

$$\int_0^{2\pi} \sin^r y \cos^r y \cos ky \, dy = \int_0^{2\pi} \cos^{2r} y \sin^k y \, dy = 0$$

$$\int_0^{2\pi} \cos^{2r} y \cos ky \, dy = \begin{cases} \frac{\pi}{2} & k=2r \\ 0 & k \neq 2r \end{cases} \quad \begin{matrix} r \geq 1 \\ k \geq 1 \end{matrix}$$

$$\int_0^{2\pi} \sin^{2r} y \cos ky \, dy = \begin{cases} -\frac{\pi}{2} & k=2r \\ 0 & k \neq 2r \end{cases}$$

$$\int_0^{2\pi} \sin^r y \cos^r y \sin ky \, dy = \begin{cases} \frac{\pi}{2} & k=2r \\ 0 & k \neq 2r \end{cases}$$

Equation (5.12) simplifies to

$$s(s+1) \begin{Bmatrix} \Delta g_s^r \\ \Delta \delta_s^r \end{Bmatrix} = -k^2 a_0^r \begin{Bmatrix} h_s^r \left(1 + \frac{a_{2r}}{2}\right) + \eta_s^r \frac{b_{2r}}{2} \\ \eta_s^r \left(1 - \frac{a_{2r}}{2}\right) + h_s^r \frac{b_{2r}}{2} \end{Bmatrix}$$

This is the first order effect, calculated from magnetic variations which are all odd (or all even) about the equator and which depend only on local time. The corrections caused by the irregularities of the oceans must be small; otherwise the fields induced in the oceans, which do not satisfy the above conditions, would have important secondary effects.

A possible representation of the earth's oceans according to (5.10 a, b) is illustrated in Figure 5.1.

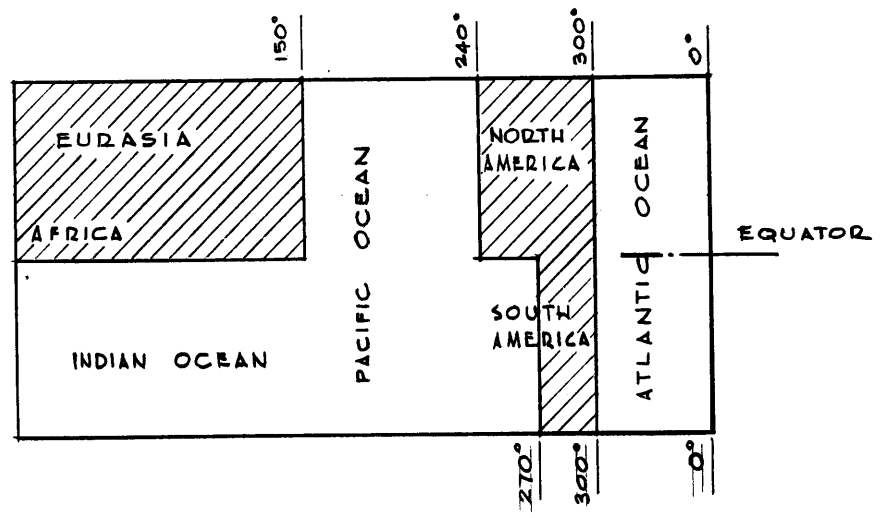


FIGURE 5.1

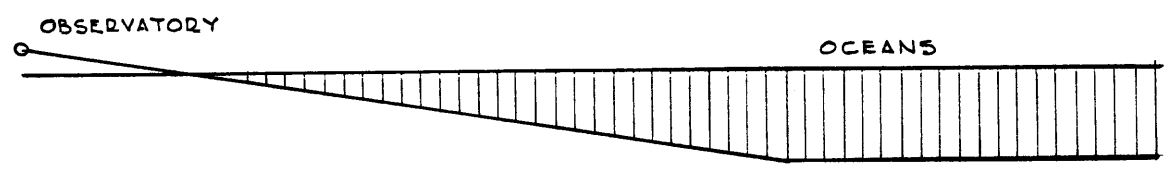


FIGURE 5.2a



FIGURE 5.2b

FROM FIGURE 5.1 :

$$a_k = \frac{3d_0}{2} \left[\frac{1}{2\pi} \int_0^{270^\circ} \cos ky \, dy + \frac{1}{2\pi} \int_0^{240^\circ} \cos ky \, dy + \frac{1}{\pi} \int_{300^\circ}^{360^\circ} \cos ky \, dy \right] =$$

$$\frac{3d_0}{4\pi k} \left[\sin 270k^\circ + \sin 240k^\circ - \sin 150k^\circ - 2 \sin 300k^\circ \right]$$

$$b_k = \frac{3d_0}{2} \left[\frac{1}{2\pi} \int_0^{270^\circ} \sin ky \, dy + \frac{1}{2\pi} \int_{150^\circ}^{240^\circ} \sin ky \, dy + \frac{1}{\pi} \int_{300^\circ}^{360^\circ} \sin ky \, dy \right] =$$

$$\frac{3d_0}{4\pi k} \left[\cos 150k^\circ + 2 \cos 300k^\circ - \cos 270k^\circ - \cos 240k^\circ - 1 \right]$$

$$a_2 = 0.413 d_0$$

$$b_2 = 0$$

$$a_4 = -0.103 d_0$$

$$b_4 = -0.179 d_0$$

$$a_6 = 0$$

$$b_6 = 0$$

For this ocean distribution, the appropriate corrections for the P_2^1 , P_3^2 and P_4^3 terms are

$$6 \begin{Bmatrix} \Delta g_2^1 \\ \Delta \gamma_2^1 \end{Bmatrix} = -k^2 a d_0 \begin{Bmatrix} 1.21 h_2^1 \\ 0.79 \eta_2^1 \end{Bmatrix}$$

$$12 \begin{Bmatrix} \Delta g_3^2 \\ \Delta \gamma_3^2 \end{Bmatrix} = -k^2 a d_0 \begin{Bmatrix} 0.95 h_3^2 - 0.09 \eta_3^2 \\ 1.05 \eta_3^2 - 0.09 h_3^2 \end{Bmatrix}$$

$$20 \begin{Bmatrix} \Delta g_4^3 \\ \Delta \gamma_4^3 \end{Bmatrix} = -k^2 a d_0 \begin{Bmatrix} h_4^3 \\ \eta_4^3 \end{Bmatrix}$$

For the fields assumed, the difference between the correction required for this ocean distribution and that of an equivalent uniform shell is small to negligible. However, attempts by earlier workers to apply the equivalent uniform shell correction resulted in impossible fields beneath the seas for all harmonics considered. It behooves us, therefore, to seek a source of systematic bias in the original data used.

Bias

The part of the varying magnetic field observed at a station that is caused by induced ocean currents may be expressed in terms of the integral

$$\vec{B} \text{ induced} = \iiint_{\text{oceans}} \frac{\nabla \times \vec{J}}{4\pi R} dV$$

where R is the distance between station and volume element. The $1/R$ term implies that the closer the currents are to the station, the

greater are their effects on the magnetic field. If a station is on a ship in the ocean, the effects are greatest; if it is continental and distant from the coast, the effects are least. For an unbiased harmonic analysis of the magnetic potential, the stations must be uniformly scattered over land and sea. Actually, however, there are no floating magnetic observatories although many stations have been established on islands and near coastlines. Let us pay particular attention to these types of stations. Since the nearby oceans are approximately planar, let the thin spherical shell of variable conductivity be approximated by an infinitesimally thin plane sheet of variable conductivity. At any coastal or island station, the ocean gradually tapers from its deep sea depth to the coastline and the altitude of the observatory is somewhat less than its distance inland from the coast (see Figure 5.2 a). The observatory is, therefore, approximately co-planar with the effective ocean (Figure 5.2 b) so any horizontal component of the induced field from nearby oceans is quite small. Unless there are floating observatories, the ocean induced part of the analyzed horizontal field is underestimated and its harmonic analysis in terms of \mathcal{O}_n^m is biased. In addition, because of the observatory distribution there may be a small bias in the harmonic analysis of the vertical field in terms of \mathcal{H}_n^m .

Let us return to the sphere and assume that the distribution of continental, coastal and island stations is such that a fraction, β_1 of the contributions to the horizontal components from the induced ocean fields is unobserved. In addition we shall assume that a fraction, β_2 , of the contributions to the vertical components from these fields

is also unobserved. For the reasons given above, we expect that β_2 is small compared with β_1 . Above the oceans an unbiased harmonic analysis of the field would give \mathcal{G}_n^m and \mathcal{H}_n^m from which, by the uniform shell approximation, we could estimate $\mathcal{G}_n^m - \Delta \mathcal{G}_n^m$ and $\mathcal{H}_n^m - \Delta \mathcal{H}_n^m$ under the shell. But, by assumption, instead of finding

$$\mathcal{G}_n^m = \mathcal{E}_n^m + \mathcal{J}_n^m$$

$$\mathcal{H}_n^m = m\mathcal{E}_n^m - (m+1)\mathcal{J}_n^m$$

the harmonic analyses of the field find

$$\bar{\mathcal{G}}_n^m = \mathcal{E}_n^m + \mathcal{J}_n^m - \beta_1 \Delta \mathcal{J}_n^m = \mathcal{G}_n^m - \beta_1 \Delta \mathcal{J}_n^m$$

$$\bar{\mathcal{H}}_n^m = m\mathcal{E}_n^m - (m+1)(\mathcal{J}_n^m - \beta_2 \Delta \mathcal{J}_n^m) = \mathcal{H}_n^m + \beta_2 (m+1) \Delta \mathcal{J}_n^m$$

Across the shell we have

$$\Delta \mathcal{H}_n^m = m\mathcal{E}_n^m - (m+1) \Delta \mathcal{J}_n^m = 0$$

$$\Delta \mathcal{G}_n^m = \Delta \mathcal{E}_n^m + \Delta \mathcal{J}_n^m$$

$$\Delta \mathcal{J}_n^m = \frac{m}{2m+1} \Delta \mathcal{G}_n^m$$

Therefore

$$\bar{\mathcal{G}}_n^m = \mathcal{G}_n^m - \beta_1 \frac{m}{2m+1} \Delta \mathcal{G}_n^m \quad (5.13a)$$

$$\bar{\mathcal{H}}_n^m = \mathcal{H}_n^m + \beta_2 \frac{(m+1)}{2m+1} \Delta \mathcal{G}_n^m \quad (5.13b)$$

We seek the ratio, S_m' , beneath the oceans. Since $\Delta \mathcal{H}_n^m = 0$

$$S_m' = S_m - \Delta S_m = \frac{m(\mathcal{G}_n^m - \Delta \mathcal{G}_n^m) - \mathcal{H}_n^m}{(m+1)(\mathcal{G}_n^m - \Delta \mathcal{G}_n^m) + \mathcal{H}_n^m} \quad (5.14)$$

Using (5.13 b) and (4.23 c)

$$\begin{aligned}\bar{H}_n^m &= H_n^m - \beta_2 \frac{k^2 a d}{2m+1} H_n^m \\ H_n^m &= \frac{\bar{H}_n^m}{1 - \beta_2 \frac{k^2 a d}{2m+1}}\end{aligned}\quad (5.15a)$$

Using (5.13 a), (4.23 c) and (5.15 a)

$$\begin{aligned}y_n^m - \Delta y_n^m &= \bar{y}_n^m - (1 - \beta_1 \frac{m}{2m+1}) \Delta y_n^m = \bar{y}_n^m + \frac{k^2 a d [(2-\beta_1)m+1]}{m(m+1)(2m+1)} H_n^m \\ y_n^m - \Delta y_n^m &= \bar{y}_n^m + \frac{[(2-\beta_1)m+1]}{m(m+1)} \frac{k^2 a d}{2m+1} \frac{\bar{H}_n^m}{[1 - \beta_2 \frac{k^2 a d}{2m+1}]}\end{aligned}\quad (5.15b)$$

Combining (5.14) and (5.15 a, b) gives

$$S_n' = \frac{m E_n^m \left[1 - \beta_2 \frac{k^2 a d}{2m+1} \right] + \frac{[(2-\beta_1)m+1]}{(m+1)} \left(\frac{k^2 a d}{2m+1} \right) \bar{H}_n^m - \bar{H}_n^m}{(m+1) \bar{y}_n^m \left[1 - \beta_2 \frac{k^2 a d}{2m+1} \right] + \frac{[(2-\beta_1)m+1]}{m} \left(\frac{k^2 a d}{2m+1} \right) \bar{H}_n^m + \bar{H}_n^m}\quad (5.16)$$

In terms of the biased ratio, $\bar{S}_n = \bar{H}_n^m / \bar{E}_n^m$, we may write

$$\begin{aligned}\bar{y}_n^m &= E_n^m (1 + \bar{S}_n) \\ \bar{H}_n^m &= E_n^m (m - (m+1)\bar{S}_n)\end{aligned}$$

If these are substituted into (5.16), the equation may be manipulated into the form

$$S_n - \Delta S_n = S_n' = \left(\frac{m}{m+1} \right) \frac{(2m+1)^2 \bar{S}_n - [(2-\beta_1)m+1] k^2 a d \left(\bar{S}_n - \frac{m}{m+1} \right) - \beta_2 m k^2 a d (\bar{S}_n + 1)}{(2m+1)^2 \frac{m}{m+1} - [(2-\beta_1)m+1] k^2 a d \left(\bar{S}_n - \frac{m}{m+1} \right) - \beta_2 m k^2 a d (\bar{S}_n + 1)}\quad (5.17)$$

For $\beta_1 = \beta_2 = 0$ (5.17) is equivalent to (4.31), the correction for a uniform shell of thickness δ . For $\beta_1 = 1$ and $\beta_2 = 0$, (5.17) is equivalent again to (4.31), but the correction is now for a thinner shell of thickness $\frac{m+1}{2m+1} \delta$. For small $k^2 a \delta$, $S'_m - \Delta S'_m \rightarrow S'_m$ and for large k^2 , $S'_m - \Delta S'_m \rightarrow \frac{m}{m+1}$. The reverse problem is, knowing the true S'_m under the oceans, to estimate the S'_m which would be measured above the oceans. The derivation of the appropriate formula is similar to that of (5.17).

$$\bar{S}_m = \left(\frac{m}{m+1}\right) \frac{(2m+1) S'_m + [(1-\beta_1)m + (1-\beta_2)(m+1)] k^2 a \delta (S'_m - \frac{m}{m+1})}{(2m+1)^2 \frac{m}{m+1} + [2m+1 + (\beta_2 - \beta_1)m] k^2 a \delta (S'_m - \frac{m}{m+1})} \quad (5.18)$$

Interpretation of Biased Sq Ratios

Neither the depth nor the conductivity of the oceans is constant. For the thin shell correction we shall, instead of using the mean of $\sigma \delta$, we shall approximate it by the mean of σ times the mean of δ . The mean depth of the oceans which is still generally used by oceanographers and geochemists was calculated by Kossina in 1921 (see Goldschmidt, 1954, for an English account of his method) by integration over five degree zones over the earth. Kossina calculated that the mean ocean depth is 3792 meters; an ocean of the same volume distributed evenly over the earth would have a depth of 2680 meters. The conductivity is a function of the salinity temperature, (see Table 5.1). The salinity is relatively uniform at 35‰ but the

Table 5.1 (Extracted from Chapman and Bartels, page 424)

Conductivities in mhos/meter

Temp. °C	Salinity	30	35	40
0		2.6	2.9	3.3
10		3.3	3.8	4.4
20		4.2	4.8	5.6

temperature falls off rapidly with depth leaving the bulk of the ocean a uniform 3° or 4° C. We shall take a mean temperature of 5° C and, by interpolating Table 5.1, the mean conductivity will be taken as 3.3 mhos/meter. The $\sigma \delta$ to be used in the thin shell approximation will then be 8.8×10^3 mhos. Table 5.2 lists $-k^2 a \delta$ and the skin depth, $\sqrt{\frac{2}{|k^2|}}$, as a function of the period, $2\pi/\omega$. It is seen that the ocean correction is unimportant for the semiannual and sunspot cycles.

Table 5.2

Period	8 hours	12 hours	24 hours	6 months	11 years
$-k^2 a \delta$	15.4 i	10.3 i	5.14 i	0.044 i	0.002 i
skin depth	47 km	58 km	81 km	1100 km	5160 km

If, in (5.18), S'_m is varied along the positive real axis, the path that \bar{S}_m takes, which depends upon β_1 and β_2 may be plotted. Since the real axis must fall below all possible S'_m ratios, the paths plotted (representing the "biased" real axis) must fall below the observed \bar{S}_m ratios. In Figure 5.3 a-c several of these paths are

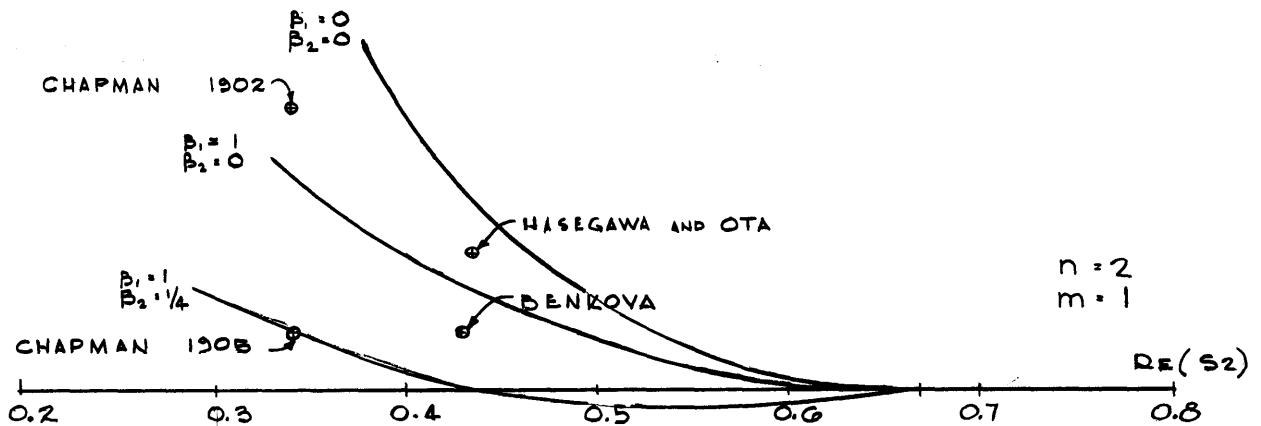


FIGURE 5.3a

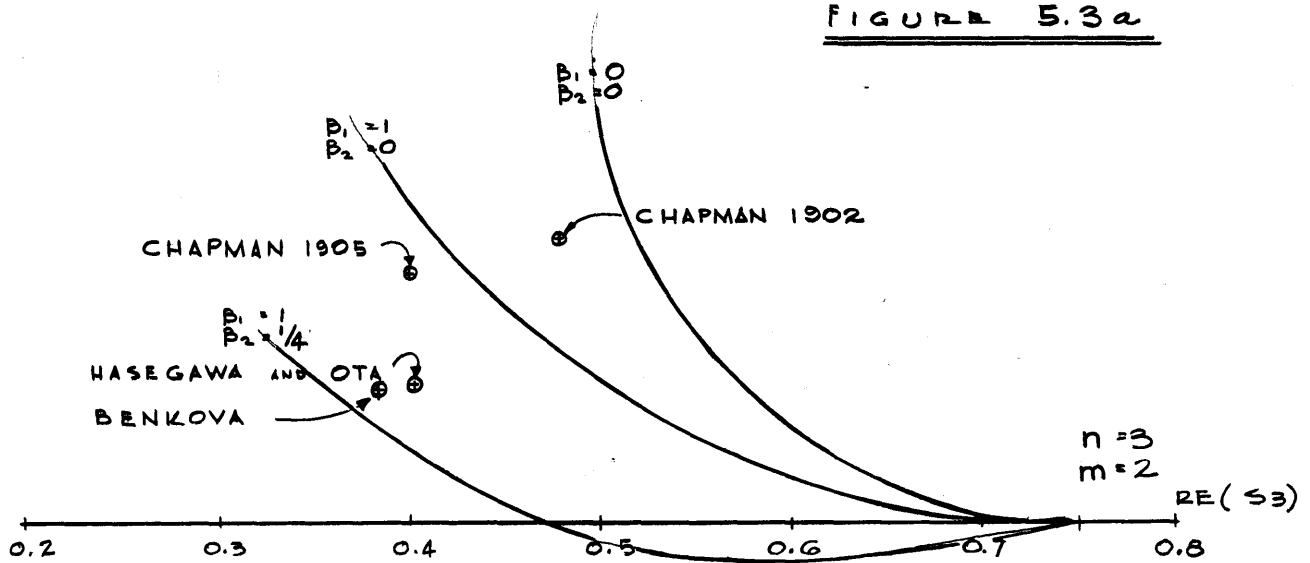


FIGURE 5.3b

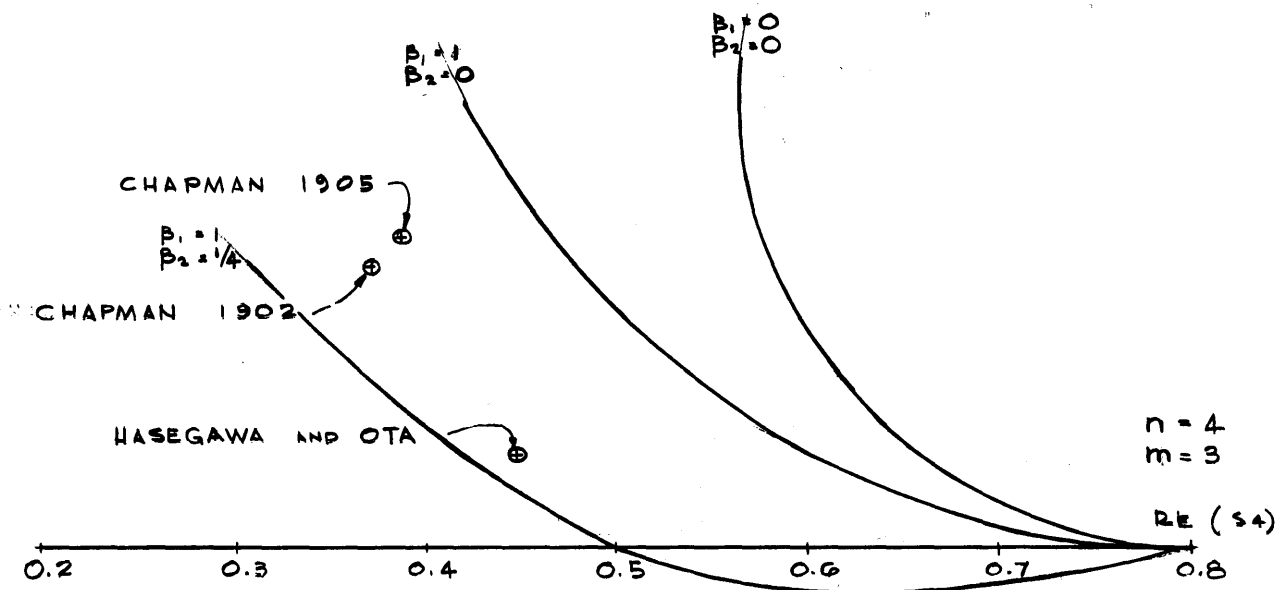


FIGURE 5.3c

shown for the P_2^1 , P_3^2 and P_4^3 terms for the daily variation which depends only on local time. Superposed on these figures are the \bar{S}_m 's calculated from the analyses Chapman (1902 and 1905), Benkova, and Hasegawa and Ota. These ratios are scattered but none falls above the zero bias curve. By choosing the bias sufficiently large, however, we can find curves which fall below any of the ratios.

Aside from the difficulty of assessing the actual amount of bias in harmonic analyses of the Sq field, the interpretation is complicated by the lack of agreement between the original harmonic analyses which are available. These discrepancies cannot be entirely attributed to ocean bias; one analyst (Chapman) calculated widely different ratios, \bar{S}_m , for the same stations but for different years. Considering all the uncertainties involved, a quantitative interpretation of the conductivity of the earth's mantle from these Sq field ratios is rather difficult. We shall, however, make an attempt to apply the straight line interpretation given at the end of Chapter IV.

The ocean and bias corrections have a relatively minor effect on

$$\operatorname{Re} \left(S_m - \frac{m}{m+1} \right) = h_m$$

so in using (4.40), (4.41) and (4.42), we may use the following approximate quantities, eclectically culled from Figures 5.3 a-c:

Approximation	Sources
$h_2(r_0) \approx 0.25$	Benkova, Hasegawa and Ota
$h_3(r_0) \approx 0.35$	Benkova, Hasegawa and Ota, Chapman (1905)
$h_4(r_0) \approx 0.40$	Hasegawa and Ota, Chapman - (1902, 1905)

The angle, γ_n , which is also required for the straight line solution is unknown. Figures 5.4 a-c plot possible solutions for different values of γ_n . For these variations any conductivity of the order of 0.3 mhos/meter or greater appears as a superconductor. This conductivity is attained at a minimum depth of about 500 kilometers. For the semiannual variation, any conductivity of the order of 0.05 mhos/meter or less appears as an insulator. This conductivity is attained from the diurnal analyses at a minimum depth of about 400 kilometers. This information will be useful in the interpretation of the semiannual variation.

$n = 2$
 $m = 1$

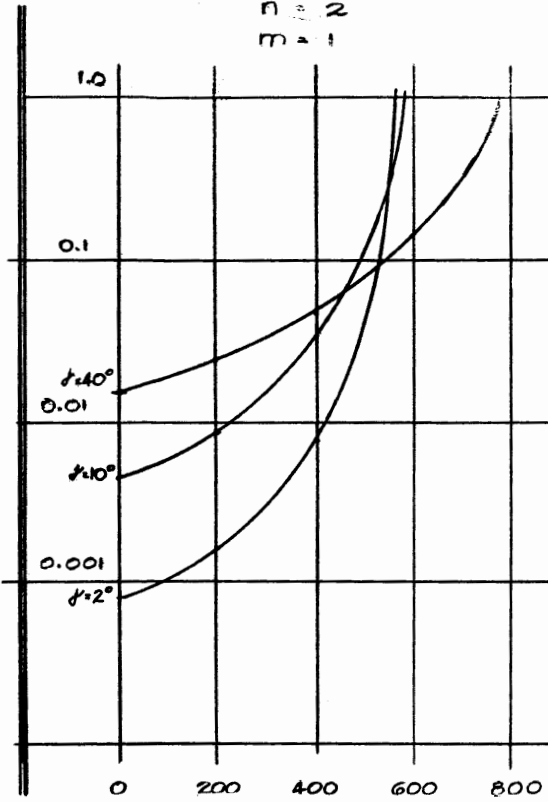


FIGURE 5.4a

$n = 3$
 $m = 2$

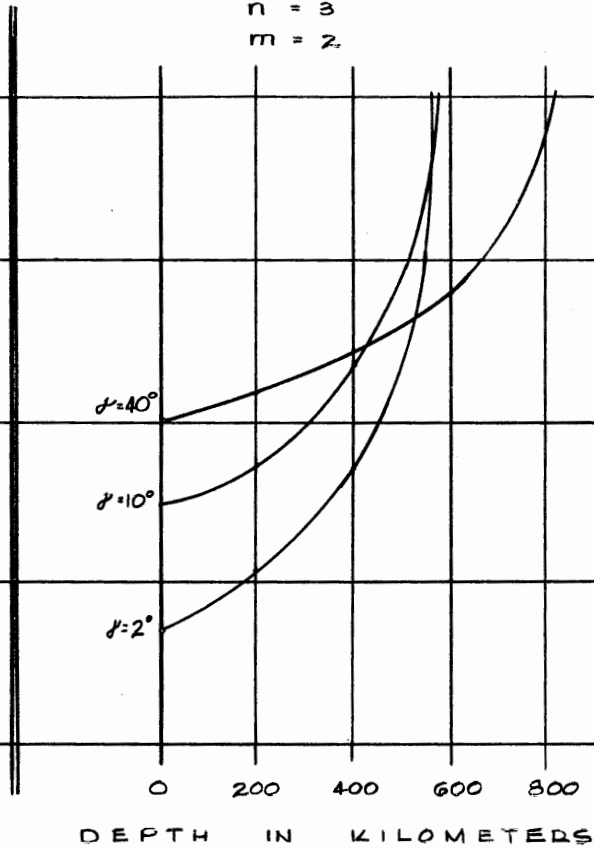


FIGURE 5.4b

$n = 4$
 $m = 3$

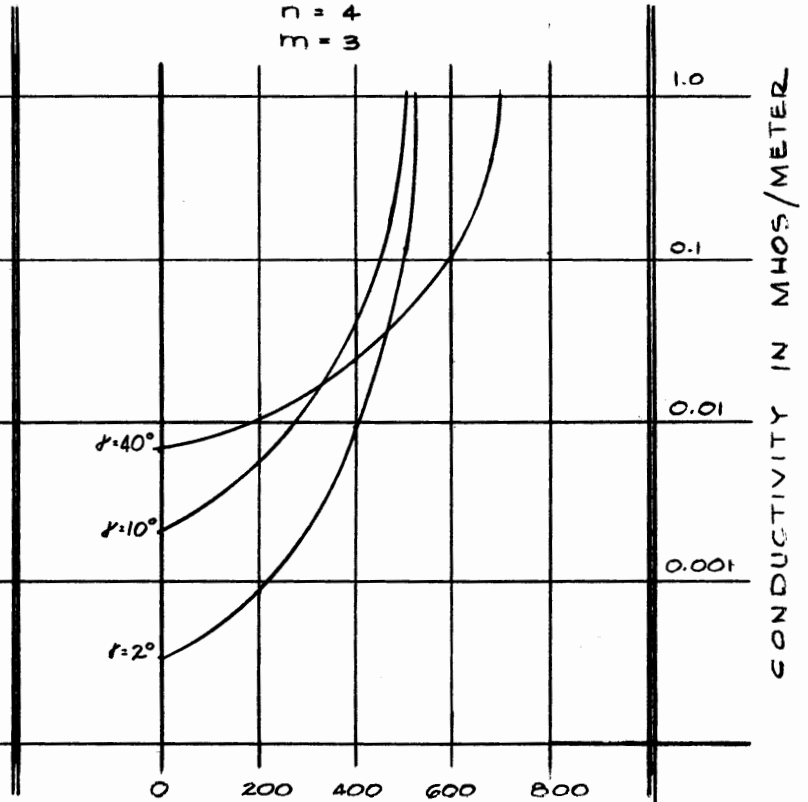


FIGURE 5.4c

CHAPTER VI
ANALYSIS OF LONG PERIOD DATA

Purpose

The first half of this chapter is concerned with the data reduction used to calculate (or to attempt to calculate) the ratio for the semiannual and sunspot cycles. The three main points to be considered are the techniques for zonal harmonic analysis, frequency harmonic analysis and prefiltering of low frequency background from the original data. In the second half of the chapter results of analyses of the semiannual and sunspot cycles by these methods are given. The semiannual analysis, using mean disturbance elements, successfully yields a complex ratio, $S_1(a)$, which proves quite useful in mantle conductivity interpretations. The sunspot cycle analysis, using mean elements, gives poor results.

Zonal Harmonic Analysis

In the non-polar latitudes we may consider the varying magnetic field in geomagnetic co-ordinates as derivable from a potential containing only a first zonal harmonic term. From Chapter III, for either cycle we have at station k

$$X'_k = -G_1(a) \sin \vartheta'_k$$

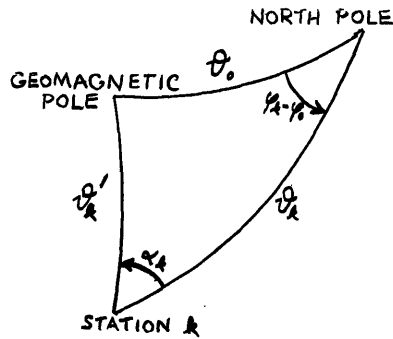
$$Y'_k = 0$$

$$Z'_k = H_1(a) \cos \vartheta'_k$$

In the geographic system we denote the colatitude and east longitude at station k by ϑ_k and φ_k , and we denote the colatitude and east longitude at the geomagnetic pole by ϑ_0 and φ_0 (see Figure 6.1).

We may then calculate the geomagnetic colatitude by using the formula

$$\cos \theta'_k = \cos \theta_k \cos \theta_0 + \sin \theta_k \sin \theta_0 \cos (\varphi_k - \varphi_0)$$



The geomagnetic components,

X'_k and Y'_k , are related to the measured geographic components, by

$$\begin{bmatrix} X'_k \\ Y'_k \end{bmatrix} = \begin{bmatrix} \cos \alpha_k & -\sin \alpha_k \\ \sin \alpha_k & \cos \alpha_k \end{bmatrix} \begin{bmatrix} X_k \\ Y_k \end{bmatrix}$$

FIGURE 6.1

where α_k , the change in declination, is determined by using

$$\sin \alpha_k = \sin \theta_0 \frac{\sin (\varphi_k - \varphi_0)}{\sin \theta'_k}$$

Weighting all K stations equally, we may determine $\mathcal{G}_1(a)$ and $\mathcal{H}_1(a)$, by the method of least squares.

$$\mathcal{G}_1(a) = - \frac{\sum_{k=1}^K X'_k \sin \theta'_k}{\sum_{k=1}^K \sin^2 \theta'_k}$$

$$\mathcal{H}_1(a) \approx \frac{\sum_{k=1}^K Z_k \cos \theta'_k}{\sum_{k=1}^K \cos^2 \theta'_k}$$

From these we calculate the ratio

$$\mathcal{S}_1(a) = \frac{\mathcal{G}_1(a) - \mathcal{H}_1(a)}{2\mathcal{G}_1(a) + \mathcal{H}_1(a)}$$

Since the first zonal harmonic is so predominant in the non-polar latitudes, $\mathcal{G}_1(a)$ and $\mathcal{H}_1(a)$ and, therefore, $\mathcal{S}_1(a)$ can be calculated from the records of only one station. The best location for such a station is in the middle latitudes where Z_k is not small. In practice,

of course, the more stations used, the better is the estimation of $S_1(a)$.

Order of Harmonic Analyses

Needed for the above calculations of \mathcal{B}_1 and \mathcal{H}_1 are the complex amplitudes X_k' and Z_k at the appropriate frequency. These may be determined at station k by frequency harmonic analyses of a sequence of measurements of the components of the geomagnetic field. This method - a frequency harmonic analysis followed by a simple zonal harmonic analysis by least squares - is used in the analysis of the semiannual variation where data from all stations used is available over a common span of time. For the sunspot cycle analysis, data from many observatories are available, but these observatories do not have continuous measurements over a common time span; operations at different observatories started at different dates and in some cases have already ceased. At any year, however, there are always many data so, in order to use as much information as possible, the procedure for the sunspot cycle analysis is the reverse of that given above: first there is a zonal harmonic analysis by least squares and then these results are subjected to a frequency harmonic analysis to determine \mathcal{B}_1 and \mathcal{H}_1 .

Frequency Harmonic Analysis

Let us consider the input for the frequency harmonic analysis as

$$g(t) = s(t) + n(t)$$

$$G(\omega) = S(\omega) + N(\omega)$$

where $s(t)$ is a pure sinusoidal signal at frequency $\frac{\omega_0}{2\pi}$ and $n(t)$ is the noise, and $S(\omega)$ and $N(\omega)$ are the frequency transforms of $s(t)$ and $n(t)$. If we write $S(\omega)$ in the form

$$S(\omega) = 2\pi S_0 e^{-i\omega_0 t_0} u_0(\omega - \omega_0) \quad u_0(\omega - \omega_0) = \text{unit impulse}$$

we find that its transform is

$$s(t) = \frac{1}{2\pi} \int_{-\infty}^{\infty} \mathcal{S}(\omega) e^{i\omega t} d\omega = \left[\mathcal{S}_0 e^{-i\omega_0 t_0} \right] e^{i\omega_0 t}$$

where the bracketed term in the above equation is the complex amplitude of the signal. This is the term we wish to estimate from a sample of $g(t)$. Since the lengths of our records are finite, rather than having $g(t)$ we have only

$$x(t) = g(t) \cdot w(t)$$

where $w(t)$ is the window which must be identically zero for $|t| \geq \frac{1}{2}T_1$, and T_1 is the total length in time of the filtered record. If $X(\omega)$ and $W(\omega)$ are the frequency transforms of $x(t)$ and $w(t)$

$$\begin{aligned} X(\omega_0) &= \frac{1}{2\pi} \int_{-\infty}^{\infty} G(\omega) W(\omega_0 - \omega) d\omega \\ \frac{X(\omega_0)}{W(0)} &= \mathcal{S}_0 e^{-i\omega_0 t_0} + \frac{1}{2\pi} \int_{-\infty}^{\infty} N(\omega) \frac{W(\omega_0 - \omega)}{W(0)} d\omega \end{aligned} \quad (6.1)$$

The first term on the right hand side of this equation is the complex amplitude which we seek and the second term is the noise contribution which we wish to make relatively small. This is done by making $W(\Delta\omega)/W(0)$ small where $N(\omega)$ is large. To diminish the effects of low frequency noise which passes through the secular variation filter, we shall peak $W(\Delta\omega)/W(0)$ at $\Delta\omega = 0$ and have it die off rapidly as $\Delta\omega$ moves away from zero.

The simplest window, which we shall represent by the transform pair $w_0(t)$ and $W_0(\omega)$ is defined as follows:

$$\begin{aligned} w_0(t) &= 1 & |t| < \frac{1}{2}T_1 \\ &= 0 & |t| \geq \frac{1}{2}T_1 \end{aligned}$$

It follows that

$$W_0(\Delta\omega) = T_1 \frac{\sin \pi \frac{\Delta\omega}{\omega_1}}{\pi \frac{\Delta\omega}{\omega_1}}$$

$W_0(\Delta\omega)/W_0(0)$ has zeroes at $\Delta\omega = \omega_1, 2\omega_1, 3\omega_1, \dots$, and it falls from its peak at $\Delta\omega = 0$ to side lobes whose absolute peaks are 22, 13, 9 percent, etc., of the central peak. Blackman and Tukey (1958) have considered a number of different windows in connection with autocorrelation function lags. For example, their second pair, the "hanning" window, is

$$w_2(t) = \frac{1}{2} (1 + \cos \omega_1 t) \quad |t| \leq \frac{1}{2} T_1$$

$$= 0 \quad |t| \geq \frac{1}{2} T_1$$

and

$$W_2(\Delta\omega) = \frac{1}{2} W_0(\Delta\omega) + \frac{1}{4} [W_0(\Delta\omega + \omega_1) + W_0(\Delta\omega - \omega_1)]$$

The central lobe of $W_2(\Delta\omega)$ is twice as broad as that of $W_0(\Delta\omega)$ and its zeroes occur at $\Delta\omega = 2\omega_1, 3\omega_1, 4\omega_1, \dots$. The absolute peaks of the side lobes are only 3, 1, 1/2 percent of the central peak.

The window used for the calculations of this thesis is the sigma smoothing factor of Lanczos (1956). This pair is

$$w_1(t) = \frac{\sin \omega_1 t}{\omega_1 t} \quad |t| < \frac{1}{2} T_1$$

$$= 0 \quad |t| \geq \frac{1}{2} T_1$$

and

$$W_1(\Delta\omega) = \frac{T_1}{2\pi} \left[\text{Si} \left(\pi \left(\frac{\Delta\omega}{\omega_1} + 1 \right) \right) - \text{Si} \left(\pi \left(\frac{\Delta\omega}{\omega_1} - 1 \right) \right) \right]$$

where $S_i(\cdot)$ is the sine integral. The transcendental zeroes of $W_i(\Delta\omega)$ occur at about $\Delta\omega = 1.64\omega_1, 2.58\omega_1, 3.56\omega_1$, etc., and the absolute peaks of the side lobes are 5, 2, 1 percent, etc., of the central peak. See Figure 6.2 for a comparison of the transforms of the three windows cited. With this choice of windows we have

$$\int_0^{\infty} e^{-i\omega_0 t} dt \approx \frac{X(\omega_0)}{W_i(0)}$$

$$X(\omega) = \int_{-\infty}^{\infty} g(t) w_i(t) e^{-i\omega t} dt = \int_{-\frac{1}{2}T_1}^{\frac{1}{2}T_1} x(t) e^{-i\omega t} dt$$

If $x(t)$ is broken into the even and odd functions

$$u(t) = x(t) + x(-t)$$

$$v(t) = x(t) - x(-t)$$

we then have

$$X(\omega) = \int_0^{\frac{1}{2}T_1} u(t) \cos \omega t dt - i \int_0^{\frac{1}{2}T_1} v(t) \sin \omega t dt$$

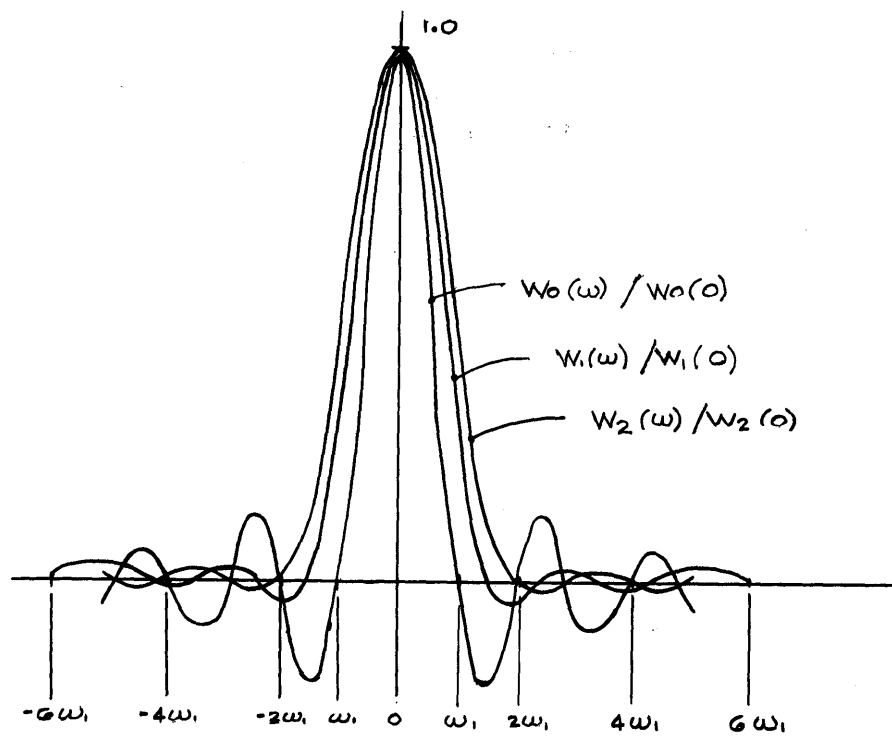
Let us solve these integrals numerically by using the trapezoidal rule of numerical integration. We shall take the increment in time as $\Delta t = 1$ year and the effective record length as the even integer, $T_1 = 2M+2$

$$X(\omega) \approx \sum'_{t=0}^{M+1} u(t) \cos \omega t - i \sum'_{t=0}^{M+1} v(t) \sin \omega t \quad (6.2)$$

The primes on the summations indicate that the first and last terms of each are taken with only half their normal values. We

note that $W_i(\pm(M+1)) = W_i(\pm \frac{1}{2}T_1) = 0$

$$u(M+1) = v(M+1) = 0$$



COMPARISON OF WINDOW TRANSFORMS

FIGURE 6.2

so $g(-M-1)$ and $g(M+1)$ are never used in the calculation. For this reason, the actual record length may be taken as $2M$, and the number of yearly means required is $2M+1$. If, further, we note that $\sin \omega_0 = 0$, (6.2) becomes

$$X(\omega) = \frac{1}{2} u(0) + \sum_{t=1}^M u(t) \cos \omega t - i \sum_{t=1}^M v(t) \sin \omega t$$

By calculating $X(k\omega_1)$ for $k = 0, 1, \dots, M+1$, we have the discrete range Fourier series coefficients (Lanczos, 1956). The real and imaginary parts of $X(k\omega_1)$ may be interpolated to find $X(\omega_0)$, but the calculations for this thesis have always used an ω_1 such that ω_0/ω_1 is an integer and interpolation is unnecessary.

From (6.1), we have, approximately

$$S_0 e^{-i\omega_0 t_0} \approx \frac{X(\omega_0)}{W_1(0)} = \frac{\pi X(\omega_0)}{\text{Si}(\pi)(2M+2)}$$

As long as all the records analyzed are over the same time span, we may drop the above normalization and consider the complex amplitude as identical with $X(\omega_0)$. This is because the significant quantity, which is the ultimate goal of these calculations, is a complex amplitude ratio.

Prefiltering

No matter in which order the frequency and zonal harmonic analyses are applied, they must be preceded by some sort of an operation which reduces the very powerful low frequency background from the original measurements. The semiannual and sunspot cycles contribute only slightly to the over-all change in the earth's measured magnetic field. Over a span of years the major change

is the secular variation of the earth's magnetic field, and its power is several orders of magnitude greater than the power of the signals sought. The secular variation usually changes slowly with time so over fifty years of records, say, it can usually be fairly well approximated by a low order polynomial. The recording instruments may drift or their baselines may be miscalibrated at different times. If these errors change slowly enough their effects and those of the secular variation may be reduced by the same method.

The effects of the secular variation, instrument drift and miscalibration may be effectively eliminated by using the mean disturbance field rather than the mean field. This is feasible for the semiannual variation which is measured in this thesis from United States Coast and Geodetic Survey magnetic observatory data. For the five internationally disturbed days and the five internationally quiet days of each month, all USC&GS observatories publish the means of the declination, total horizontal flux density and vertical flux density. Their differences constitute the elements of the monthly mean disturbance field used. Magnetic variations, such as the secular variation, which are causally unrelated to magnetic disturbance fields and which change *little* in a month cancel themselves out in the subtractions of the means. Unfortunately, data currently available to the author are inadequate to successfully apply this method to the sunspot cycle.

For the sunspot cycle, we require a filter which eliminates low order polynomial terms but passes the eleven year period unattenuated. Vestine (1947 b) uses the differences between the annual means and a quadratic fit by the method of least squares to all the annual means. This method, however, does not constrain the signal

frequency to remain unaffected; in fact, Vestine notes that using the differences between the annual means and a least squares cubic fit seemed to remove part of the signal.

One method for accomplishing the desired result has been suggested by T. R. Madden. It is based upon the filter whose response to the unit impulse at time t is

$$h(t) = -\frac{1}{2} u_0(t - \frac{1}{2} T_0) + \frac{1}{2} u_0(t)$$

where $u_0(t)$ is the unit spike at $t = 0$ and $T_0 = \frac{2\pi}{\omega_1}$ is the period of the signal, eleven years. If we pass our data, represented by $f(t)$, through this filter once, we get the output $g_1(t)$ which may be written in terms of the convolution integral

$$g_1(t) = \int_{-\infty}^{\infty} f(\gamma) h(t - \gamma) d\gamma = \frac{1}{2} f(t) - \frac{1}{2} f(t + \frac{1}{2} T_0) = -\frac{1}{2} \Delta f(t)$$

where Δ is the first forward difference operator for the interval $(1/2) T_0$. If the transforms of $f(t)$, $g_1(t)$ and $h(t)$ are, respectively, $F(\omega)$, $G_1(\omega)$ and $H(\omega)$, we have in the frequency domain

$$G_1(\omega) = F(\omega) H(\omega)$$

where

$$H(\omega) = \int_{-\infty}^{\infty} e^{-i\omega t} h(t) dt = \frac{1}{2} (1 - e^{-i\omega \frac{T_0}{2}}) = \frac{1}{2} (1 - \cos \frac{\omega T_0}{2} + i \sin \frac{\omega T_0}{2})$$

$$\text{At } \omega = \omega_0 \quad H(\omega_0) = 1$$

$$G_1(\omega_0) = F(\omega_0) H(\omega_0) = F(\omega_0)$$

No frequency has a gain greater than 1 although there are an infinite number of frequencies that also pass unattenuated; their angular frequencies are all the odd harmonics of ω_0 , that is, $3\omega_0$, $5\omega_0$, etc.

If we apply this filter k times we have

$$g_k(t) = \left(-\frac{1}{2}\right)^k \Delta^k f(t)$$

$$G_k(\omega) = F(\omega) H^k(\omega)$$

where Δ^k is the k^{th} forward difference operator. Taking the k^{th} forward difference reduces the polynomial part of $f(t)$ by k degrees and at $\omega = \omega_0$

$$H^k(\omega_0) = 1$$

$$G_k(\omega_0) = F(\omega_0)$$

and the signal frequency is unattenuated, so the filter has the criteria required. For discrete data, the filtering operation then is simply a matter of taking forward differences. For instance, if we wish to remove all constant, linear and quadratic terms and reduce the cubic term to a constant we operate on $f(t)$ as follows:

$$g_3(t) = -\frac{1}{8} \Delta^3 f(t) = \frac{1}{8} f(t) - \frac{3}{8} f\left(t + \frac{T_0}{2}\right) + \frac{3}{8} f(t + T_0) - \frac{1}{8} f\left(t + \frac{3T_0}{2}\right)$$

For the sunspot cycle, though, $T_0/2$ and $3T_0/2$ correspond, respectively, to 5 1/2 and 16 1/2 years. Since we have only mean yearly data, we are forced to compromise by linear interpolation. Letting the unit of time be one year, the above operation is replaced by

$$g_3(t) \approx \frac{1}{8} f(t) - \frac{3}{16} f(t+5) - \frac{3}{16} f(t+6) + \frac{3}{8} f(t+11) - \frac{1}{16} f(t+16) - \frac{1}{16} f(t+17)$$

(6.3)

Analysis of the Semiannual Variation

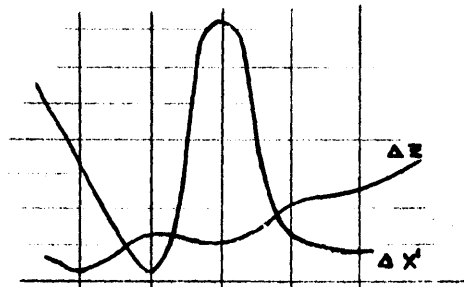
The data used in the analysis of the semiannual magnetic variation came from the four non-polar geomagnetic observatories operated by the United States Coast and Geodetic Survey: Honolulu, San Juan, Tucson and Cheltenham (now transferred to Fredricksburg).

Ten cycles were covered in the five relatively quiet years 1951 - 1955. At each station the tabulated mean elements D, H and Z for the five internationally quiet days of each month were subtracted from the corresponding mean elements for the five internationally disturbed days of each month giving the monthly mean disturbance elements ΔD , ΔH and ΔZ . In the five years covered, the elements X and Y changed only a little, so the values half way between their extremes were used, along with ΔD and ΔH , in Equations 2.1 a, b to calculate the monthly mean disturbance elements ΔX and ΔY . These were converted to the geomagnetic co-ordinate elements $\Delta X'$ and $\Delta Y'$ using the magnetic pole axis for 1945 given by Vestine et al (1947 b). Its north magnetic pole is at latitude = $78^{\circ}6'N$ and longitude = $289^{\circ}9'E$. The elements were then harmonically analyzed (frequency-wise) using the sigma smoothing window.

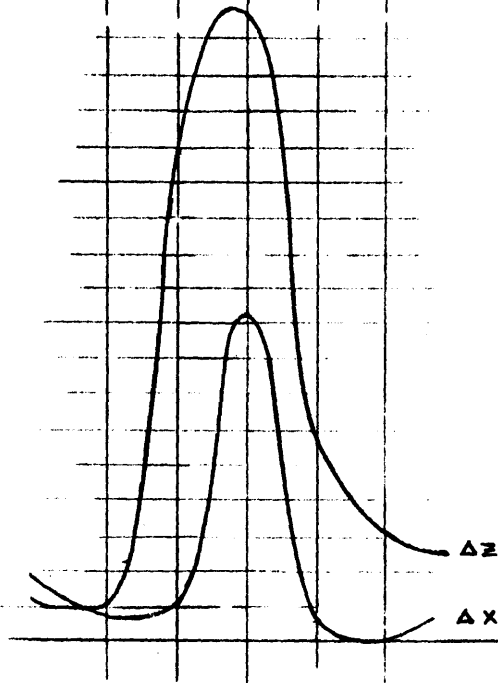
In Figure 6.3 are plots of the power spectra of $\Delta X'$ and ΔZ from the harmonic analysis of the monthly mean disturbance field. As would be expected for a zonal field there are no significant peaks in the power spectra of $\Delta Y'$ so they are not plotted. Clear peaks at the six month period are recognized at all four stations with but two exceptions: the ΔZ spectra of Honolulu and San Juan. Honolulu is close to the geomagnetic equator so its ΔZ component should be small and the lack of a power peak in ΔZ is not unexpected.

MONTHLY MEAN DISTURBANCE FIELD
POWERS IN GAMMAS²

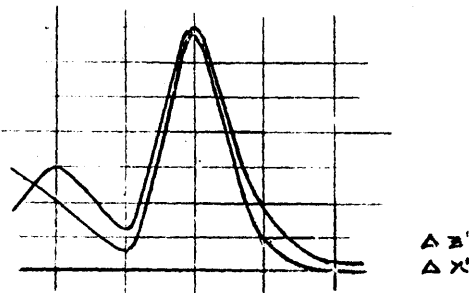
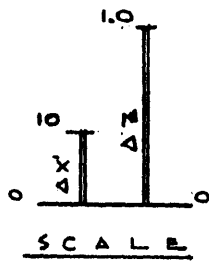
FIGURE 6.3



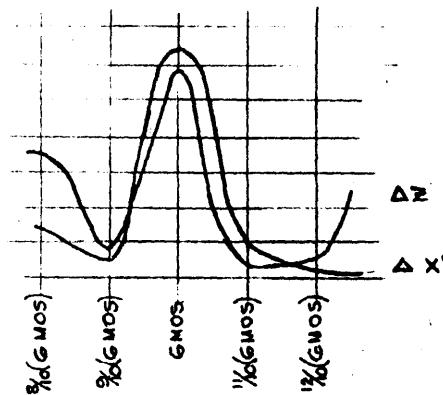
HONOLULU
GEOMAGNETIC LATITUDE
20.6° N



SAN JUAN
GEOMAGNETIC LATITUDE
28.4° N



TUCSON
GEOMAGNETIC LATITUDE
40.2° N



CHELTENHAM
GEOMAGNETIC LATITUDE
49.7° N

San Juan has a peak for ΔZ , but it does not fall at exactly six months; the ΔZ complex amplitude derived from San Juan data is therefore questionable.

In Figure 6.4 are plotted the complex amplitudes ΔX^1 , and ΔZ . There is good agreement in the phases with the same two exceptions in ΔZ noted above: Honolulu and San Juan. The small ΔZ amplitude of Honolulu receives little weight in the least squares zonal harmonic analysis and does not have much effect on the $\mathcal{H}_1(a)$ determined. The phase and amplitude of ΔZ for San Juan are discordant with those of Tucson and Cheltenham. Because of this and because of its questionable power spectrum, the ΔZ amplitude of San Juan was not used in the least squares determination of $\mathcal{H}_1(a)$.

By the least squares method given in Chapter VII, $\mathcal{L}_1(a)$ and $\mathcal{H}_1(a)$ were found to be the following quantities:

$$\mathcal{L}_1(a) = -6.55 + i 3.56 \text{ gammas (using HO, SJ, TU and CH)}$$

$$\mathcal{H}_1(a) = -1.08 + i 1.09 \text{ gammas (using HO, TU and CH)}$$

It follows that

$$S_1(a) = 0.37/6^\circ$$

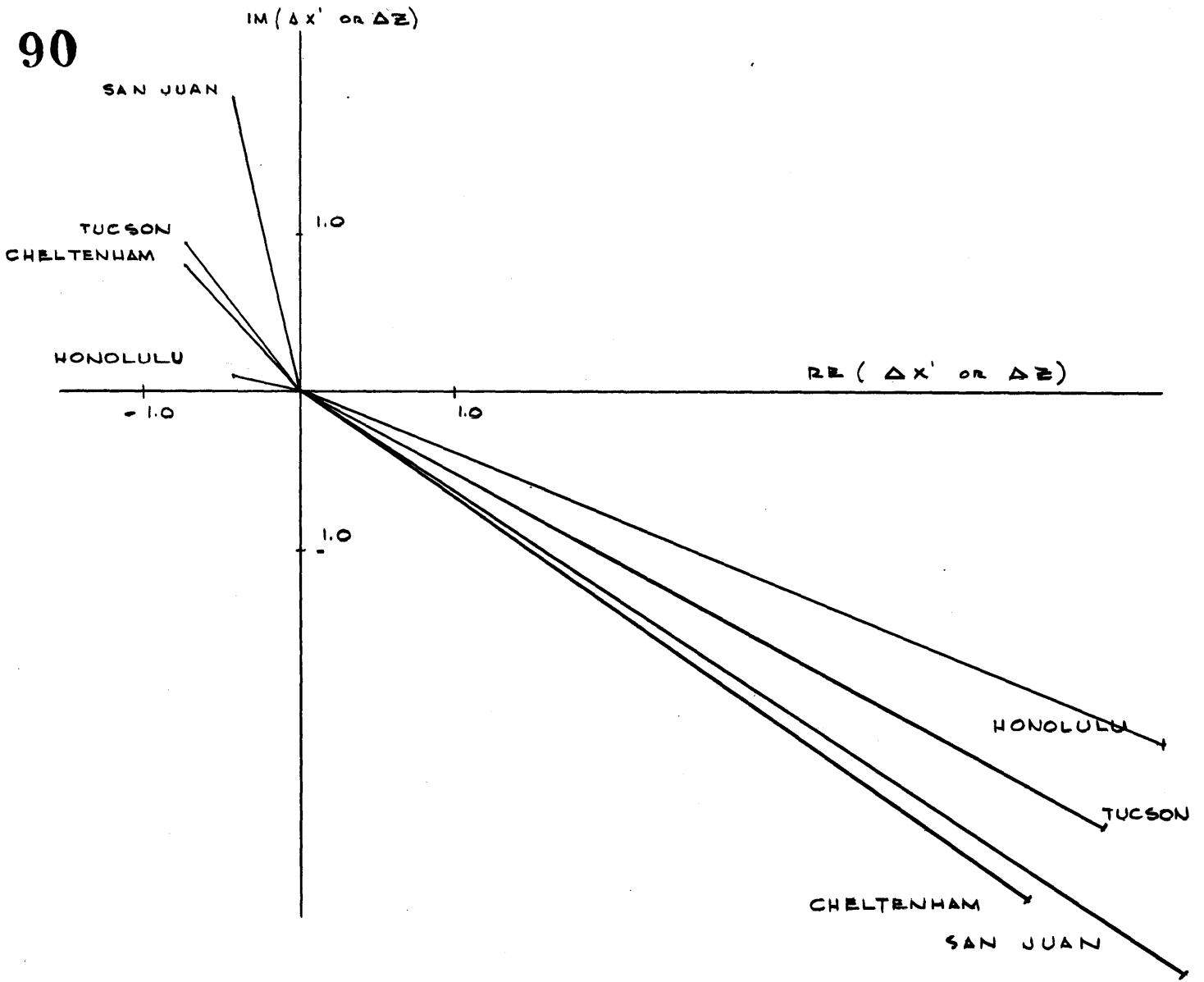
This is the complex ratio used in Chapter VII for conductivity calculations.

It is of interest to derive $S_1(a)$ from the monthly mean disturbance data of only one station. This was done for Tucson and for Cheltenham. The ratios calculated are as follows:

$$S_1(a) = 0.35/9^\circ \text{ (TU)}$$

$$S_1(a) = 0.39/3^\circ \text{ (CH)}$$

90



SCALE IN GAMMAS

FIGURE 6.4

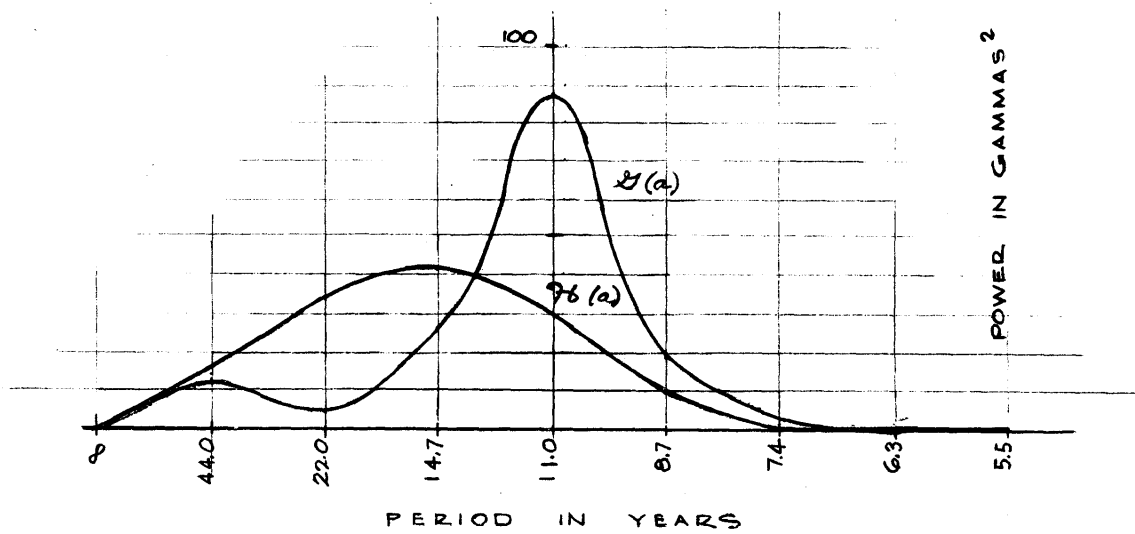


FIGURE 6.5

Vestine et al (1947 a) present tables of the "estimated symmetrical part of annual variation" in the geomagnetic north component and in the vertical component for every month from 1905 to 1942. Also presented are "multiplicative latitude factors for obtaining symmetrical part in any latitude from given values". (The method for obtaining these data is not given.) Frequency harmonic analyses of the data were made in search of the six month period. The resulting complex amplitudes times the latitude factors at $\cos \vartheta'_k = 0.0, 0.1, 0.2, \dots, 0.8$ (geomagnetic non-polar latitudes $0^\circ, 6^\circ, 12^\circ, 17^\circ, 24^\circ, 30^\circ, 37^\circ, 44^\circ$ and 53°N) were used to find $S_1(a)$ and $H_1(a)$ by least squares. The complex ratio calculated from these turned out to be

$$S_1(a) = 0.39 \underline{-1^\circ}$$

Although this is an impossible ratio, it is encouraging that it does not differ by very much from the ratio calculated above from the mean disturbance field.

Analysis of the Sunspot Cycle

Yearly mean values of the geomagnetic elements, such as were used in the sunspot cycle analysis, are available in graphical form for many stations operating between 1905 and 1945 in Vestine et al (1947 a). They have been tabulated from time to time by Fleming and Scott (1943, 1944, 1948) and Johnston (1951, 1956). Used in this thesis are unpublished elements compiled by the Physics Research Division of Emmanuel College, Boston, under the U. S. Air Force Contract AF19(604)-2192. The compilation was done under the direction of M. Patricia Hagen of Emmanuel College and the data, in punched card form, were made available by Paul F.

Fougere of the Geophysics Research Directorate, Air Force Cambridge Research Laboratories in Bedford, Massachusetts. The stations used, their latitudes and longitudes and the spans of coverage are given in Table 6.1. The 1922 magnetic pole axis (north magnetic pole latitude = 78.5°N , longitude = 291.0°E - Vestine, 1947 a) - was used to convert from geographic to geomagnetic co-ordinates.

In Figure 6.5 are plots of the spectra calculated for $\mathcal{G}_1(a)$ and $\mathcal{H}_1(a)$. The $\mathcal{G}_1(a)$ spectrum shows a distinct eleven year period peak with a lesser peak at lower frequencies which is caused by the low frequency background passing through the numerical filter. For $\mathcal{H}_1(a)$, the background is considerably stronger and the eleven year signal is weaker and concealed. (This is the same trouble as beset Vestine et al, 1947 b, in their attempt to analyze Z.) The real part of $\mathcal{G}_1(a)$ was found to be

$$5.0 \cos \left(\frac{Y - 1900}{11} 360^{\circ} \right) + 7.3 \sin \left(\frac{Y - 1900}{11} 360^{\circ} \right)$$

where y is the year. This function is maximized at about $y = 1902$, 1913, etc., which are years of sunspot minima. This is in accordance with the fact that the X^1 flux density decreases at times of high magnetic activity.

Since a substantial portion of the least-squared Z data analyzed for the sunspot cycle is random noise, the correct way to calculate its power spectrum is to find the frequency transform of its autocorrelation function. Using a program written by J. Galbraith this was done for 55 years of filtered Z data. However, the 11 year period peak in $\mathcal{H}_1(a)$ was hardly perceptible in the presence of the high Z noise.

Table 6.1 (When observatories have been transferred locally, only one is listed.)

Station	Latitude	Longitude	Span Used
Amberley	-43° 09'	172° 43'	1902-1957
Melbourne	-37° 50'	144° 58'	1916-1957
Capetown	-34° 25'	19° 14'	1933-1956
Pilar	-31° 40'	296° 07'	1905-1950
Watheroo	-301° 90'	115° 52'	1919-1957
Vassouras	-22° 24'	316° 21'	1915-1955
Maurituis	-20° 06'	57° 33'	1898-1954
Tananarive	-18° 55'	47° 32'	1902-1922, 1929-1954
Apia	-13° 48'	188° 14'	1905-1957
Huancayo	-12° 03'	284° 40'	1922-1949
Elisabethville	-11° 40'	27° 28'	1932-1952
Antipolo	14° 36'	121° 10'	1911-1938
San Juan	18° 23'	293° 53'	1903-1957
Taungoo	18° 56'	96° 27'	1905-1923
Honolulu	21° 19'	201° 34'	1902-1957
Hong Kong	22° 18'	114° 10'	1898-1939
Helwan	29° 52'	31° 20'	1903-1951
Dehra Dun	30° 19'	78° 03'	1903-1943
Zik-a-wei	31° 19'	121° 02'	1908-1933
Tucson	32° 15'	249° 10'	1910-1957
Ksara	33° 49'	35° 53'	1937-1954
San Fernando	36° 28'	353° 50'	1898-1957
San Miguel	37° 46'	334° 21'	1911-1957
Cheltenham	38° 44'	283° 10'	1901-1955
Coimbra	40° 12'	351° 35'	1898-1954
Ebro	40° 49'	0° 31'	1910-1937
Keles	41° 25'	69° 12'	1936-1955
Tiflis	41° 50'	44° 42'	1898-1934, 1938-1955
Agincourt	43° 47'	280° 44'	1899-1954
Nantes	47° 15'	358° 27'	1923-1955
Chambon-la-Forêt	48° 01'	2° 16'	1898-1957
Munich	48° 10'	11° 17'	1939-1957
Vienna	48° 12'	16° 14'	1929-1950
Greenwich	51° 28'	0° 00'	1898-1956
Valentia	51° 56'	349° 45'	1899-1956
Niemegk	52° 04'	12° 40'	1931-1957
Swider	52° 07'	21° 15'	1921-1951
Potsdam	52° 23'	13° 04'	1898-1929
Eskdalemuir	55° 19'	356° 48'	1908-1957
Zaymistche	55° 50'	48° 51'	1914-1954
Vyssokaya Dubrava	56° 44'	61° 04'	1900-1955
Sverdlovsk	56° 50'	60° 38'	1898-1931
Lovo	59° 21'	17° 50'	1929-1959
Slutsk	59° 41'	30° 29'	1898-1941

CHAPTER VII
CONDUCTIVITY INTERPRETATIONS OF THE MANTLE

Resolution of Conductivities

The reckoned diurnal ratios, S_2 , S_3 and S_4 , are predominantly influenced by the oceans and shallow mantle conductivities and the semiannual ratio, S_1 , is most affected by greater and deeper mantle conductivities. When ratios from both variations are used together, conductivity interpretations over a wide range of conductivities and through a considerable fraction of the mantle are possible. Lacking a sunspot ratio, the higher conductivities in the lower mantle are best appraised by methods other than those treated in detail in this thesis.

The Conductivity of The Mantle - Specific Models

If the semiannual ratio calculated in Chapter VI, $S_1(a) = 0.370/6^\circ$, is used in the straight line conductivity solution (Equations 4.40 - 4.42), a conductivity-depth structure (labelled A in Figures 7.1 and 7.2) is obtained as follows:

Depth	Conductivity (mhos/meter)
0	1.5
200	2.2
400	3.6
600	6.8
800	20
1000	180
1100	∞

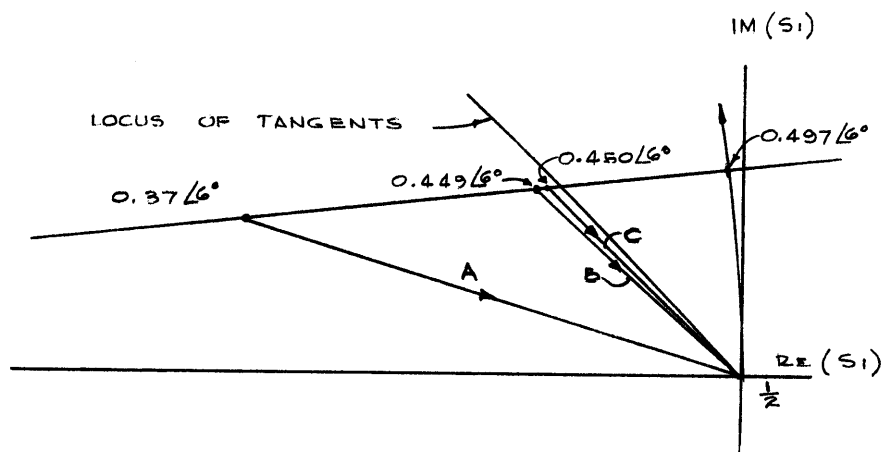


FIGURE 7.1

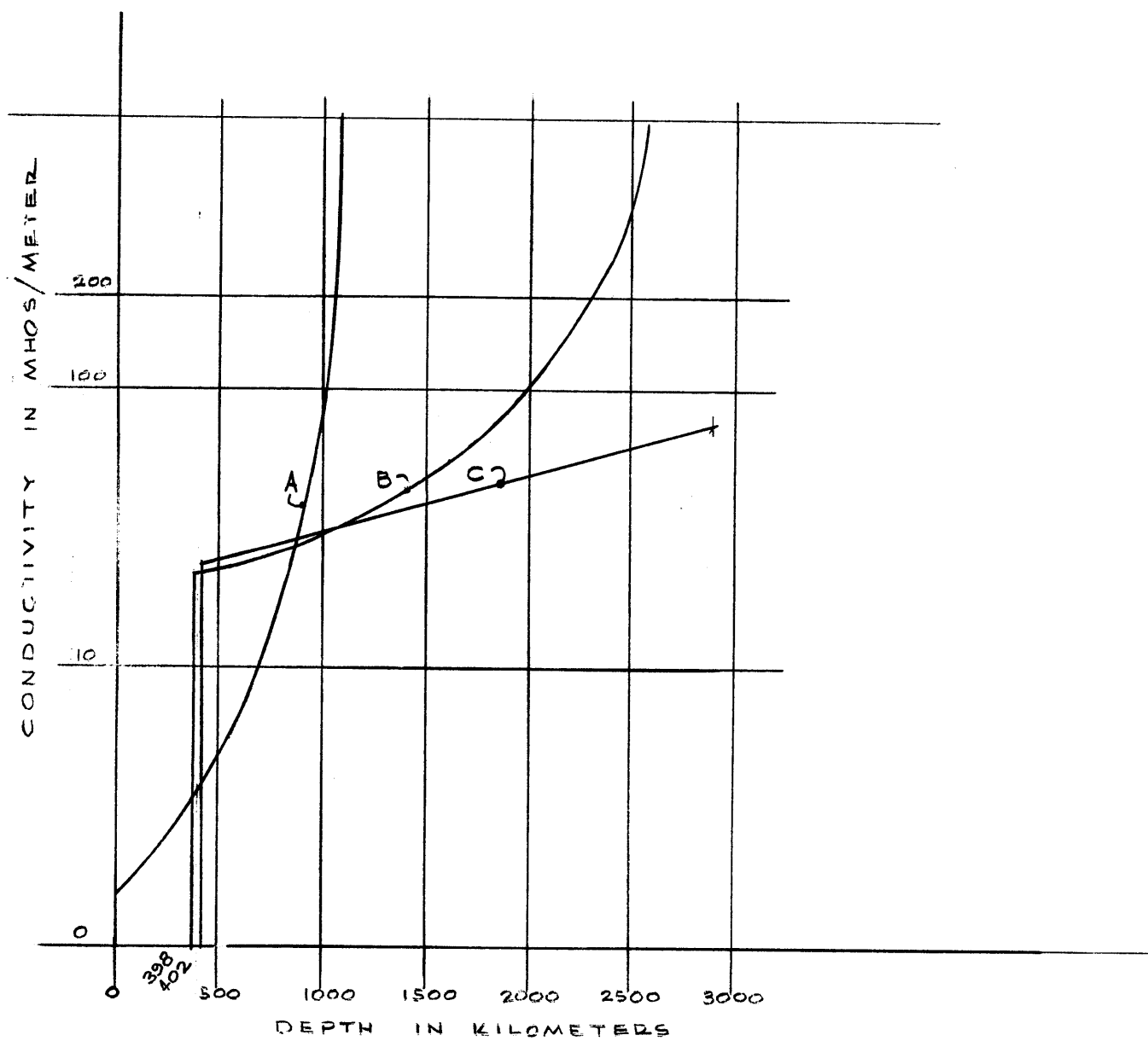


FIGURE 7.2

However, a conductivity of 1 1/2 mhos/meter is excessive at or near the surface of the earth. A much better conductivity estimate can be obtained by first using the results of the diurnal variation analysis.

In the last paragraph of Chapter V it was pointed out that the minimum depth at which the conductivity may significantly affect the semiannual variation is about 400 kilometers. The effect on $S_1(a)$ as it travels downward through this relatively nonconducting outer layer is that its magnitude increases and its phase remains constant. The ratio increases as the cube of the radial distance so at a depth δ

$$S_1(a-\delta) = \left(\frac{a}{a-\delta}\right)^3 S_1(a)$$

At the depth $\delta = 402$ kilometers

$$S_1(5968 \text{ km}) = 0.450/6^\circ$$

which is on the locus of tangents. (See Figure 7.1.) At a depth $\delta = 600$ kilometers

$$S_1(5770 \text{ km}) = 0.498/6^\circ$$

which is on the outer boundary of the semicircular region inside of which S_1 must fall. There is only one possible path which can lead away from this point (along the outer semicircular arc counter-clockwise to the origin), and this requires an infinitesimally thin superconducting shell surrounding an insulating sphere. This is clearly implausible.

If, corresponding to Path 5 of Figure 4.9, $S_1(r)$ is taken to a depth just short of the locus of tangents and the straight line solution of Chapter IV is used, the conductivity below this depth increases inversely as the square of the radial distance until it approaches the center of the earth and then it rapidly increases to infinity. With this interpretation (labelled C in Figures 7.1 and 7.2) the conductivity rises rapidly to 25 mhos/meter at a depth of 402 kilometers and increases thereafter as r^{-2} . At the depth of the core boundary, 2900 kilometers, the conductivity is 75 mhos/meter. But, since $\sigma \propto r^{-2}$

$$k^2 \propto r^2$$

$$kr = \text{constant}$$

and the conductivity does not approach that of an equivalent superconductor for the semiannual period except right at the center of the earth.

The starting depth for the straight line model can be chosen so that the conductivity becomes infinite at the core boundary, and near the locus of tangents this superconducting depth is extremely sensitive to the starting depth. Starting at a depth of 398 kilometers

$$S_1(5972 \text{ km}) = 0.449/6^\circ$$

Very close to this choice

$$\frac{h_1}{\cos \delta_1} = 0.402$$

and, by (4.42), the superconductor occurs at

$$r_s = 3470 \text{ km}$$

which is the core boundary. The conductivity-depth structure for this model (labelled B in Figures 7.1 and 7.2) is as follows:

Depth	Conductivity (mhos/meter)
0-398 km	0 (apparent insulator, $\sigma < 0.05$)
400 km	22
900 km	30
1400 km	45
1900 km	87
2400 km	310
2900 km	∞ (apparent superconductor, $\sigma > 200$)

The conductivities required by models B and C at depths between 400 and 500 kilometers are much too high to be consistent with those allowed by the diurnal variation analyses at the end of Chapter V. The semiannual and diurnal ratios are consistent only if the semiannual ratio, S_1 , crosses the locus of tangents. Beyond the locus of tangents the straight line solution is no longer applicable.

The Conductivity of the Mantle - Generalizations

An examination of the terms in Equation 4.30 as S_1 crosses the locus of tangents and continues to the right shows that r and $(S_1 - 1/2)^2$ decrease and $1/r$ and S_1 increase. Thus, before S_1 leaves its restricting semicircle at a depth of 600 kilometers, the first term of (4.30) must counteract the second term and this is possible only for conductivities exceeding the conductivity which exactly balances the two terms at the locus of tangents. We may conclude that the diurnal and semiannual ratios are consistent only if a conductivity in excess of 25 mhos/meter is attained at a depth between 500 and 600 kilometers.

There are an infinite number of possible monotonic conductivity-depth distributions which satisfy our data for the diurnal and semiannual variations and which are compatible with lower mantle conductivity estimates. All of them have the following properties:

1. From the surface to a depth of 500 kilometers the conductivity increases to no more than 0.3 mhos/meter. This is an apparent superconductivity to the diurnal variation. The absolute magnitudes of S_2 , S_3 , and S_4 are too low to allow superconductivity at any depth shallower than 500 kilometers.
2. At depths greater than 600 kilometers, the conductivity is at least 25 mhos/meter. At these depths the first term of Equation 4.30 must be large enough to counteract the second term. This is in order to keep S_1 (for the semiannual variation) within the semicircle to which it is restricted as (4.30) is solved working downwards.
3. The lower mantle conductivity is of the order of 100 mhos/meter. The reasons are reviewed in Chapter I.

Thus, for a mantle in which the electrical conductivity increases monotonically with depth, the conductivity changes by several powers of ten in the outer 600 kilometers and by no more than a factor of about ten in the remaining 2300 kilometers.

CHAPTER VIII

SUGGESTIONS FOR FUTURE WORK

The purpose of this chapter is to suggest possible avenues of future work on this and related problems.

The Sunspot Cycle

It is probable that the sunspot variation penetrates the mantle to a significant degree as far as the core-mantle boundary and that a successful analysis of this variation would contribute much information about the electrical conductivity of the mantle. Part of the problem of the detection of the elements of this cycle is the low frequency, high power noise background, and part of the problem is the long duration of the cycle. The former difficulty can probably be overcome by using the mean disturbance field such as was done for this thesis in the analysis of the semiannual cycle; the latter difficulty is a matter of time, but over a century of data is required to match just five years of data for the semiannual cycle. Mean disturbance elements have been measured by many observatories for many years; the practical problem is to acquire these data. Once acquired, they will not cover many sunspot cycles but this may possibly be offset by using data from many stations.

Other Cycles

Analyses of other periodic magnetic variations may be feasible. The 22 year cycle, because of its length, is probably not one of these at present. The annual variation may well be detectable in all of its elements, but its mantle conductivity and depth resolution would be only slightly different from that of the semiannual variation.

The 27 day cycle falls between the semiannual and diurnal variation, and if it could be analyzed it might illuminate the nature of the rapid rise in the conductivity of the upper mantle. This cycle is very weak, but comparatively many cycles of data are available for its analysis.

Survey of Mantle Models

The electrical conductivity distribution of the earth's mantle is strongly dependent on its temperature profile and it also depends somewhat on its fairly well-known pressure profile. MacDonald (1959) has presented numerical calculations of the thermal history of the earth for a number of different models. For any assumed conductivity mechanism each of MacDonald's models (and any others) can be tested for compatibility with observed complex ratios, S_m^s , by numerically integrating Equation 4.30. Such testing may help to circumscribe possible temperature profiles and conductivity mechanisms within the mantle and it may throw some light on the thermal history of the earth.

Mantle Shielding

Equations 4.26 a, b may be of use in investigating the shielding by the mantle of secular variations. For any mantle conductivity distribution, these equations relate the measurable secular variation field components at the earth's surface to its source field components at the core boundary. The equations may be used in either of two ways: knowing or assuming the conductivity structure, what is the field at the core; or assuming the field at the core, what is the conductivity structure.

Complex Ratios in Geophysics

Many problems in geophysics are concerned, like this thesis, with ratios such as current/voltage, \vec{E} field/ \vec{H} field, etc. The

utility of the approach of this thesis in which a differential equation for the ratio itself is considered (rather than its numerator and denominator separately) suggests that it may be fruitful to use this method of attack for other problems. For instance, in the one dimensional magnetotelluric problem (Cagniard, 1953) for which an electromagnetic wave with an implicit $e^{-i\omega t}$ time variation and components $\mathbf{E} = (E_x, 0, 0)$, $\mathbf{H} = (0, H_y, 0)$ penetrates vertically into the earth (z positive downward), the complex ratio $R = E_x / H_y$ is of importance. From Maxwell's equations

$$\sigma E_x = -\frac{dH_y}{dz}$$

$$-\frac{dE_x}{dz} = i\omega\mu H_y$$

Thus

$$\frac{d\left(\frac{E_x}{H_y}\right)}{dz} = \frac{1}{H_y} \frac{dE_x}{dz} - \frac{E_x}{H_y^2} \frac{dH_y}{dz}$$

$$\frac{dR}{dz} = -i\omega\mu + \sigma R^2$$

This equation may be of use for the numerical solution of R when the conductivity changes continuously or discontinuously with depth. Its qualitative effect on R in the complex plane is easily perceived.

When $\frac{dR}{dz} = 0$ we get the familiar uniform earth ratio, $R = \sqrt{\frac{i\omega\mu}{\sigma}}$.

BIOGRAPHICAL NOTE

Donald Eckhardt was born in 1932 in Flushing, New York, and attended school in Bayside, New York. He received a B.S. in Geophysics from M.I.T. in 1955. From 1955 to 1958 he was employed by the Socony Mobil Oil Company in Nebraska and Venezuela. He is currently an off-campus Research Associate of the Ohio State University Research Foundation.

BIBLIOGRAPHY

- Benkova, N. P. (1940) Spherical Harmonic Analysis of the Sq-Variations, May-August, 1933, Terr. Mag., 45, pp. 425-432.
- Benkova, N. P. (1957) Current Systems of Magnetic Storms, Trans. of Toronto Meeting IAGA, IAGA Bull. No. 16, pp. 350-351.
- Blackman, R. B. and J. W. Tukey (1958) The Measurement of Power Spectra, Dover Publications.
- Bullard, E. C., C. Freedman, H. Gellman and J. Nixon (1950) The Westward Drift of the Earth's Magnetic Field, Phil. Trans. R. Soc. Lond., A. 243, pp. 67-92.
- Cagniard, L. (1953) Basic Theory of the Magnetotelluric Method, Geophys. 18, pp. 605-635.
- Chapman, S. (1919) The Solar and Lunar Diurnal Variations of Terrestrial Magnetism, Phil. Trans. R. Soc. Lond., A. 218, pp. 1-118.
- Chapman, S. and T. T. Whitehead (1923) The Influence of Electrically Conducting Material Within the Earth on Various Phenomena of Terrestrial Magnetism, Trans. Phil. Soc., Cambridge, 22, pp. 463-482.
- Chapman, S. and A. T. Price (1930) The Electric and Magnetic State of the Interior of the Earth, as Inferred from Terrestrial Magnetic Variations, Phil. Trans. R. Soc. Lond., A. 229, pp. 427-460.
- Chapman, S. and J. Bartels (1940) Geomagnetism, Oxford Univ. Press.
- Chapman, S. (1951) The Earth's Magnetism, John Wiley, Second Edition.
- Cynk, B. (1939) Variations in the Disturbance Field of Magnetic Storms, Terr. Mag., 44, pp. 51-57.
- Cynk, B. (1941) Some Relationships in the Fields of Geomagnetic Storms, Terr. Mag., 46, pp. 431-433.
- Elsasser, W. M. (1950) The Earth's Interior and Geomagnetism, Rev. Mod. Phys., 22, pp. 1-35.

- Fleming, J. A. and W. E. Scott (1943, 1944, 1948) List of Geomagnetic Observatories and Thesaurus of Values, Terr. Mag., 48, pp. 97-108, 171-182, 237-242; 49, pp. 47-52, 109-118, 199-205, 267-269; 53, pp. 199-240.
- Goldschmidt (1954) Geochemistry, Oxford Univ. Press.
- Hasegawa, M. and M. Ota (1948) On the Magnetic Field of Sq in the Middle and Lower Latitudes During the II Polar Year, Trans. of 1948 Oslo Meeting IATME, IATME Bull. No. 13, pp. 426-430.
- Hildebrand, F. B. (1948) Advanced Calculus for Engineers, Prentice-Hall.
- Hughes (1953) The Electrical Conductivity of the Earth's Interior, Ph. D. thesis, Univ. of Cambridge.
- Hughes (1959) The Conductivity Mechanism in the Earth's Mantle (Abstract), J. Geophys. Res., 64, pp. 1108.
- Johnston, H. F. (1951, 1956) List of Geomagnetic Observatories and Thesaurus of Values, J. Geophys. Res., 56, pp. 431-438; 61, pp. 273-282.
- Lahiri, B. N. and A. T. Price (1939) Electromagnetic Induction in Nonuniform Conductors, and the Determination of the Conductivity of the Earth from Terrestrial Magnetic Variations, Phil. Trans. R. Soc. Lond., A. 237, pp. 509-540.
- Lanczos, C. (1956) Applied Analysis, Prentice-Hall.
- MacDonald, G. J. F. and L. Knopoff (1958) On the Chemical Composition of the Outer Core, Geophys. J. of R. Astron. Soc., 1, pp. 284-295.
- MacDonald, G. J. F. (1959) Calculations on the Thermal History of the Earth, J. Geophys. Res., 64, pp. 1967-2000.
- McDonald, K. L. (1957) Penetration of the Geomagnetic Secular Variation through a Mantle with Variable Conductivity, J. Geophys. Res., 62, pp. 117-141.
- McNish, D. H. (1959) On the Annual Variation of Magnetic Disturbance, Phil. Trans. R. Soc. Lond., A. 251, pp. 525-552.
- Munk, W. and R. Revelle (1952) On the Geophysical Interpretation of Irregularities in the Rotation of the Earth, Mon. Not. Roy. Astron. Soc., Geophys. Suppl., 6, pp. 331-347.

- Rikitake, T. (1950) Electromagnetic Induction within the Earth and its Relation to the Electrical State of the Earth's Interior, Bull. Tokyo Univ. Earthquake Res. Inst., 28, pp. 45-98.
- Runcorn, S. K. (1955) The Electrical Conductivity of the Earth's Mantle, Trans. Am. Geophys. Un., 36, pp. 191-198.
- Runcorn, S. K. (1956) The Magnetism of the Earth's Body, Handbuch der Physik, 47, pp. 498-533.
- Sommerfeld, A. (1952) Electrodynamics, Academic Press.
- Stratton, J. A. (1941) Electromagnetic Theory, McGraw-Hill.
- Tozer, D. C. (1959) The Electrical Properties of the Earth's Interior, Chapter 8, Physics and Chemistry of the Earth, 3, Pergamon Press, London.
- U. S. Dept. of Commerce, Coast and Geodetic Survey (1948, 1949) Magnetic Hourly Values.
- U. S. Dept. of Commerce, Coast and Geodetic Survey (1950-) Magnetograms and Hourly Values.
- Vestine, E. H., L. Laporte, I. Lange, C. Cooper and W. C. Hendrix (1947a) Description of the Earth's Main Magnetic Field and Its Secular Change, 1905-1945, Carnegie Inst., Wash., Pub. No. 578, pp. 1-100.
- Vestine, E. H., L. Laporte, I. Lange and W. E. Scott (1947b) The Geomagnetic Field, Its Description and Analysis, Carnegie Inst., Wash., Pub. No. 580.
- Yukutake, T. (1959) Attenuation of Geomagnetic Secular Variation through the Conducting Mantle of the Earth, Bull. Earthquake Res. Inst., 37, pp. 13-32.